Chrome spinel grains from the Komstad Limestone Formation, Killeröd, southern Sweden: A high-resolution study of an increased meteorite flux in the Middle Ordovician

Ellinor Martin

Dissertations in Geology at Lund University,
Master's thesis, no 421
(45 hp/ECTS credits)

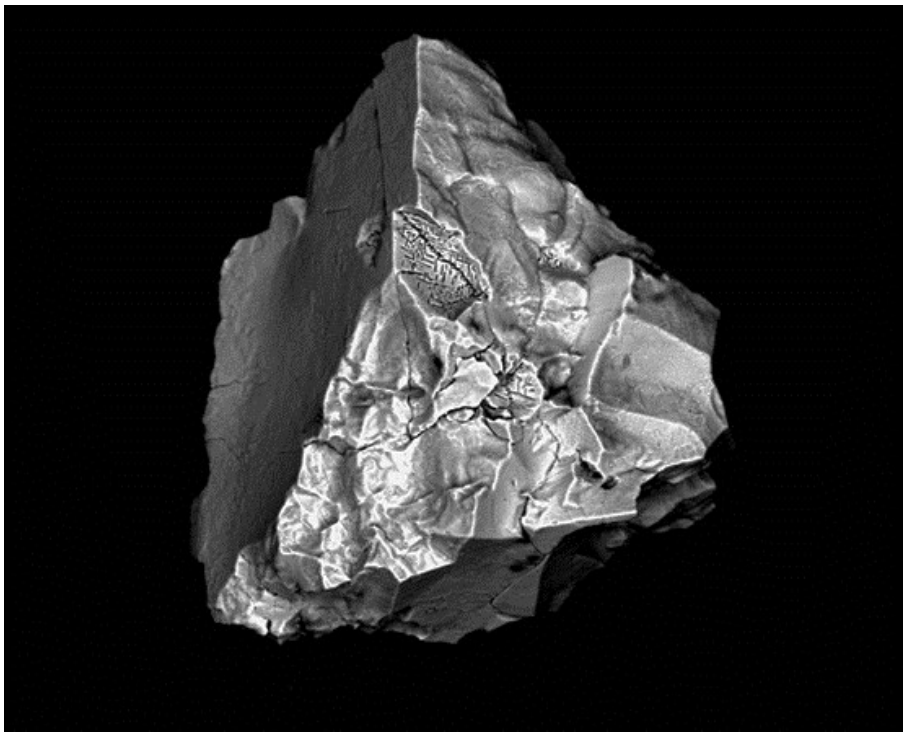

Department of Geology
Lund University
2014

Chrome spinel grains from the Komstad Limestone Formation, Killeröd, southern Sweden: A high-resolution study of an increased meteorite flux in the Middle Ordovician

Master's thesis

Ellinor Martin

Department of Geology
Lund University
2014

Contents

Cover Picture: SEM-image of EC grain #367 (grain size = 133 × 111 μm) photograph by E. Martin

Chrome spinel grains from the Komstad Limestone Formation, Killeröd, southern Sweden: A high-resolution study of an increased meteorite flux in the Middle Ordovician

ELLINOR MARTIN

Martin, E., 2014: Chrome spinel grains from the Komstad Limestone, Killeröd, southern Sweden: A high-resolution study of an increased meteorite flux in the Middle Ordovician. *Dissertations in Geology at Lund University*, No. 421, 35 pp. 45 hp (45 ECTS credits) .

Abstract: In the Middle Ordovician period the influx of cosmic material to Earth was increased, following the breakup of the L-chondrite parent body in the Main Asteroid Belt, enriching the ancient shelf environment with meteorites and cosmic dust. The Komstad Limestone Formation in Killeröd, Scania, contains an interval exceptionally rich in L chondritic chromite grains indicating a very high degree of condensation. The interval also has very low amounts of terrestrial chromium-rich spinels. This facilitates the search for chromite from other, rarer types of meteorites, including lunar meteorites potentially ejected by impacts of L-chondritic asteroids on the Moon. Especially interesting is also to look for grains similar to those from the recently found fossil winonaite-like meteorite at Kinnekulle. This meteorite may be a fragment of the body that hit and disrupted the L-chondrite parent body.

One hundred kilograms of a thin interval of the Komstad Limestone from the Killeröd quarry was dissolved in acids. Chromite grains were picked and analyzed in SEM and EDS for chemical composition, and divided into extraterrestrial (ordinary chondritic) chromite (EC) grains and other chrome-spinel (OC) grains. One recently recovered fossil meteorite, Grå 002, from the Thorsberg quarry at Kinnekulle was also included in this study. Polished thin sections were made from the studied interval that naturally subdivides into four sub-beds. Sedimentological facies and features were determined.

The results from the sedimentological study indicate a rather active environment with a gradual regression of the sea level with the increase in number of skeletal grains and the transition from wackestone/packstone to packstone/grainstone, and back to wackestone.

In the 100 kg of rock 507 EC grains (4.95 grains/kg) and 17 OC grains (0.17 grains/kg) were found. Based on the chemical affinity of the grains they were further divided into subcategories. The average chemical composition of the EC grains plot within the range of L chondrites. Six grains contain nickel, which is interpreted to represent chromite that resided in the fusion crust of micrometeorites. No typical lunar chrome spinel grains were discovered. Based on chemistry and size of the chromite grains the fossil meteorite Grå 002 was determined to be an L chondrite of petrological type 5. Of the OC grains 12 could be terrestrial based on their similar composition as chrome spinel from igneous ultramafic and mafic rocks from subduction regimes, however, an extraterrestrial origin cannot be excluded. One OC grain in particular has a composition similar to that of the fossil winonaite chrome spinel and deviates from both terrestrial and chondritic chromite. The single OC grain falls within the ranges of the fossil winonaite-like meteorite in all oxides except for a somewhat smaller amount of FeO. The Cr/(Cr+Al) and Fe^{2+}/($Mg+Fe^{2+}$) ratios are also similar to the fossil winonaite meteorite. A second grain is also similar with a good match in the ratios, but deviates in more than one oxide. One or two winonaite-like grains among 500 EC grains supports the contention, based on the recovery of 1-20 cm large fossil meteorites from Kinnekulle, that winonaite-like meteorites represented on the order of one percent of the meteorite flux to Earth in the mid-Ordovician.

Keywords: chrome spinel, fossil meteorites, Komstad Limestone, winonaites, Middle Ordovician, carbonate sedimentology

Supervisor(s): Birger Schmitz, Mats Eriksson and Anders Lindskog

Subject: Bedrock Geology

Ellinor Martin, Department of Geology, Lund University, Sölvegatan 12, SE-223 62 Lund, Sweden.
E-mail: ellinor.martin@gmail.com

Kromspinell från Komstadformationen, Killeröd, södra Sverige: En detaljerad studie av ett ökat inflöde av meteoriter i mellan-ordovicium

ELLINOR MARTIN

Martin, E., 2014: Kromspinell från Komstadformationen, Killeröd, södra Sverige: En detaljerad studie av ett ökat inflöde av meteoriter i mellanordovicium. *Examensarbeten i geologi vid Lunds universitet*, Nr. 421, 35 sid. 45 hp.

Sammanfattning: I mellersta ordovicium var inflödet av kosmiskt material till jorden högre än idag, i sviterna efter uppbrytningen av den L-kondritiska asteroidkroppen i asteroidbältet mellan Mars och Jupiter, vilket berikade den forna havsbottnen med meteoriter och kosmiskt damm. Komstadformationen i Killeröd, Skåne, innehåller ett lager särskilt rikt på L-kondritiska kromitkorn vilket indikerar en hög grad av kondensation. Intervallet har dessutom lågt innehåll av andra typer av kromspinell. Detta möjliggör sökandet efter kromit från andra typer av mer ovanliga meteoriter, till exempel månmeteoriter som potentiellt slungats ut till följd av impakter från den uppbrutna L-kondritiska kroppen. Särskilt intressant är också att söka efter kromitkorn liknandes dem som hittats i den nyligen funna fossila winonait-liknande meteoriten i Kinnekulle. Denna meteorit som kan vara ett fragment av den himlakropp som splittrade den L-kondritiska föräldrakroppen.

Etthundra kilogram av ett tunt interval av Komstadformationen från Killerödsbrottet löstes upp i syror. Kromitkorn plockades och analyserades i SEM och EDS för kemisk sammansättning och indelades i utomjordisk (kondritisk) kromit (EC) och andra kromspineller (OC). En nyligen upptäckt fossil meteorit, Grå 002, från Thorsbergsbrottet i Kinnekulle inkluderades i studien. Polerade tunnslip tillverkades från det studerade intervallet, som naturligt är uppdelat i fyra delinterval. Sedimentologiska facies och karaktärer fastställdes.

Resultatet från den sedimentologiska studien indikerar en relativt aktiv miljö med gradvis regression av havsnivån med ökat antal skalkorn och en övergång från wackestone/packstone till packstone/grainstone och tillbaka till wackestone.

I hundrakilosprovet hittades 507 EC-korn (4.95 korn/kg) och 17 OC-korn (0.17 korn/kg). Baserat på den kemiska sammansättning av kornen så delades dessa vidare in i subkategorier. Den genomsnittliga sammansättningen på EC -kornen sammanfaller inom ramen för L-kondritiska korn. Sex kromitkorn innehåller nickel, vilket tolkas som att kornen suttit i smältskorpan på mikrometeoriter. Inga typiska kromspineller från månen kunde hittas. Baserat på kemisk sammansättning och storlek på kromitkornen från den fossila meteoriten Grå 002 klassificeras den som en L-kondritisk meteorit av petrologisk typ 5.

Av OC-kornen kan 12 vara terrestriska, baserat på deras liknande sammansättning med kromspinell från magmatiska ultramafiska och mafiska bergarter från subduktionsmiljöer. Dock kan en utomjordisk härkomst inte uteslutas. Ett av OC-kornen har en sammansättning som stämmer bra överens med kromspinell från den fossila winonait-lika meteoriten och samtidigt avviker från terrestrisk och kondritisk kromit. OC-kornets sammansättning sammanfaller inom oxidernas respektive intervall för den fossila meteoriten utom FeO-halten som är något lägre. Cr/(Cr+Al) och $Fe^{2+}/(Mg+Fe^{2+})$ stämmer också bra överens med meteoriten. Ett andra OC-korn är liknande med avseende på Cr# och Fe# men skiljer sig i fler än en oxid. En eller två winonait-lika korn bland 500 EC korn, baserat på fynden av 1-20 cm stora fossila meteoriter i Kinnekulle, stödjer hypotesen att winonait-lika meteoriter representerar i storleksordningen en procent av inflödet av meteoriter till jorden under mellanordovicium.

Nyckelord: kromspinell, fossila meteoriter, Komstadkalksten, winonaiter, mellanordovicium, karbonatsedimentologi

Ellinor Martin, Geologiska institutionen, Lunds Universitet, Sölvegatan 12, 223 62 Lund, Sverige.
E-post: ellinor.martin@gmail.com

1 Introduction

The carbonate rocks of the Middle Ordovician in Baltoscandia, harbor an interval with increased levels of extraterrestrial chrome spinel grains – the only common mineral in a meteorite known to survive long-term diagenesis and weathering on Earth (Thorslund et al. 1984). The increase of chrome spinel in these layers has been linked to the break-up of the L-chondrite parent body in the main asteroid belt at ~470 Ma. Together with abundant sediment-dispersed chromite grains (ca. 63-300 μm large) more than a hundred L-chondritic fossil meteorites have been discovered in a quarry in SW Sweden (Schmitz 2013) together with a single, more unusual, winonaite-like fossil meteorite (Schmitz et al. 2014). The meteorites fell into a broad shallow sea in a time when life, in geological terms, suddenly took a turn and diversity was booming, the so called Great Ordovician Biodiversification Event (GOBE). There have been attempts to link the increased influx of cosmic material with the sudden increase in biodiversity on Earth (Schmitz et al. 2008). The bombardment of meteorites and asteroids has has been a common feature through the history of the Earth and the solar system. Impact craters of different ages are known worldwide, and, so far four craters, Lockne, Granby, Kärdla and Tvären are known from the Ordovician Period in Baltoscandia (Puura & Suuroja 1992; Lindstrom et al. 1994; Alwmark 2009). Several studies on coeval strata in Sweden, Russia and China have been published where the sediment-dispersed chromite grains have been quantified and their extraterrestrial provenance deduced (Schmitz et al. 2001; Schmitz & Häggström 2006; Heck et al. 2008; Cronholm & Schmitz 2010; Lindskog et al. 2012).

In the carbonate rocks there are also other chrome-rich spinels present whose origin have not yet been determined. The finding of a single winonaite-like fossil meteorite, has led to the conclusion that the meteorite is a possible fragment from the impactor that disrupted the L-chondritic parent body. Following this new meteorite find, sediment dispersed chromite grains from the mysterious impactor could theoretically be found amongst the myriad of L-chondritic chromite grains. There is also a small chance that sediment-dispersed chrome-spinel grains from the Moon could have accumulated in the sediments following the increased bombardment of the Earth-Moon system during this time in the Middle Ordovician.

Previous studies have located a bed in the mid-Ordovician Komstad Limestone Formation in the Killeröd quarry, southeastern Scania, that is extremely rich in extraterrestrial chromite (EC) grains, with up to 5 grains >63 μm per kilogram rock (Häggström and Schmitz 2007). The bed is unusual also because it contains only few chrome spinel grains that do not have ordinary chondritic composition. The bed contains significantly fewer terrestrial chrome spinel grains than the stratigraphic levels below and above. In intervals with many terrestrial chrome spinels the search for extraterrestrial grains from other types of meteorites than ordinary chondrites becomes more difficult, if not near impossible. This makes this bed at Killeröd particularly favorable for extraction of chrome spinel grains from more rare types of meteorites. The mysterious relict winonaite-like meteorite recently found could very well be one of many similar meteorites and micrometeorites in the Middle Ordovician. This is the first attempt to search for winonaite-like grains among sediment-dispersed chromite grains. In the bed of concern here, one would expect to also find a small fraction of lunar chrome spinel grains from ejecta related to impacts on the Moon (Artemieva and Shuvalov, 2008).

The study also aims at characterizing in greater detail the ordinary chondritic grains in the bed and compare with results from other localities, such as the Lynna River section in western Russia (Lindskog et al. 2012). The Killeröd section represent an unusual setting compared to other coeval EC-rich beds in having formed under reducing conditions. By comparing the composition of EC grains from different environments better insights can be gained into the diagenetic processes that may alter the composition of EC grains. A further objective has been to better characterize the sedimentary environment using petrological studies of the bed in thin sections. This may add understanding how hydrodynamic processes on the sea floor affected the extraterrestrial heavy mineral assemblages in the bed.

2 Background

2.1 Meteorites and meteorite classification

A meteorite is an impact-derived fragment larger than 1 mm (Gounelle 2011), originating from one of approximately 85 parent bodies (Keil et al. 1994), including asteroids, comets, Mars, and the Moon. Micrometeorites represent the dust fraction and are less than 1 mm in diameter (Gounelle 2011). It is believed that most impactors on Earth originate from the inner parts of the Main Asteroid Belt between Mars and Jupiter (Fig. 1). Meteorites are crudely divided into chondrites, achondrites and primitive achondrites (Weisberg et al. 2006). Chondrites are meteorites that have 'solar-like' composition and typically, but not always, contain small spherules called chondrules (Fig. 2). Chondrites derive from parent bodies that have not differentiated. Achondrites are meteorites that originate from differentiated parent bodies. Primitive achondrites are more closely related to chondrites and preserve a primitive chemical affinity but have achondritic textures. There are three major chondrite classes: carbonaceous, ordinary, and enstatite chondrites. The ordinary chondrites are the dominant class representing 80% of the meteorite falls today hence their name,

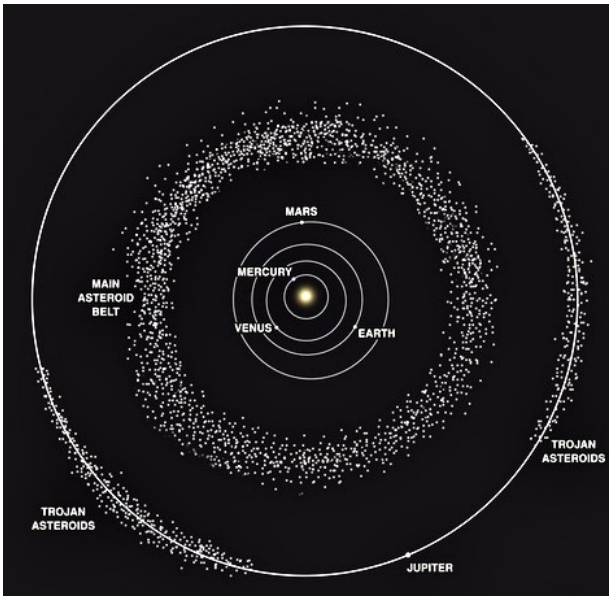

Fig. 1. Schematic image of the solar system with the main asteroid belt that lies between Mars and Jupiter. Most meteorites that reach the inner parts of the solar system and Earth, stem from the main belt or the Trojan asteroid clusters in Jupiter's orbit. Modified from NASA (2014) .

7.9% are achondrites, 4.8% iron meteorites, and 4.6% carbonaceous and anomalous chondrites (Bevan et al. 1998). In the micrometeorite fraction, however, the carbonaceous chondrites dominate (e.g. Engrand & Maurette 1998). Class is further divided into two or more groups that share oxygen isotopic and primary whole-rock chemical properties. Meteorites within one group commonly indicate that they originate from the same parent body, and group is thus the most important unit in meteorite taxonomy (Weisberg et al. 2006). The ordinary chondrites have three groups: H, L, and LL, reflecting their iron content and the ratio of metallic Fe to oxidized Fe (H, 0.58; L, 0.29; LL, 0.11). All chondrites, even though not differentiated, display some degree of metamorphism. Ordinary chondrites

Fig. 2. Photograph of the polished L3 chondritic meteorite NWA 5411, containing small chondrules. Found in Sahara desert, Northwest Africa in 2008. Scale bar = 5 mm. Edited photograph, original image courtesy of F. Terfelt and B. Schmitz.

are further divided into subgroups, i.e. L3-L6, where the higher number indicate higher metamorphic grade (Bunch et al. 1967). Winonaites are a meteorite group belonging to the primitive achondrites. Winonaites (together with e.g., lodranites and acapulcoites) show clear signs of being residues of partial melts. Winonaite meteorites have a fine to medium grained texture, contain olivine, Ca-pyroxene, traces of low Ca-pyroxene, plagioclase, minor amounts of metal, and contain other minerals like troilite, daubreelite, schreibersite, graphite and chromite (Weisberg et al. 2006; Schmitz et al. 2014). The chromite amount is generally less per gram in winonaites compared to equilibrated L-chondrites (Bjärnborg & Schmitz 2013). The chromite grains in winonaites are often

2.2 Lunar meteorites

The outer layer of the Moon is composed of loose sediments, derived from the many impacts during its existence the last 4 Ga. This layer, the lunar regolith, has a thickness of a meter up to a kilometer (Joy & Arai 2013). The regolith changes in composition with each new impact. It is from this regolith that lunar meteorites spawn.

When many large projectiles bombard Earth there will also be many impacts on the Moon (Artemieva & Shuvalov 2008). During the meteorite shower in the Middle Ordovician, high-velocity ejecta from the Moon could have been transported to Earth and accumulated in the ancient marine sediments. Lunar meteorites are found in cold and hot deserts, such as Antarctica and Oman amongst others, but no lunar meteorite fall has been witnessed as of yet (Joy & Arai 2013). Almost 200 individual meteorites have been found, where grouping of rocks with similar chemical composition, isotopic ratios and mineralogy, give up to about 50-85 separate impact events on the Moon during the last 20 million years.

Remote-sensing has shown that remarkably high volumes of spinels are present at the lunar surface (Pieters et al. 2011). Oxides are the second most common mineral on the moon after silicates, where spinels can constitute up to ten volume percent of Mare basalts (Papike et al. 1998). Chrome spinel grains from the Moon could prove difficult to distinguish from terrestrial chrome spinels because they have identical oxygen isotopic ratios (Clayton et al. 1976; Clayton 2003). There are differences, however, in the mineral compositions due to the lack of water and the low oxygen fugacity on the Moon compared to Earth (Papike et al. 1991). This could provide the opportunity to search among the extracted OC grains for lunar-derived chrome spinel.

2.3 Fossil meteorites and dispersed extraterrestrial chromite grains

In the Middle and Late Ordovician the flux of extraterrestrial material was increased by up to two orders of magnitude (Schmitz et al. 2001), estimates based on fossil meteorite finds. This can be compared to the flux today that based on osmium isotopes from marine sediments is estimated to 30 000 ± 15 000 tons per year (Peucker-Ehrenbrink & Ravizza 2000).

Since 1993 a total of 102 fossil meteorites have been found in the Thorsberg quarry, Kinnekulle, Southern Sweden (Fig. 3). Of these, 101 have been classified as L chondrites of petrologic type 3 to 6 (Schmitz et al. 2001; Bridges et al. 2007; Alwmark & Schmitz 2009). The fossil meteorites are most likely related to the ca. 30 % of recent meteorites, all L chondrites, which have K-Ar retention ages around 500 Ma (Keil et al. 1994). Recent argon isotope data suggest these meteorites originate from a break-up event at 470 ± 6 Ma (Korochantseva et al. 2007) that was first thought to have created the Flora asteroid family (Nesvorny et al. 2007). Later works suggests the Gefion asteroid family is a more likely candidate based on composition and position in the main belt (Vernazza et al. 2008; Nesvorny et al. 2009). These ages found in many recent meteorites infers that, still today, fragments from the breakup event of the L-chondrite parent body are ejected from their orbits in the asteroid belt on a trajectory towards Earth. The section with the fossil meteorite finds at Kinnekulle also displays elevated iridium concentrations indicating 2 to 3 times higher iridium influx than today (Schmitz et al. 1996). The meteorites are often found on hardgrounds together with other large objects such as cephalopods, which would indicate that they have accumulated partly through sediment winnowing by currents, similar to the accumulation of recent meteorites in deserts (Schmitz et al. 2001). One meteorite found recently is different from the others, however, and bears closer resemblance to the meteorite group winonaites. The identification of the fossil winonaite meteorite is based on chemical composition and oxygen isotope ratios from extracted chromite grains (Schmitz et al. 2014). Schmitz et al. (2014) speculates that it could be a fragment of the body that collided with the L-chondrite parent body ~470 Ma ago as this is the only type of fossil meteorite found besides L chondrites. The fossil meteorites fell during a time interval of ca. 2 Ma in the Mid-Ordovician. On Earth the meteorites weather relatively quickly and the original mineral assemblages are replaced by secondary minerals. The minerals of the Ordovician fossil meteorites have mainly been replaced by calcite (Thorslund et al. 1984).

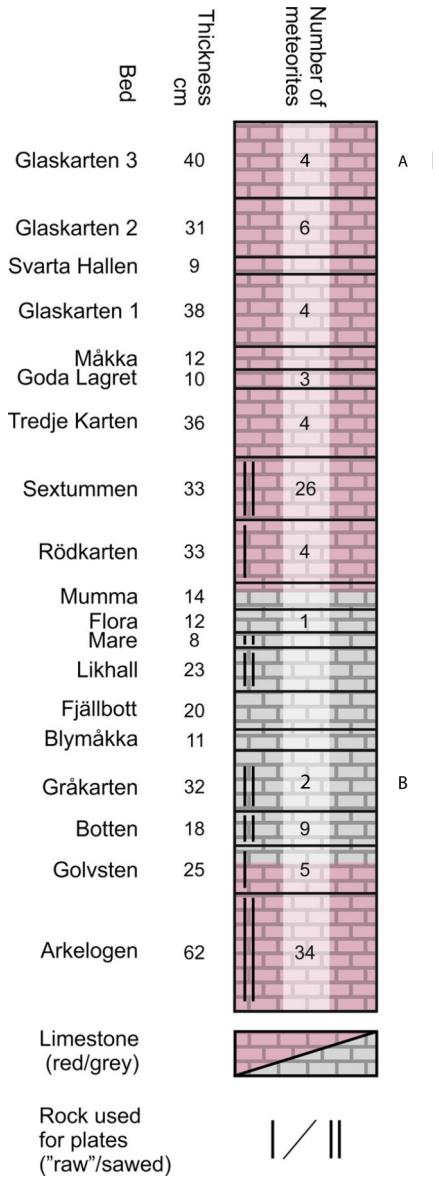

Fig. 3. The distribution of the fossil meteorites found so far in Kinnekulle. **A:** The stratigraphical level of the fossil winonaite-like meteorite. **B:** The level where the fossil meteorite Grå 002 included in this study was found. Modified from Schmitz et al. (2014).

Sediment-dispersed extraterrestrial chromite grains have been found in coeval Middle Ordovician strata in Sweden, Russia and China. At Kinnekulle, Sweden, the Arkeologen bed is the level where the amount of EC grains >63 µm suddenly increase with up to two orders of magnitude (Schmitz et al. 1996; Schmitz et al. 2001). The richest bed in this time interval was found at Lynna River, Russia, with ~10 grains per kilogram of rock in the lowermost part of the *Asaphus raniceps* trilobite Zone (Lindskog et al. 2012). The sediment-dispersed chromite grains are interpreted to originate mainly from micrometeorites (less than 1

mm in diameter) based on their content of the noble gases ^{3}He and ^{21}Ne induced by solar wind, whose ions only penetrate a few tens of nanometers beneath the surface (Heck et al. 2008). In another study by Meier et al. (2010) thirty percent of the sediment-dispersed EC grains had very high cosmic-ray exposure ages (several 10 Ma), higher than would be expected for micrometeorites travelling to Earth from the asteroid belt considering the limitation of <1 Ma travel times by the Poynting-Robertson drag. These grains were hypothesized to have gained their extra ^{21}Ne from high -energy cosmic rays when they were situated in the regolith breccia of the parent body. Numerous extra-terrestrial chromite grains were extracted by Alwmark & Schmitz (2007) from resurge deposits of the Ordovician Lockne crater of central Sweden. The crater measures 10 kilometres across. More than 75 EC grains per kilogram of rock was found, which is the most EC-enriched layer found so far. These grains probably represent fragments of the impactor that formed the Lockne crater.

3 Geological setting, locality and regional geology

3.1 Baltoscandia during the Ordovician period

During the Cambrian and Ordovician period the terrane of Baltica was situated in the Southern hemisphere and drifted from higher to lower latitudes (Fig. 4). The Scandinavian Caledonides started to deform already in the late Cambrian and Early Ordovician in the collision between Laurentia and Baltica, later climaxing in the Scandian orogeny in the Silurian (Cocks & Torsvik 2005). As the continent drifted through different palaeolatitudes in the Ordovician the climate also changed and the shelf environment shifted from a cold-water siliciclastic ramp to warm-water tropical carbonates (Dronov & Rozhnov 2007).

A large part of Baltoscandia was covered by an epicontinental sea during the Ordovician (Lindström 1963). The sea was bordered by the Caledonian geosyncline in the northwest and joined with the sea of the Moscow Basin in the east. Ordovician strata thin out substantially in the southeast in the Belorussian area that according to Jaanusson (1973) was land during most of the period. Coarse fractions of the sediment supply have formed rocks like conglomerate, greywacke and sandstone in the northwest that reflect a near-shore depositional environment. Peniplanization was in an advanced state especially in the north and

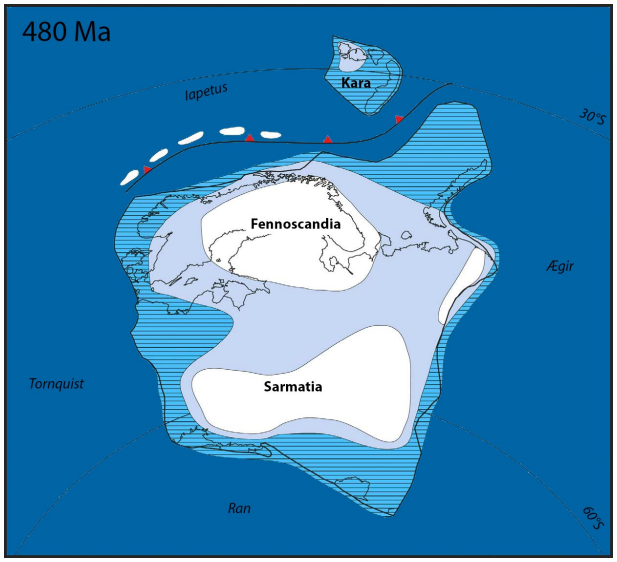

Fig. 4. Map showing the position of Baltica in relation to the paleo-equator in the Middle Ordovician. White areas: land, light grey: shallow shelf, light blue: deep shelf, and dark blue: ocean. Modified from Cocks and Torsvik (2005).

east of the East Baltic area, terrigenous material would thus have been in short supply. The sea-floor is believed to have been extraordinarily flat with a gentle slope (and with low-energy). As sedimentation kept pace with the subsidence, carbonate sediments were rarely deposited below the photic zone. The inferred depth for the deposition of Ordovician limestone in Baltoscandia varies with author and locality. The sea has been considered to be fairly deep in an outer shelf environment with depths of 130-300 m, based on for example the collapse of cephalopod shells (Chen & Lindström 1991). This has however been debated since there is evidence of sub-aerial conditions with desiccation cracks in the Öland region (Nordlund 1989) and formation of microbialites in the photic zone (depths of tens of meters) in other regions (Lindskog 2014). A difference in interpreted depth would naturally occur depending on where in the basin the study takes place, as is also evident from the difference in thickness and preservation for one and the same interval in different areas.

With subsidence in mind, the net deposition rate during the Ordovician is estimated to 2.5 mm per 1000 years. However, the deposition during the ~60 million year period fluctuated between hundreds of mm per year, with growth of stromatolitic algal mats, to zero (Jaanusson 1973).

3.2 Regional geology of Scania

The Scanian region is underlain by the Proterozoic Baltic shield of crystalline rocks in the north and Palaeozoic sedimentary rocks laying on top of the Baltic

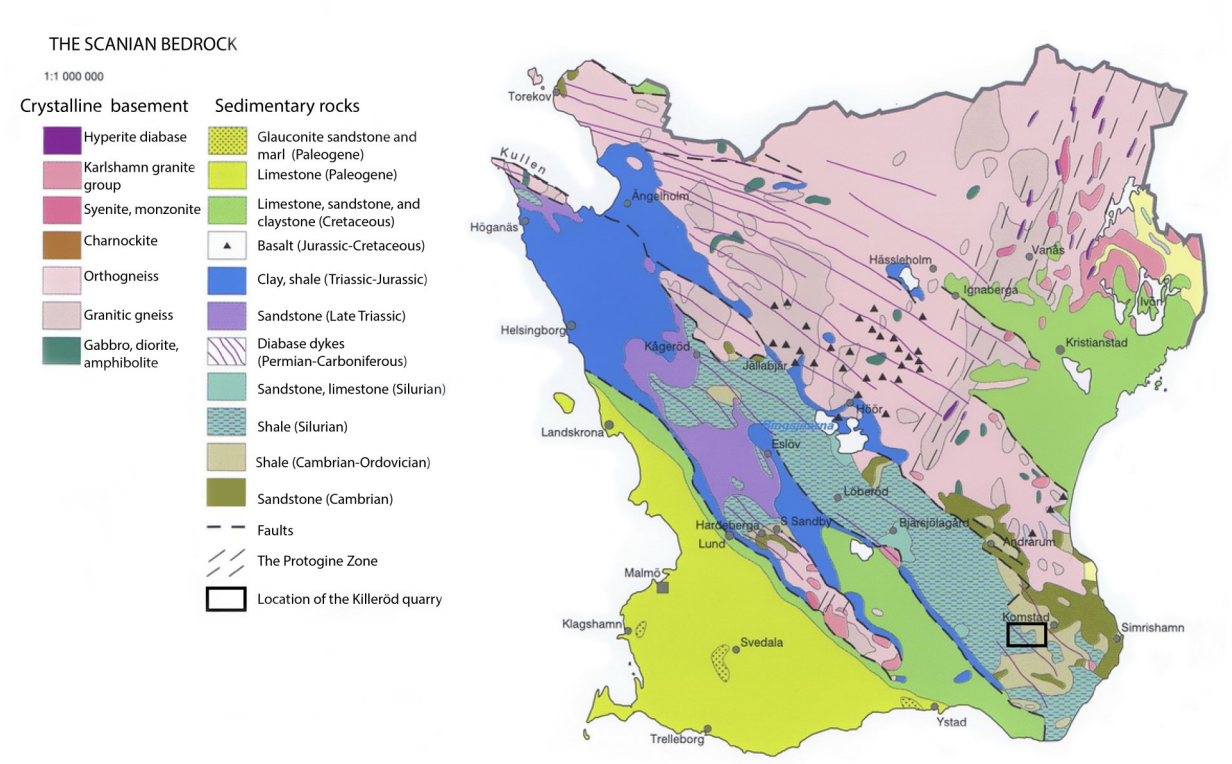

Fig. 5. Geological map of the Scanian bedrock, composed of igneous and sedimentary rocks. Location of the study area at Killeröd is marked. Modified from Erlström et al. (1999).

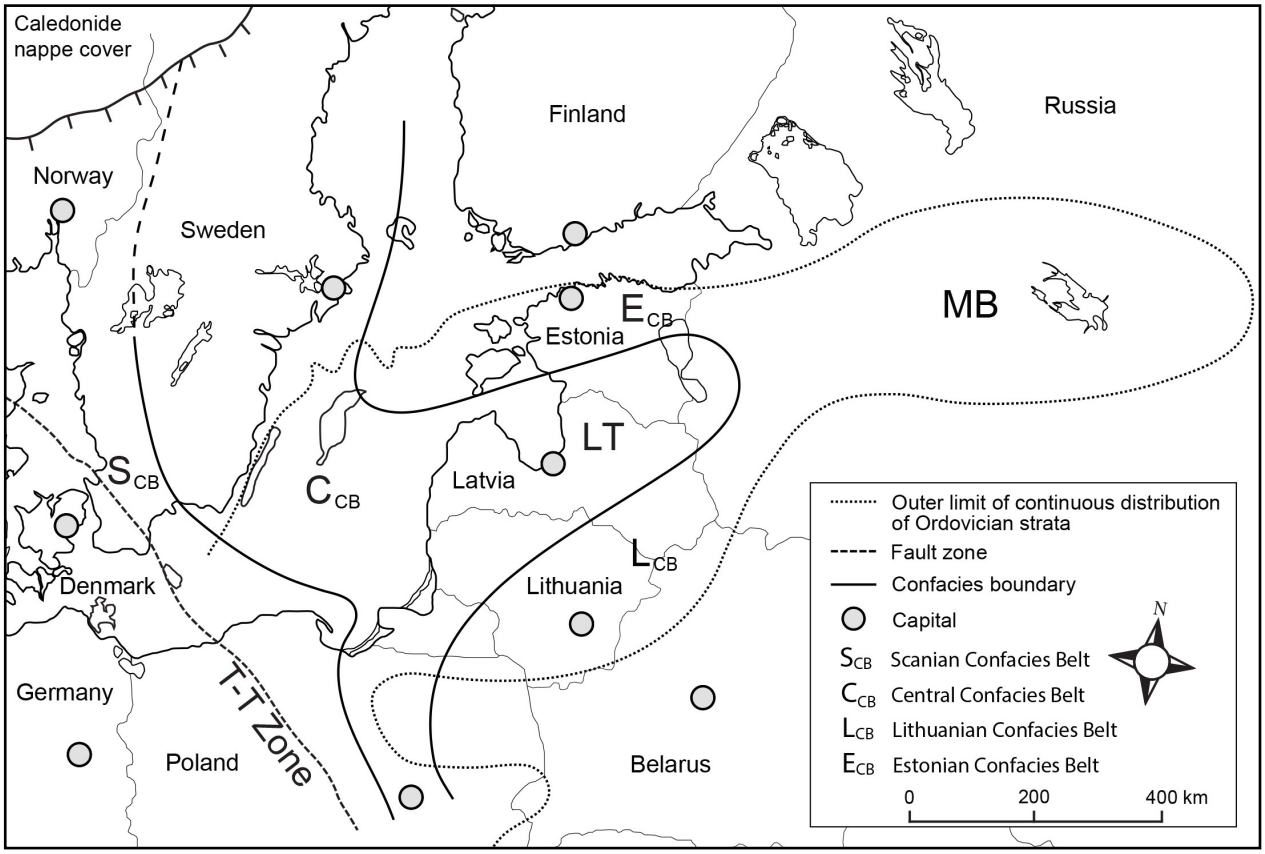

Fig. 6. Map showing the lateral extension of the Baltoscandian Confacies Belts. Modified from Eriksson et al. (2012).

shield in the south (Fig. 5). Scania and the different rock types are divided diagonally on a SE to NW trend by the tectonically active Tornquist Zone (Bergerat et al. 2007). The zone was formed in a collision between Baltica and the micro-continents Eastern Avalonia and the European massif during Late Ordovician times (Torsvik et al. 1992). This zone has seen compression, extension and shear during the last 450 million years with horst-graben systems as a result with intermittent diabase dykes along the zone (Bergerat et al. 2007). The Ordovician beds reside in the so-called Scanian Confacies Belt (Fig. 6).

3.2.1 The Komstad Limestone Formation

The section comprises a dark, organic-rich limestone deposited in the Middle Ordovician period, during the Volkhov and Kunda Baltoscandian stages. The limestone is sitting on top of, and overlain by Ordovician shale. In field the layers alternate between condensed fairly homogenous and well-cemented almost shaly layers, by more light colored marly limestone intercepted by thin weathered clay-rich bands (see Fig. 8). The layers have an average strike and dip of 141.8° S/5.3°. The Komstad Limestone is very similar in lithology to the 'orthoceratite limestone' that was the dominating sediment in the Baltoscandia during the Ordovician period (Nielsen 1995). The Komstad Limestone would for that similarity, rather be part of the distal parts of the Central Confacies Belt. For the deposition of the Komstad Limestone a depth of less than 100 m is inferred by Nielsen (1995). Based on the relatively uniform thicknesses of the trilobite zones in Killeröd and Kinnekulle the net rate of deposition was

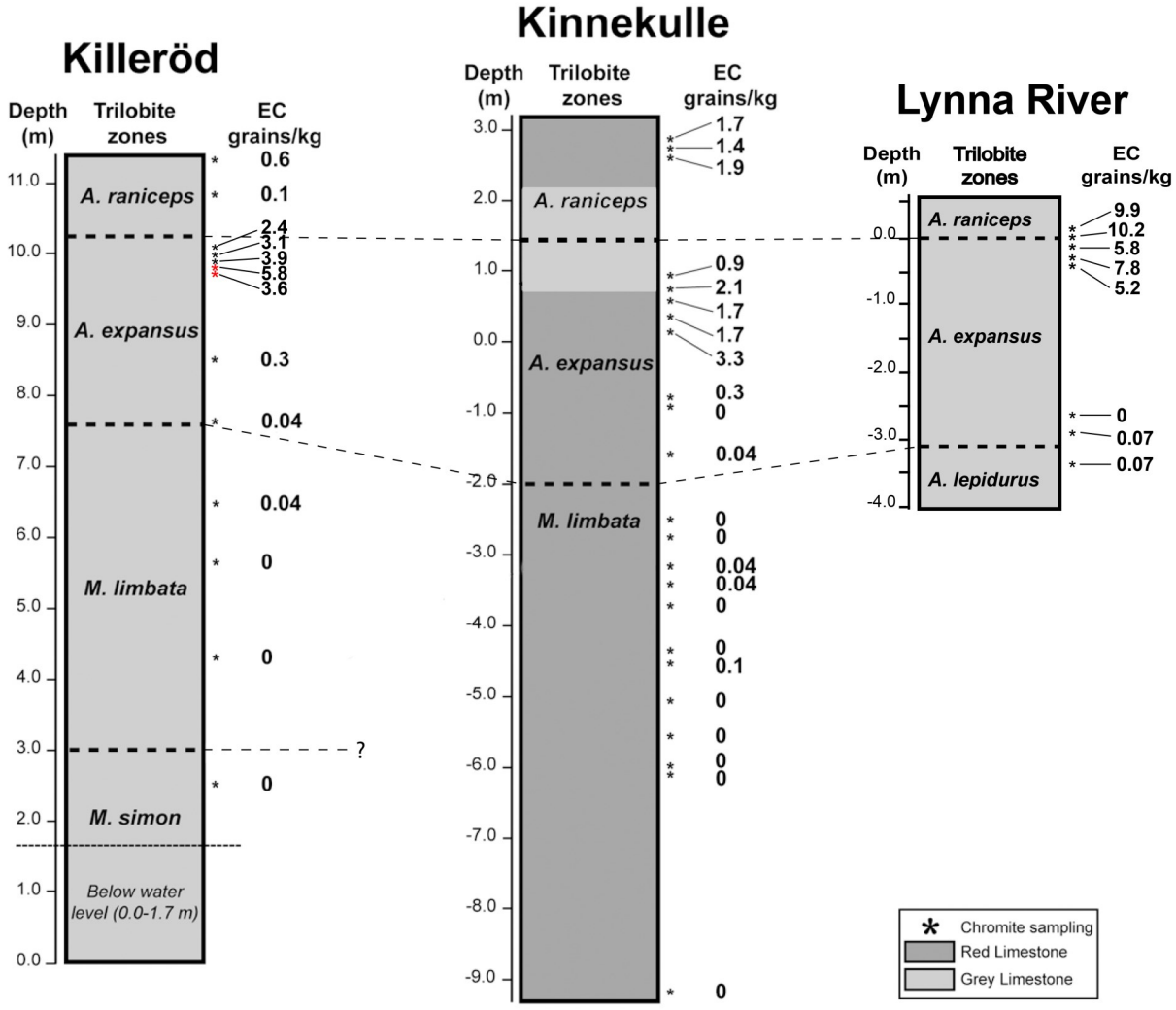

Fig. 7. Logs from Killeröd, Kinnekulle and Lynna River sections. Five intervals around 10 m in the Killeröd log were corrected as the bottom two levels were missing in the original figure and one level had incorrect grains/kg. The interval sampled in this study is marked with red asterisks. Modified from Häggström & Schmitz (2007).

probably analogous, with a few millimeters per thousand years. The layer rich in sediment-dispersed EC grains in Killeröd also correlates with the EC-rich layers in Hällekis, Sweden, and at the Lynna River section in Russia, where the layers in the latter are situated in the uppermost part of the *Asaphus expansus* Zone and a bit into the basal part of the *Asaphus raniceps* Zone (Fig. 7).

3.2.2 The Killeröd locality

The location of this study is set in south-east Scania, Sweden, 13 km west of the town Simrishamn (marked area in Fig. 5). The Komstad limestone outcrops in the Killeröd main quarry. The sampling area for this study is denoted Killeröd 'site b' by Nielsen (1995) with coordinates 55° 34' 20.95" N and 14° 7' 54.72" E, a smaller quarry a few tens of meters from the main quarry. The thickness of the Komstad Limestone in the Killeröd area is estimated to a minimum of 15 m (Nielsen 1995). In this study, at the smaller quarry 'Killeröd site b' the thickness was estimated to ca. 4 m, measured from the small hill down to the water level (Fig. 8). The studied section is in the lower Kundan stage and comprises the trilobite zones *A. expansus* and the basal part of *A. raniceps*. A diabase dyke cuts through the river channel between the main quarry and the smaller quarry.

4 Materials and methods

4.1 Samples and processing

A large sample of 102.4 kilograms of the Komstad limestone was extracted from the Killeröd quarry. The sample was taken from within level +35 in Nielsen (1995) in the uppermost *A. expansus* Zone, and around level 9.71-9.79 m in Häggström & Schmitz (2004). In 21.1 kg of the sampled level these authors found 5.45 EC grains and 0.19 OC grains per kilograms of rock (see Fig. 7 where the interval is marked). The chosen interval in this study has a small lateral variation in thickness but measures around 12 cm. A pilot sample of one kilogram was also extracted for making sure the right interval was chosen.

In the laboratory the sample was weighed, larger rock pieces were washed with a high-pressure washer and smaller rock pieces were hand-washed in warm water and scrubbed with a nail brush and detergent to remove dirt, mosses and loose sediments. When thoroughly cleaned the rocks were put in a 400 liter plastic barrel, and 6 M hydrochloric acid was added to decalcify the rocks in room temperature.

When the samples were completely dissolved the excess hydrogen chloride was decanted and water refilled until neutralized. The residual material, consisting of clay and sand fractions, was poured into 5 liter plastic beakers and sieved in a 32 µm sieve to remove the clay fractions. Material above 355 µm was sieved off and stored. The 32-355 µm fraction was put in 11 M hydrofluoric acid in room temperature and the material was kept in the acid for two days with stirring several times a day. After neutralization the material left was fractionated into 32-63 µm and 63-355 µm. Only the 63-355 µm fraction was studied further. Under a stereo optical light microscope the opaque grains

Fig. 8. Photographs of the smaller Killeröd quarry, 'site b'. The studied interval is marked with an arrow in the top picture, and a closeup of the interval with sub-intervals marked in the photograph below.

were picked with a fine brush and mounted onto carbon tape for chemical analysis in an Oxford Instruments INCA X-Sight energy-dispersive spectrometer (EDS), attached to a Hitachi S-3400N scanning electron microscope (SEM). The mounted grains were first quickly scanned for chromium content. Each chromium-rich grain was further analyzed semi-quantitatively in 1-2 points in 30 seconds counting live-time to preliminarily determine which ones were EC grains and which ones were other chrome spinel grains. All grains were photo-captured and images were put in Excel documents together with the chemical data.

The grains were measured on the long axis and short axis. Grain shape and general appearance was also noted. The grains were molded in epoxy, polished with diamond paste and carbon coated for further analysis in SEM-EDS with 80 seconds counting live-time in 3 points. Only analyses with a total oxide sum deviating with a maximum of 2 % from 100 % were accepted. Residual minerals other than chrome spinels that did not dissolve in acid treatment were also analyzed with SEM and EDS.

The studied interval is in closer examination separated into four subintervals corresponding to the superficial bedding. The four samples were cut perpendicular to bedding and manufactured into thin-sections that were studied under a petrographic microscope. The exposed succession was measured from top to bottom, which was the easiest since the rock crops out in natural terraces. From bottom of the interval the samples were denoted KIL14-EC4 (2 cm thick), KIL14-EC3 (3 cm), KIL14-EC2 (3.5 cm), and KIL14-EC1 (4 cm). Sedimentological characteristics and microfacies of the subsections was determined. The microfacies was characterized based on Dunham (1962). One kilogram of each subinterval was also extracted and treated with the same procedure as the main large sample to identify any difference in chromite content.

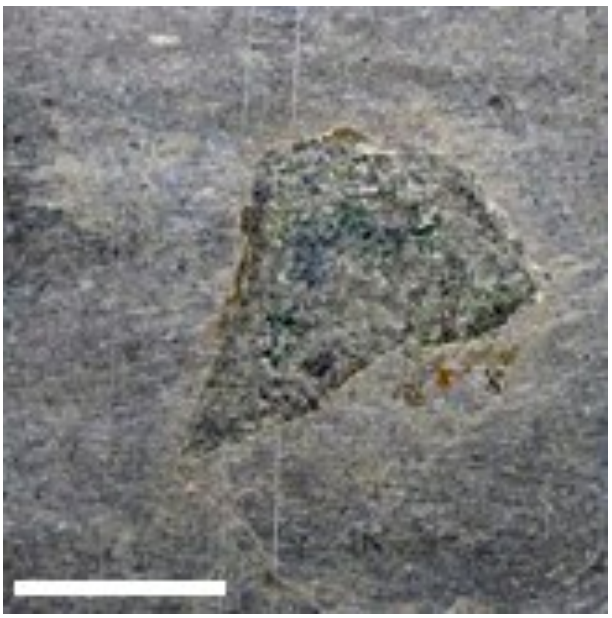

Fig. 9. Photograph of the fossil meteorite Grå 002 residing in a rock slab, discovered in the Gråkarten bed at Kinnekulle (see Fig 3). Scale bar = 20 mm. Courtesty of B. Schmitz.

From the newly found fossil meteorite Grå 002 a mass of 0.17 g was separated and dissolved in hydrochloric acid. The meteorite was found in the Gråkarten interval at the Thorsberg quarry, Kinnekulle. The meteorite measures 3.0 × 4.0 cm in cross section in a limestone plate (11 × 15 × 2.5 cm) (Fig. 9). The acid-resistant residue of Grå 002 was scanned under the light microscope and chromite grains were picked and molded in epoxy, polished and carbon coated. Since all chromite grains recovered are extraterrestrial only

4.2 Characteristics of extraterrestrial chromite grains

Chromite ($FeCr_2O_4$) is an iron chromium oxide belonging to the mineral group spinel of the isometric crystal system. The color is jet black to black brown with a glassy shine beneath a light microscope. Cr^{3+}, Al^{3+} and Ti^{4+} occupy the octahedral positions in the crystal, whereas the smaller ion Fe^{2+} can occupy both the octahedral and the tetrahedral positions (Papike et al. 1991). Fe^{2+} and Mg^{2+} are diadochic, i.e. they have similar ionic radii and have the same charge, and can thus readily substitute one another in the octahedral positions (Nesse 2000). Chromite is a refractory mineral, formed at high temperatures and is very resistant to weathering and diagenesis. However, some of the compounds in chromite are susceptible to alteration, e.g. MnO, FeO and ZnO and their percentage will thus vary in contrast to Cr_2O_3, Al_2O_3, and TiO_2 that are more stable (Wlotzka 2005) The chemical compositional characteristics for extraterrestrial chromite used in this study is according to the ranges defined by Schmitz & Häggström (2006) together with a revised TiO_2 range by (Cronholm & Schmitz 2010): MgO ~1.5-4.0 wt%, Al_2O_3 ~5.0-8.0 wt%, TiO_2 ~1.4-3.5 wt%, V_2O_3 ~0.6-0.9 wt%, Cr_2O_3 ~55-60 wt%, and FeO ~25-30 wt%. The relatively high concentrations of TiO_2 and V_2O_3 are considered diagnostic for EC grains (Bunch et al. 1967). Grains with oxide weight percentage falling outside of their respective ranges were put in an EC sub-category or in a separate category as OC: 'other chromium-rich spinel'.

4.3 Characteristics of terrestrial chrome spinel grains

Spinels crystallize from mafic and ultramafic magmas over a wide range of conditions, where chromite is among the first phases to do so (Barnes & Roeder 2001). Spinels are found in a large part of terrestrial mafic and ultramafic rocks. Spinels also display an extensive range of solid solution. The chromium content can vary from less than 30 wt% to more than 60 wt% (Stevens 1944).

Extracted OC grains were compared to a multitude of analyses from the literature, and performed on terrestrial chrome spinel grains from a variety of magmatic regimes. As the EDS in this study does not distinguish between the two oxidation states of iron, the total iron is displayed as FeO. Total iron (FeOT) was added to chrome spinel data from other studies using equation ($Fe_2O_3 \times 0.8998$) + FeO = FeOT (Winter 2010).

The oxide weight percentage of OC grains were calculated in INCA for both V_2O_3 and V_2O_5. The latter was done to be able to compare with terrestrial grains as V_2O_5 is more commonly used in those studies. All ratios are in mole fractions, and to be able to handle the large amount of data from the studies of terrestrial spinel the ratios were calculated using an Excel spread sheet from Barnes & Roeder (2001). As noted by Barnes & Roeder (2001), minor elements like V in particular, and Mn and Zn are not detected or measured in many of the terrestrial spinel studies. Emphasis is therefore mainly put on the major elements, and molar ratios of Cr/(Cr+Al) and $Fe^{3+}/(Cr+Al+Fe^{3+})$ versus $Fe^{2+}/(Mg+Fe^{2+})$ presented in simple x-y plots. The ratios are also expressed as 'Cr#', 'Fe/3+' , and 'Fe#', respectively. The mean compositions of chromite from ordinary chondrites (H, L, and LL) from Wlotska (2005) were added to the plots as a reference.

5 Results

5.1 Sedimentologic thin-section analyses

The lowermost sample, KIL14-EC4, is characterized as a wackestone/packstone (Fig. 10 A). The sample was collected on a visible bedding surface/firm-/hardground. Skeletal grain abundance increase from the middle of the thin section upward. The bed appears to have been deposited on an undulating sea-floor surface. In the top of the thin section the grains are more abundant and lying horizontally, plausibly representing the exposed sea floor. Trilobite sclerites dominate the grain assemblage. There are a few hematite-stained grains. Endolithic borings are present within some skeletal grains. Some grains have diffuse outlines.

The overlying sample, KIL14-EC3, is regarded as a packstone (Fig. 10 B). The energy level increased from the previous sample and the environment is becoming turbulent. Trilobite fragments still dominate in the sediment. More endolithic borings than in the previous thin section. The hematite coated grains increase significantly, and there are putative signs of microbial growth. Large (~2-5 mm) intraclasts with hematite coating. Diffuse outlines of grains become more abundant.

The second sample from the top, KIL14-EC2 (Fig. 10 C), is classified as a grainstone/packstone. Hematite and limonite rims increase further. A distinct oncoid of 1 × 1.5 mm is present in the bottom of the thin section. The outline of the oncoid is uneven but the preservation is fairly good. A few macroscopic (ca. 5 mm) oncoids occur. Trilobite sclerites are abundant and borings become more abundant than previous. The larger skeletal shells have borings, the smaller ones are usually spared. The sediment appears more bioturbaded than previously. A small number of fossils are etched. There is also what could be a microtektite filled with calcite along the right side of the thin section.

The top most sample KIL14-EC1 (Fig. 10 D) is within a large cephalopod, which in itself could be a micro-environment and could thus represent another environment than in the rest of the subsection. The subinterval contains many cephalopods in horizontal position that are visible in the field. The section mostly forms a wackestone with larger trilobite sclerites in the bottom part. Some limonite stained grains occur and the sample is similar in that respect to the lowest thin section KIL14-EC4. Two oncoids occur (1-2 mm in length) and are hematite stained. Some bioerosion and borings occur.

5.1.2 Residual material

The minerals left after leaching in acid (besides Cr spinel), are in descending order of abundance: titanium sulfides (milky white, translucent, tetragonal to rounded in shape), pyrite (amorphous, cone-shaped, pyramidal, cubic), zinc sulfide, titanium disulfide, cupper sulfide, and iron sulfide. Also a fair amount of amorphous coal grains is present. Some silicates have remained even after treatment in strong hydrofluoric acid, e.g. feldspar, and small round "fluffy" shells of silicon oxide. From the one-kilogram pilot sample that was only treated with HCl, many zircons were recovered, and biotite was common.

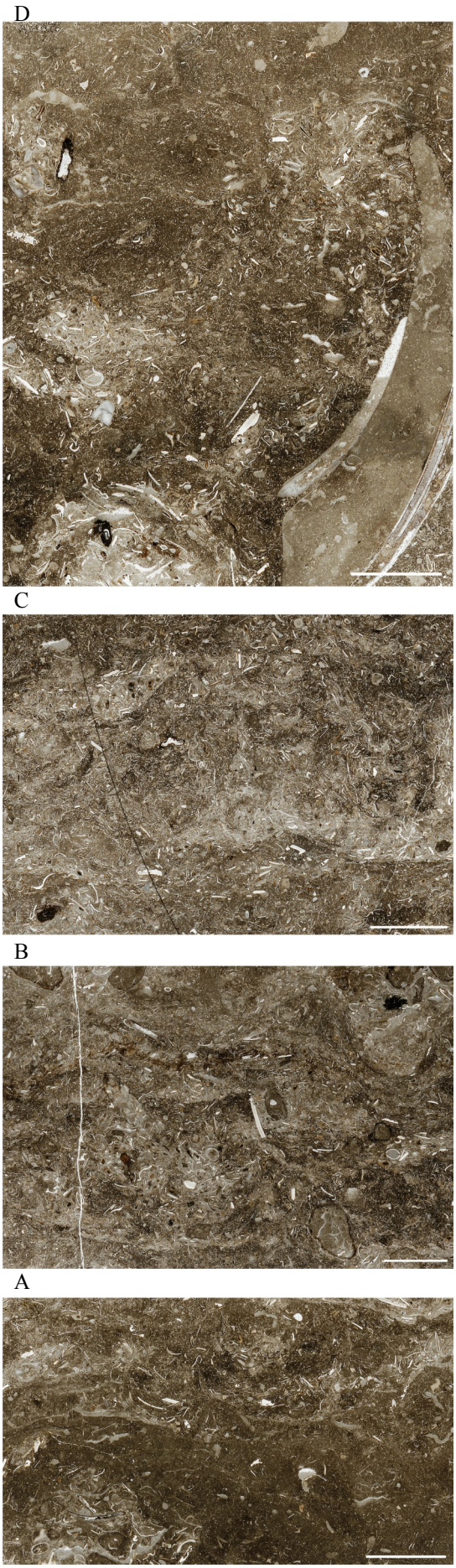

Fig. 10. Composite image of the thin sections from the sub-intervals. **A.** KIL 14-EC4. **B.** KIL14-EC3. **C.** KIL14-EC2. **D.** KIL14-EC1. Scale bars = 5 mm.

Among the four sub-intervals, of which one kg from each was dissolved, the two in the middle, EC 2 and EC 3, contained more clay than EC 1 and EC 4, which was evident when dissolving the samples. The topmost and lowermost samples reacted more vigorously with the HCl indicating a higher carbonate and lower clay content. Each sample was density-separated with LST (lithium heteropolytungstate). When scanning through the samples in a light microscope the number of chromite grains appear to be more or less the same in each of them.

5.2 EC and OC grains

In the 63-355 µm fraction a total of 527 chromium-rich grains were found. 507 were classified as EC grains with an average of 4.92 grains/kg. 17 grains fell significantly outside of the chemical definitions of EC grains and were classified as OC grains (0.17 grains/kg). From the total grain amount, 405 grains are considered to have 'true' EC composition and 43 grains have one or more elements diverging from the EC definition. Among the EC grains 23 completely lack magnesium and are enriched in zinc and were placed in an EC subcategory (see Table 1 for definitions). Six grains contain nickel. Three of those containing nickel have a composition near that of an EC grain and the other three significantly fall outside the definition and were classified as OC grains.

Of the 527 grains recovered 29 were lost during polishing, but were preliminary analyzed in SEM-EDS. Among the lost grains 26 are classified as EC grains, but not included in any of the EC subcategories in Table 1. Three of the lost grains are either EC or OC. The lost EC grains are excluded from plots and averages, except for the average number of grains per kilogram of rock. The three EC/OC grains are completely excluded since their affinity could not be determined with confidence. Among the EC grains (including EC outliers) 39 have a TiO_2 content between 1.38 and 2.21 wt%.

The overall grain shape, for both EC and OC grains, is dominated by angular grains (47%) followed by sub-angular (23%), very angular (21%), and sub-rounded (2%). In Fig. 11 some of the different unpolished morphologies of EC and OC grains are shown. No grains were rounded or very rounded. The grain size measured on the long-axis varies from 45 µm to 311 µm and the average length of the grains is 113 µm on the long-axis and 78 µm on the short-axis. A quite

Table 1. EC and OC grains from this study in Killeröd and the study from the Lynna River section (Lindskog et al. 2012) divided into separate categories and subcategories. Three grains from the russian samples were lost during processing but were included in an EC sub-category.

Sub-/Category	Definition	Number of grains	
		Komstad	Lynna
EC	**Extraterrestrial (chondritic) chromite grains with composition defined by Schmitz & Häggström (2006) and Cronholm & Schmitz (2010)**	**507**	**313**
-True EC	Composition that follow the strict definition by Schmitz & Häggström (2006) and Cronholm & Schmitz (2010)	405	239
-Outlier EC	One or more elements fall outside of the strict definition of an EC grain	43	60
-MgO-depleted EC	Fulfill the criteria for an EC grain but lack MgO.	23	0
-EC-NiO	Fulfills the definition of an EC/EC Outlier grain but also contain NiO	3	13
-EC low-TiO_2	EC grains with TiO_2 <1.4 wt%	7	1
-Lost EC grains	Grains with an EC composition lost during polishing	26	–
OC	**Significantly diverge from the definition an EC grain**	**17**	**7**
-OC		2	7
-OC-NiO	Significantly diverge from the definition of an EC grain and contain NiO	3	0
-OC-X	Significantly diverge from the definition an EC grain, but have a Cr/(Cr+Al) ratio of 0.8-1.0, indicative of a chondritic source (Roeder 1994)	12	0

large number of EC grains display fractures and have reaction rims (Fig. 12).

In a randomized test of one hundred SEM photos 81 % of the polished grains have two or more fractures and 22 % of the grains have crossing fractures in a perpendicular or slightly oblique angle towards each other and/or parallel fractures. 47 % had reaction rims on the rims of the grains or inside fractures. Reaction rims included recrystallization of the grains, which is assumed for grains that display aggregates of smaller crystals at the rim of the grain. In comparison, the same randomized test of the EC grains from Lynna

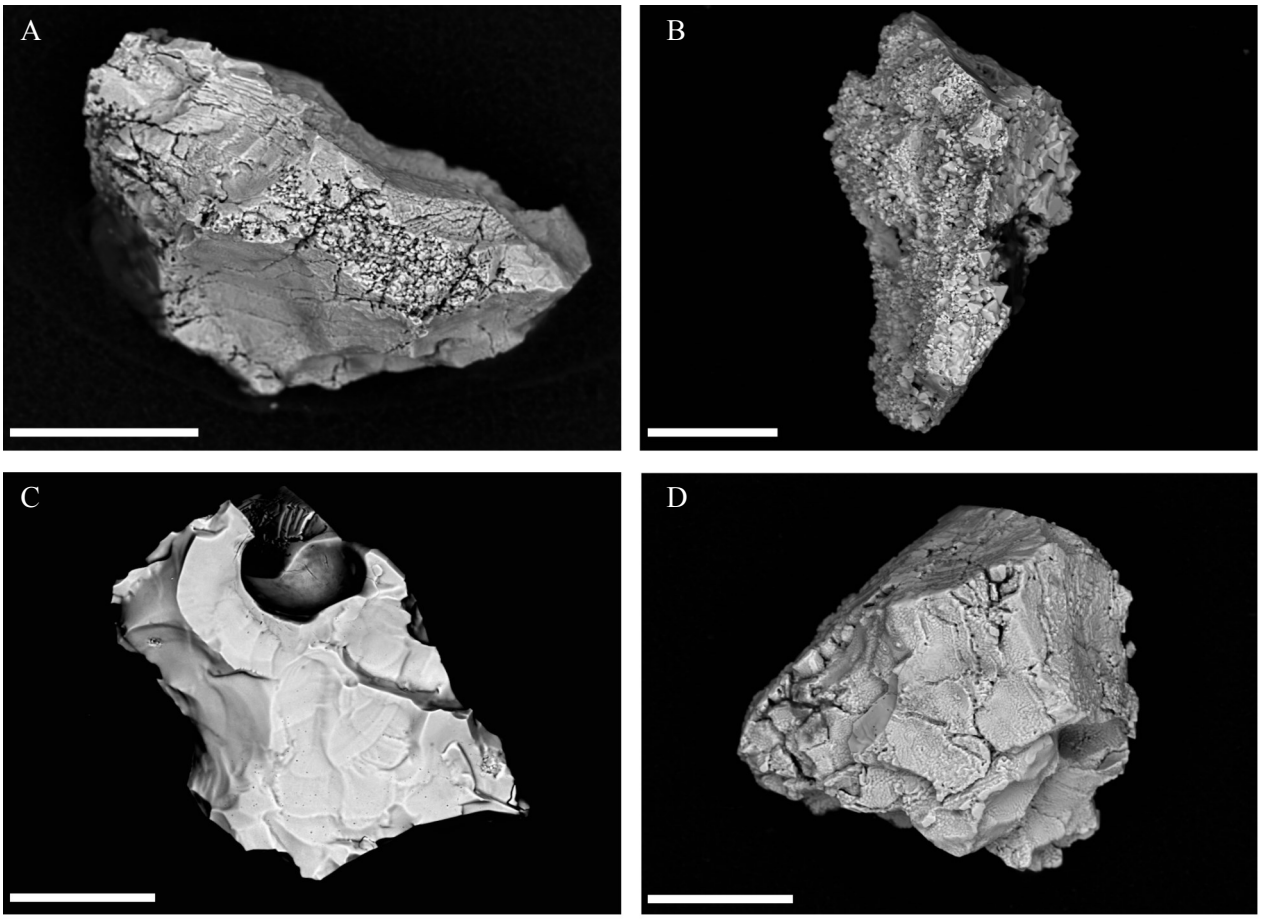

Fig. 11. SEM images of unpolished EC grains. Scale bars = 50 µm. **A.** A typical EC grain with fractured surface. **B.** An EC grain with untypical aggregate structure. **C.** A typical very angular/angular EC grain with smooth surface, and with a large cavity where an inclusion once resided. **D.** An EC grain with fractures and an etched surface.

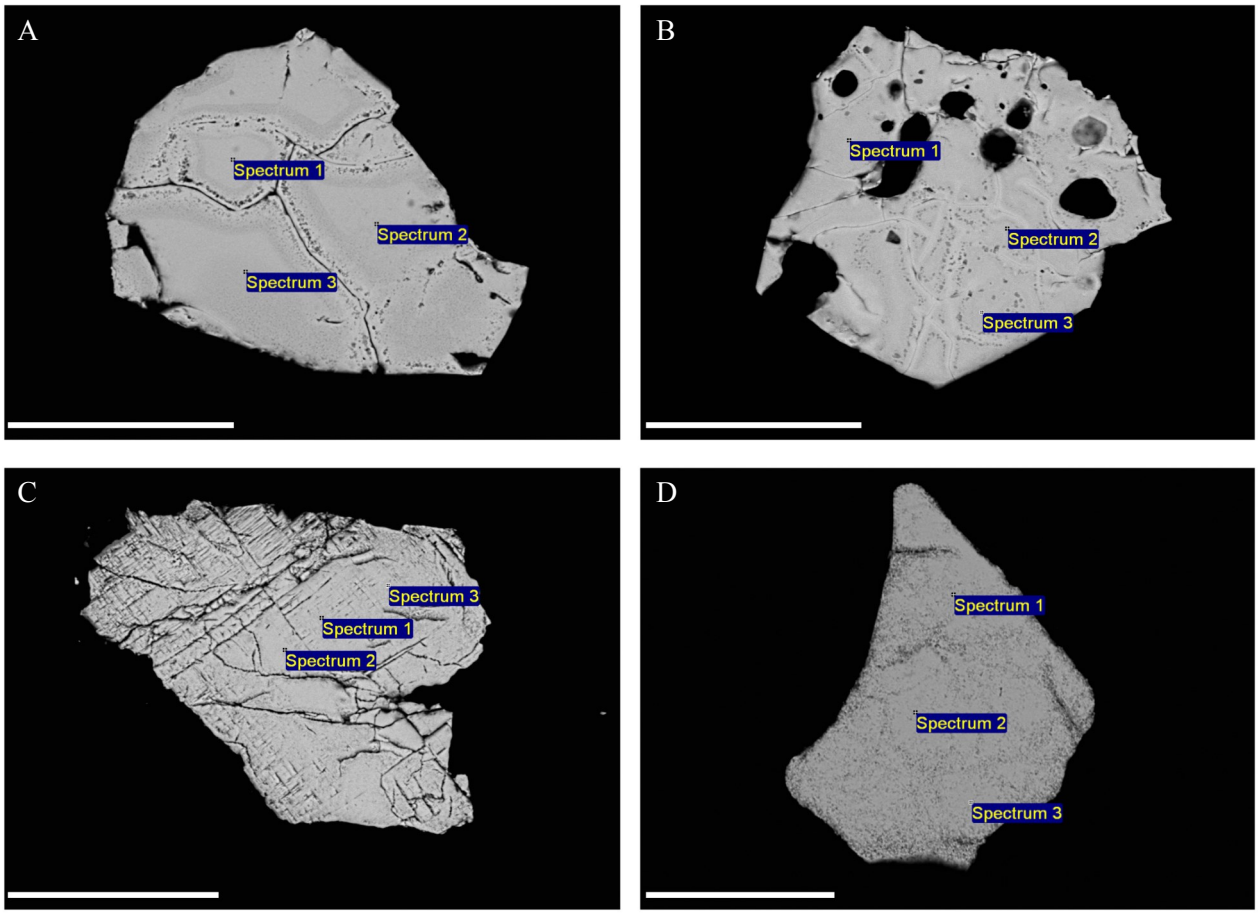

Fig. 12. SEM images of polished EC grains. Scale bars = 50 µm. **A.** A typical EC grain with fractures and reaction rims along fractures. **B.** Grain with many cavities where inclusions once resided. One inclusion is still present in the upper right corner. **C.** Grain with pronounced crossed/perpendicular fractures. **D.** One of the MgO-depleted EC grains with a common blotchy/spotted surface.

display fractures in 79% of the grains, of which 20% are crossed fractures, and 8% have reactions rims.

The composition of each individual grain from this study was plotted together with the average composition of chromite from recent ordinary chondrites (Fig. 13). In the major element plot of Al_2O_3 vs. MgO, most grains plot in a narrow band around 5 wt% Al_2O_3, with the exception of one EC grain low in TiO_2, and most of the OC grains. The MgO content varies a bit more in the EC grains, and one EC-NiO grain and the three OC-NiO grains are enriched in MgO. The two OC grains ('sensu stricto') are deviating most from the other grains in this plot. In relation to the ordinary chondrites the EC grains plot around the L-chondritic average.

In the plot with ZnO vs. FeO, the MgO-depleted grains form a tail of negative correlation towards higher ZnO content with decreasing FeO. Most of the EC grains plot around 25 to 30 wt% FeO and between 0 and 2 wt% ZnO. The 'true' EC grains generally have less FeO than all the ordinary chondritic chromite grains but are closer to the H chondrite in this plot. The grains not following the trend of increasing ZnO with decreasing FeO are the two OC grains, the OC-NiO grains and one EC-NiO grain, one EC grain low in TiO_2, and a couple of the OC-X grains.

Plotting Cr_2O_3 with MnO+FeO+ZnO the EC grains form a rather narrow band at a Cr_2O_3 content between 55 and 60 wt%. The MgO-depleted grains have Cr_2O_3 contents like that of the 'true' EC grains, but are enriched in the divalent oxides. The OC-X grains scatter around the EC grains together with some outlier EC grains, one of the low-TiO_2 grains, the OC-NiO grains, and one of the EC-NiO grains. The two OC grains are deviating from the rest with both low Cr_2O_3 content and low divalent oxide content. The EC grains also in this plot are closer to H chondritic chromites. For the minor elements, TiO_2 and V_2O_3, the EC grains have a quite wide span in TiO_2 (between 1.5 and 3.5 wt%) but cluster around 3 wt%. The V_2O_3 content has a narrower range between 0.6 and 0.9 wt% and is as densest around 0.7 wt%. The EC-NiO grains

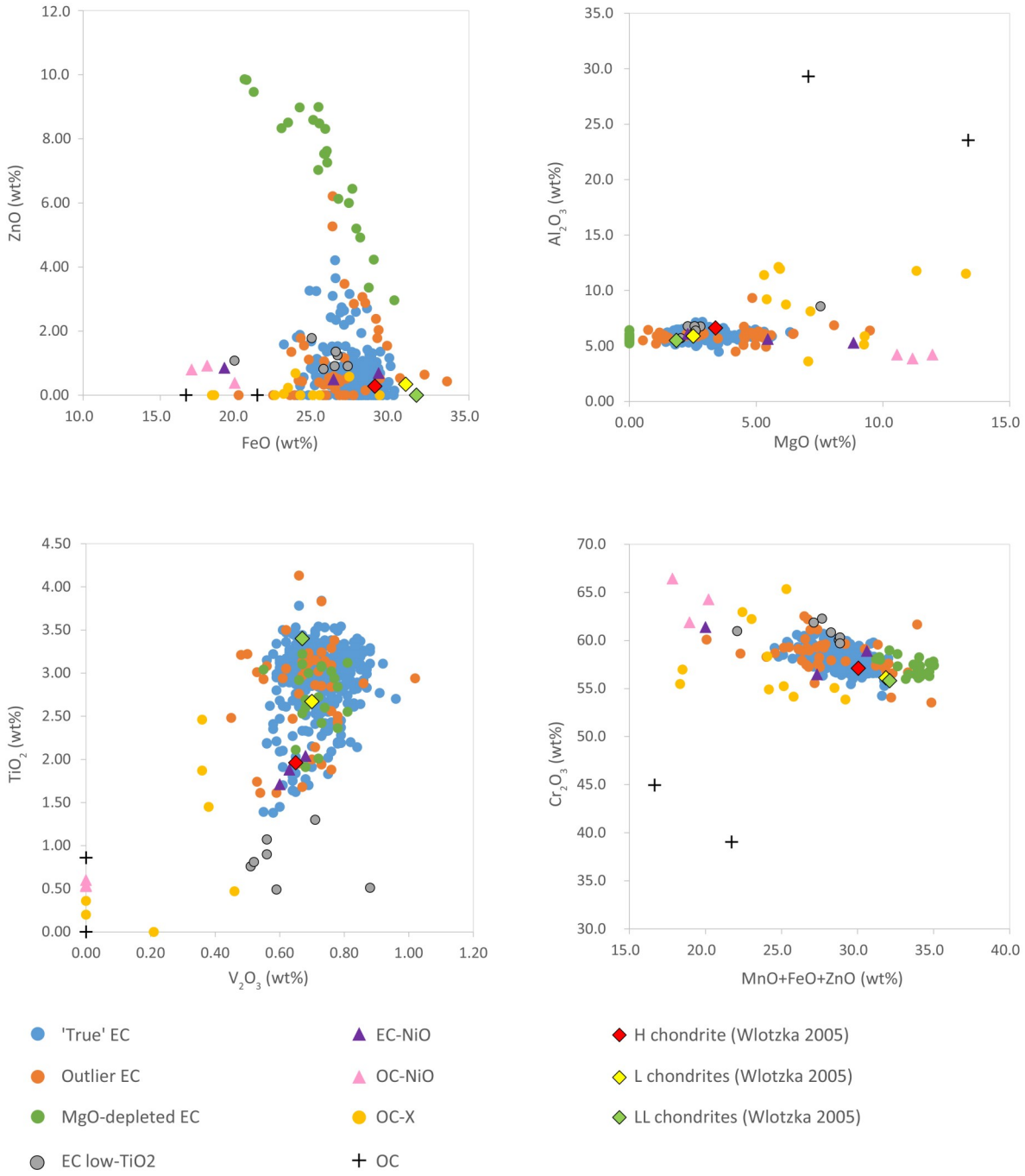

Fig. 13. All grains in this study plotted together with the average composition of chromite from recent ordinary chondrites from Wlotzka (2005). Grains are separated into their respective sub-group (see legend).

and the low-TiO_2 grains have a similar amount of V_2O_3 as the 'true' EC grains. Some of the OC-X grains have TiO_2 levels as that of EC grains but have much lower V_2O_3 amounts. The two OC grains as well as the OC-NiO grains have both very low TiO_2 and V_2O_3 amounts. This plot is the only one where the densest area of the 'true' EC grains is closest to an average L chondritic chromite composition.

The averages differ slightly between studies, and one thing noted is that in some studies, the presumed diagenetically altered EC grains are included among the unaltered EC grains thus giving a slightly skewed average. To test if there would be a significant difference in the averages, the data of altered EC grains from the Lynna River study (Lindskog et al. 2012) were separated in sub-categories as done in this study.

Table 2. Average compositional data from this study and a variety of other studies of extraterrestrial chrome spinel. All values are in compound weight % ± 1 standard deviation. n.d. = not detected.

Grain source Study	MgO	Al_2O_3	TiO_2	V_2O_3	Cr_2O_3	MnO	FeO	NiO	ZnO	Cr/Cr+Al	Fe/Fe+Mg
Chromite from 13 recent H chondrites Wlotzka (2005)	3.40 ± 0.18	6.64 ± 0.41	1.96 ± 0.29	0.65 ± 0.03	57.10 ± 1.10	0.88 ± 0.07	28.90 ± 0.60	n.d	0.28 ± 0.14	0.85	0.83
Chromite from 6 recent L chondrites Wlotzka (2005)	2.52 ± 0.21	5.90 ± 0.19	2.67 ± 0.44	0.70 ± 0.06	56.10 ± 0.80	0.63 ± 0.08	30.90 ± 0.60	n.d	0.34 ± 0.06	0.86	0.87
Chromite from 4 recent LL chondrites Wlotzka (2005)	1.85 ± 0.14	5.52 ± 0.17	3.40 ± 0.57	0.67 ± 0.10	55.80 ± 0.56	0.51 ± 0.04	31.60 ± 0.62	n.d	n.d	0.87	0.91
39 sediment-dispersed EC grains, Osmussaar breccia Estonia Alwmark et al. (2010)	2.54 ± 0.22	6.08 ± 0.25	3.00 ± 0.26	0.73 ± 0.05	56.71 ± 0.48	0.79 ± 0.19	29.20 ± 0.53	n.d	0.08 ± 0.21	0.86	0.87
291 sediment-dispersed EC grains, Puxi River Cronholm & Schmitz (2010)	2.88 ± 0.88	6.00 ± 0.36	2.91 ± 0.40	0.71 ± 0.08	57.84 ± 1.14	0.80 ± 0.26	27.40 ± 1.84	n.d	1.09 ± 1.12	0.87	0.84
73 sediment-dispersed EC grains, Lockne crater Alwmark & Schmitz (2007)	1.59 ± 1.54	5.74 ± 0.75	2.48 ± 0.38	0.72 ± 0.05	57.87 ± 1.09	1.44 ± 0.47	26.83 ± 1.84	0.05 ± 0.14	2.35 ± 2.10	0.87	0.90
274 sediment-dispersed EC grains, Komstad Limestone Häggström & Schmitz (2007)	2.69 ± 1.10	6.08 ± 0.73	2.95 ± 0.44	0.74 ± 0.07	56.93 ± 1.29	0.87 ± 0.25	28.74 ± 1.72	n.d	0.71 ± 0.84	0.86	0.86
276 sediment-dispersed EC grains, Kinnekulle Schmitz & Häggström (2006)	2.58 ± 0.79	6.07 ± 0.76	3.09 ± 0.33	0.75 ± 0.07	57.61 ± 1.58	0.78 ± 0.20	27.36 ± 2.63	n.d	0.53 ± 0.50	0.86	0.86
594 EC grains from fossil meteorites Schmitz et al. (2001)	2.57 ± 0.83	5.53 ± 0.29	2.73 ± 0.40	0.73 ± 0.03	57.60 ± 1.30	1.01 ± 0.33	26.94 ± 3.89	n.d	1.86 ± 2.43	0.87	0.85
239 sediment-dispersed 'true' EC grains, Lynna River Lindskog et al. (2012)	2.64 ± 0.53	6.04 ± 0.32	3.07 ± 0.31	0.73 ± 0.07	58.91 ± 0.99	0.81 ± 0.18	26.45 ± 1.82	n.d	0.97 ± 1.11	0.87	0.85
60 outlier sediment-dispersed EC grains, Lynna River Lindskog et al. (2012)	2.74 ± 1.47	6.14 ± 0.60	2.86 ± 0.60	0.78 ± 0.11	61.10 ± 1.79	0.72 ± 0.26	23.90 ± 2.55	n.d	1.55 ± 1.95	0.87	0.84
13 sediment-dispersed EC-NiO grains, Lynna River Lindskog et al. (2012)	5.22 ± 2.64	5.77 ± 0.54	2.49 ± 0.51	0.67 ± 0.09	59.40 ± 1.31	0.73 ± 0.25	23.80 ± 2.20	0.50 ± 0.16	0.83 ± 0.96	0.87	0.73
1 sediment-dispersed EC low-TiO_2 grain, Lynna River Lindskog et al. (2012)	2.38 ± 0.00	6.26 ± 0.00	1.27 ± 0.00	0.88 ± 0.00	62.23 ± 0.00	1.11 ± 0.00	17.98 ± 0.00	n.d	7.31 ± 0.00	0.87	0.81
405 sediment-dispersed 'true' EC grains Komstad Limestone This study	2.90 ± 0.35	5.99 ± 0.20	2.94 ± 0.20	0.72 ± 0.09	58.10 ± 0.62	0.86 ± 0.17	27.48 ± 0.80	n.d	0.59 ± 0.34	0.87	0.84
43 sediment-dispersed outlier EC grains, Komstad Limestone This study	3.77 ± 0.65	6.00 ± 0.24	2.79 ± 0.26	0.68 ± 0.09	58.39 ± 0.87	0.73 ± 0.16	26.54 ± 1.38	n.d	1.09 ± 0.74	0.87	0.80
23 sediment-dispersed MgO-depleted EC grains, Komstad Limestone This study	n.d	5.76 ± 0.14	2.69 ± 0.14	0.71 ± 0.09	57.28 ± 0.43	0.90 ± 0.19	25.47 ± 0.88	n.d	7.20 ± 0.76	0.87	1.00
7 sediment-dispersed EC low-TiO_2 grains, Komstad Limestone This study	3.21 ± 0.38	6.78 ± 0.30	0.83 ± 0.11	0.62 ± 0.12	60.85 ± 0.83	1.00 ± 0.16	25.21 ± 0.58	n.d	1.16 ± 0.37	0.86	0.82
9 chromite grains from fossil meteorite Grå 002 This study	2.44 ± 0.09	5.75 ± 0.20	3.11 ± 0.12	0.72 ± 0.07	57.87 ± 0.36	0.83 ± 0.17	29.71 ± 0.42	n.d	0.07 ± 0.05	0.87	0.87
3 sediment-dispersed EC-NiO grains, Komstad Limestone This study	5.53 ± 0.61	5.68 ± 0.71	1.88 ± 0.70	0.64 ± 0.22	58.92 ± 1.53	0.47 ± 0.73	24.84 ± 0.54	0.46 ± 0.46	0.68 ± 0.53	0.87	0.72
3 sediment-dispersed OC-NiO grains, Komstad Limestone This study	11.23 ± 0.96	4.12 ± 0.12	0.56 ± 0.13	n.d	64.19 ± 1.30	n.d	18.29 ± 1.79	0.79 ± 0.25	0.70 ± 0.40	0.91	0.48
41 high aluminum chromite grains from the fossil winonaite Schmitz et al. (2014)	4.74 ± 1.04	25.93 ± 4.42	0.61 ± 0.33	0.49 ± 0.14	40.82 ± 4.55	0.15 ± 0.23	25.90 ± 1.22	n.d	0.66 ± 0.24	0.52	0.76
3 aluminium low chromite grains from the fossil winonaite Schmitz et al. (2014)	1.70 ± 0.15	0.17 ± 0.12	0.19 ± 0.17	1.01 ± 0.13	69.50 ± 0.70	0.89 ± 0.05	22.20 ± 2.07	n.d	1.14 ± 0.43	1.00	0.88
13 chrome spinel grains from the winonaite Winona Schmitz et al. (2014)	10.42 ± 0.59	0.66 ± 0.25	0.41 ± 0.07	0.25 ± 0.17	68.68 ± 0.89	2.85 ± 0.29	15.02 ± 0.16	n.d	2.00 ± 0.19	0.99	0.40
16 chrome spinels from winonaite NWA 725 Schmitz et al. (2014)	9.92 ± 0.56	5.45 ± 1.00	0.88 ± 0.08	0.63 ± 0.08	62.08 ± 0.83	2.24 ± 0.39	18.64 ± 0.31	n.d	n.d	0.88	0.49
14 chrome spinels from winonaite NWA 4024 Schmitz et al. (2014)	3.82 ± 0.40	12.38 ± 1.58	1.22 ± 0.27	0.74 ± 0.14	53.44 ± 1.50	1.25 ± 0.10	27.71 ± 0.48	n.d	n.d	0.74	0.80

5.2.1 'True' EC grains

All the EC grains and their compositions are shown in Appendix A. All values are in oxide weight percentage. Average compositional data from sediment-dispersed EC grains from previous studies, chromite from fossil meteorites, and chromite from recent ordinary chondrites and winonaites are displayed in Table 2. The average composition of the true EC grains in comparison with the average composition of the grains from Lynna River, are within one standard deviation of the grains.

In Fig. 14 four element plots are shown of average compositions of grains from previous EC studies and recent ordinary chondritic chromite. Major elements Al_2O_3 vs. MgO do not differ a lot from the previous study at Killeröd, but MgO is slightly higher, which is probably due to the MgO-depleted grains being included in the average of the previous study (as previously discussed). The grains from this study have average Al_2O_3 and MgO concentrations matching those from the Puxi River section, China (Cronholm & Schmitz 2010). The average of the 'true' EC grains cluster with most of the other studies close to the average L chondritic chromite composition.

ZnO vs. FeO shows a trend of increasing ZnO with decreasing FeO, where EC grains of this study plot in the middle of the averages. None of the averages from this or the previous EC studies, except the study from the Osmussaar breccia, Estonia (Alwmark et al. 2010), have a good match with any of the recent ordinary chondrites in their average ZnO and FeO content.

In the plot with Cr_2O_3 versus the divalent oxides (MnO, FeO, and ZnO), the grains plot close to the grains from China (Cronholm & Schmitz 2010) and Kinnekulle (Schmitz & Häggström 2006). In this study and the previous ones the averages are closest to an H-chondritic composition.

In the V_2O_3 vs. TiO_2 plot the 'true' EC grains have a near match with the sediment-dispersed EC grains from Puxi River in China (Cronholm & Schmitz 2010). The average from this study, like the previous studies, also come closest to the chromite grains extracted from recent L chondrites (Wlotska, 2005).

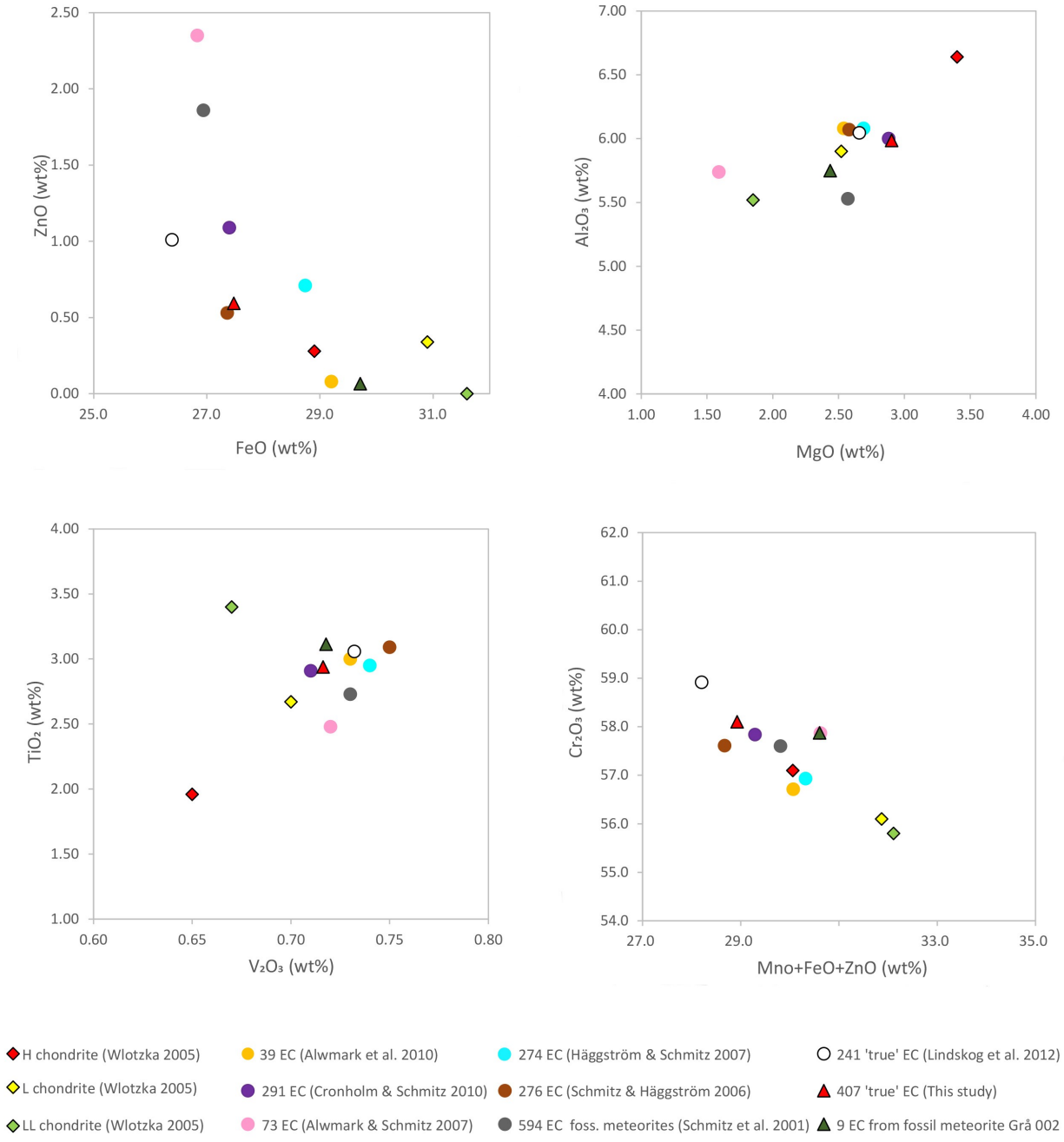

Fig. 14. Plots of the average chemical composition of sediment-dispersed EC grains and the fossil meteorite Grå 002 from this study and sediment-dispersed chromite from previous studies , chromite from fossil meteorites, and chromite from recent ordinary chondrites. Number of grains included in each average are displayed.

Since it is considered that TiO_2 and V_2O_3 are the less mobile oxides during diagenesis it is likely that this plot is defining for the sediment-dispersed grains. The Cr# ratio of the true EC grains is 0.87 and Fe# ratio is 0.84. The same category of grains from Lynna have ratios of 0.87 and 0.85 respectively.

5.2.2 Outlier EC grains

Outlier EC grains are defined by that one or more elements diverge from the definition of an EC grain, where 43 grains are in this subcategory. The studied interval in Killeröd has a smaller percentage of outlier EC grains compared to chromite grains from the 3 samples, Ly1, Ly2Ö, and Ly5 from Lynna. The outlier grains in Killeröd makes up 8% of the total EC grains. Including all the EC subcategories (76 grains in total, including low-TiO_2 grains, nickel-bearing EC grains, and MgO-depleted EC grains) gives a percentage of 15

of the total amount of EC grains found. For comparison, the outlier grains in Lynna, gives a total of 19% outlier EC grains (Ly1: 18%; Ly2Ö: 20%; and Ly5: 20%). Including nickel-bearing grains and low-TiO2 grains (69) that percentage is 24. Out of the 43 outlier grains in Killeröd 98% have fractures, 9% are crossed or parallel fractures, and 35% have reaction rims.

The average compositions of the outlier EC grains from Killeröd and Lynna are displayed in Table 2. In comparison between the two localities, the Cr_2O_3 percentage in Lynna is slightly higher than that of the Killeröd grains and also above the upper limit of 60 wt% for an EC composition, but still within one standard deviation. The FeO concentration in Lynna outlier grains is slightly lower than the lower limit for an EC composition (25 wt%), but also within one standard deviation. The EC outlier grains have a Cr# ratio of 0.87 and a Fe# ratio of 0.80. Lynna outlier grains have 0.87 and 0.84, respectively, for the two ratios.

5.2.3 MgO-depleted EC grains

The MgO-depleted chromite grains have the characteristic EC composition except for the enrichment in ZnO and lack of MgO through the grain. The average composition of the 23 grains with one standard deviation is displayed in Table 2. The amount of ZnO is 7.20 ± 0.76 wt% which is large compared to the true EC grains with 0.59 ± 0.34 wt%. When plotting the minor elements TiO_2 with V_2O_3 the MgO-depleted grains plot in the midst of the EC grains (Fig. 13). The average Cr# ratio is 0.87 and only has a small variation between 0.86 and 0.88 for individual grains. The Fe# ratio is 1.00 on average and for all the individual grains as MgO is absent. Morphological features were also studied in the grains. More than half (52%) of the grains have a small-spotted pattern on the surface (Fig. 12 D) and 87 % have fractures.

5.2.4 EC low-TiO_2 grains

Seven of the EC grains have low TiO_2 (<1.4 wt%). Two of the grains (grain #321 and #429) match an EC composition in the remainder oxides. Four of the other grains have an exceeding Cr_2O_3 content (60.8-62.3 wt%), two have V_2O_3 lower than 0.6 wt%, and one has slightly (0.59 wt%) more Al_2O_3 and MgO with 7.54 wt% (an excess of 3.54 wt% from the upper limit) and FeO at 19.81 wt% (a deficit of 5.19 wt% from the lower limit). Two of the grains have TiO_2 content in the range of 0.49-0.51 wt%. The Cr# ratio for the grains varies between 0.83 and 0.88 and the average is 0.86. The Fe# ratio is also high and varies between 0.60 and 0.88, with an average of 0.82. The single low TiO_2 grain from Lynna River has Cr# and Fe# of 0.87 and 0.81 respectively and has an increase in Cr_2O_3 and ZnO, and a decrease in FeO (Table 2).

5.2.5 Nickel-bearing EC and OC grains

Three of the six nickel-bearing chromite grains show compositions more or less in agreement with typical EC grains. Besides containing nickel the three grains also have a largely varying MgO and FeO content (see Appendix A, Table 5). Two of the unpolished nickel-bearing grains are composed of pyramidal aggregates (Fig. 15). In polished samples, the two grains have a "melted" appearance with a "spongy" surface with some fractures. One of them, grain #304 has a homogenous NiO-content. The second grain, #497 has an increase of NiO from core to rim. The third grain, #243, has a general "EC-appearance", both unpolished and polished, but displays a lot of fractures and only has nickel enriched in the rim. The amount of NiO lies between 0.21 and 0.62 wt% in the mean value for each grain and between 0.32 and 0.76 wt% for individual points. The Cr# and Fe# for the EC-NiO grains is 0.87 and 0.72 respectively with a Fe/3+ of 0.01.

The amount of nickel in the OC grains is larger than in the EC grains. The mean NiO amount for the grains falls between 0.75 and 0.84 wt% and between 0.49 and 1.27 for individual analysis points. The NiO is more or less homogenously distributed in all the grains. Compared to EC grains there is a large increase in MgO (10.6-12.0 wt%) at the expense of FeO (17.0-19.8 wt%) that was also noted by Lindskog et al. (2012) in the Russian section. There is also a decrease in Al_2O_3 (3.88-4.24 wt%) and an increase in Cr_2O_3 (61.9-66.4 wt%). TiO_2 is 0.53-0.60 wt% and V_2O_3 is not detected or absent. ZnO is present with between 0.38 and 0.92 wt%. The unpolished appearance for two of the grains is 'onion'-layered or has growth-rings with sharp crystal surfaces (Fig. 16 B and C). The third grain (Fig. 16 A) is small, sub-angular with irregular surface. The polished grains have similarities with two of the nickel-bearing EC grains: a melted appearance with a few to many formless small voids. The grains display no particular chemical zoning of NiO from core to rim, and are fairly homogenous in that aspect. The Cr# and Fe# is 0.91 and 0.48 and 0.05 for the Fe/3+.

5.3 OC grains

The visual appearance of OC grains generally does not differ much from EC grains, but the grains more commonly display pyramidal and octahedral crystal faces that are usually not seen in the EC grains (Fig. 17). The 14 OC grains (the 3 nickel grains excluded) in this study vary in composition (see Appendix A table 7).

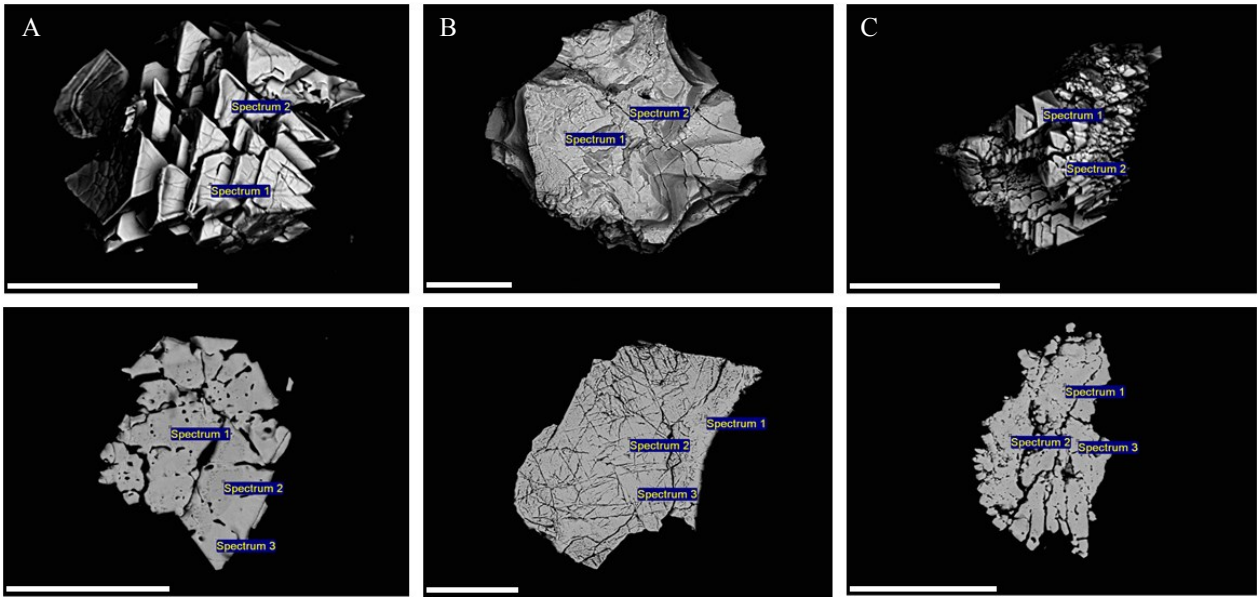

Fig. 15. Six SEM photographs showing the three nickel-bearing EC grains before (above) and after polishing (below). Scale bars = 50 µm. **A.** Grain #304. **B.** Grain #243. **C.** Grain #497.

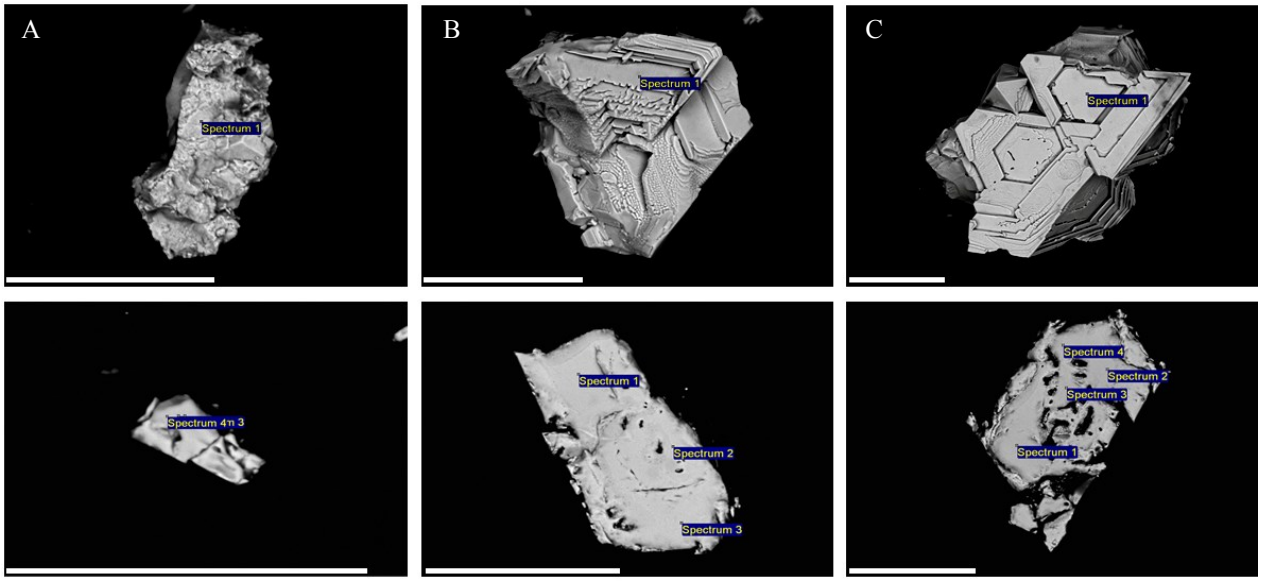

Fig. 16. Six SEM photographs showing the three nickel-bearing OC grains before (above) and after polishing (below). Scale bars = 50 µm. **A.** Grain #48. **B.** Grain #49. **C.** Grain #50. Note the 'onion'-layered appearance, or growth-rings, in the two unpolished grains in B and C.

Nine grains lack vanadium completely or the amount was below the detection limit. Six of the grains lacking V_2O_3/V_2O_5 also lacked TiO_2. Six grains have MnO+FeO+ZnO in the range of an EC grain (~25-30 wt%), but also have higher MgO content than EC grains. Twelve of the grains have a Cr# between 0.75 and 0.92 (mean value of 0.82) which when rounded are between the 0.8 and 1.0 ratio for ordinary chondrites according to Roeder (1994). These twelve grains are in the OC sub-category 'OC-X' in Table 1. The two OC grains 'sensu stricto' have ratios that are much lower than for the OC-X grains.

In Fig. 18 and Fig. 19 the OC grains are plotted with terrestrial grains from various ultramafic and mafic regimes (see Appendix D for chemical compositional data of terrestrial chrome spinel), together with the OC grains from Lynna and the OC grains from the previous study at Killeröd. The average compositions of ordinary chondrites are included as a reference. In the plot with the major oxides Al_2O_3 vs. MgO in Fig. 18 the OC-X grains follow the trend of increasing Al_2O_3 with increasing MgO together with the terrestrial grains. They plot mainly together with komatiites, boninites and picrite basalt. OC grain #94 plots outside of the terrestrial grains, and grain #436 plots with pillow basalts. The OC-NiO grains plot in the lower ed-

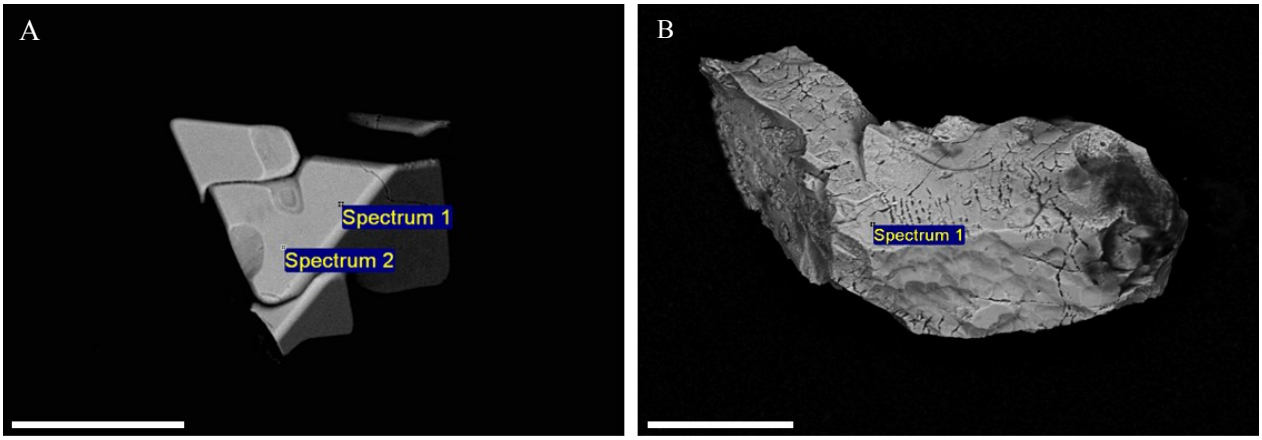

Fig. 17. SEM images of the two OC grains 'sensu stricto'. Scale bars = 50 µm. A. OC grain #436 with smooth surface and very angular/angular octahedral shape. B. OC grain #94 with fractures and angular/subangular shape.

ges of the terrestrial field, together with boninite and dunite. The OC grains from the previous study at Killeröd plot with komatiites, picrite basalt, and troctolite/peridotite. Two of the OC grains from Lynna plot closely to the average ordinary chondrite grains and with komatiites and possibly the gabbro-wehrlite grains. One of the grains plots between komatiites and troctolite/peridotite. Three of the grains plot more or less outside of the terrestrial grains.

The second plot in Fig. 18 shows the Cr_2O_3 amount versus the three divalent oxides: MnO, FeO, and ZnO. Some studies of terrestrial chrome spinels lack data for MnO and/or ZnO and the value represents only FeO or FeO with one of the other oxides. The OC-X grains as well as the OC-NiO grains have a high Cr_2O_3 content with lower MnO+FeO+ZnO. The grains plot with komatiite, boninite, dunite, and close to the average of chondritic chromite. Grain #94 plots with pillow basalt and grain #436 plots close to e.g. lherzolite xenoliths, dunite, and LIP basalt. Three of the Lynna grains plot with or close to the OC-X grains. Two of the grains plot with pillow basalt and troctolite/peridotite, respectively. One grain has very low Cr_2O_3 content and high MnO+FeO+ZnO content and plots with gabbro-wehrlite.

When plotting the ratios Cr# with Fe# the OC-X and OC-NiO grains have high Cr# with intermediate Fe# (Fig. 19). They plot together with boninite and komatiite. Grain #94 has similar Fe# as the OC-X grains but with much lower Cr#. The grain plots with or slightly below troctolite/peridotite. Four of the OC grains from Lynna plot in the outskirts of the komatiite, picrite basalt, and troctolite/peridotite fields. Two of the grains plot close to grain #94 below the troctolite/peridotite field. One of the previous Killeröd grains from the Häggström & Schmitz (2007) study plots with troctolite/peridotite, and three of the grains plot with komatiite, picrite basalt and possibly with gabbro-wehrlite. Two of these grains also plot next to average chondritic chromite. The overall trend in the diagram is increasing Cr# at low Fe# and at a certain constant Cr#, around 0.6, the Fe# increases.

In the last plot in Fig. 19 the $Fe^{3+}/(Cr+Al+Fe^{3+})$ vs. $Fe^{2+}/(Mg+Fe^{2+})$ is shown. Generally the Fe/3+ is low for most grains, both terrestrial and extraterrestrial. Most of the OC-X grains, as well as the OC-NiO, grain #436, one grain from Lynna, and one of the Killeröd grains from the previous study plot with komatiite and picrite basalt. Four of the OC-X grains, grain #94, and three of the Lynna grains plot below the terrestrial grains. One of the Lynna grains and two of the previous Killeröd grains plot with average chondritic chromite. The last Lynna grain plots with gabbro-wehrlite with high Fe/3+ and high Fe#. The Fe/3+ ratio of the OC grains is low: less than 0.1 (from 0 to 0.09) with an average of 0.03. Terrestrial grains have a wider range in Fe/3+, also generally low, but clusters around 0.05 for a majority of the mafic rocks. Terrestrial Fe# is lower than for chondrites, where the former mostly scatter between 0.2 and 0.6 (Roeder, 1994).

5.3.1 Results for grains #94 and #436:

As noted, one grain in particular (#94) plots outside of the fields for terrestrial chrome spinels. In Fig. 20 the grain is plotted with chrome spinels from the fossil winonaite-like meteorite, and three recent winonaite meteorites from Schmitz et al. (2014), together with the other 16 OC grains in this study. Grain #94 has a composition similar to that of the high-aluminum fossil winonaite chrome spinel compositions. Compared to the average composition (Table 2), all oxides have a good match except for a somewhat lower FeO content (4.62 wt% lower than the average, and ~2.0 wt% from the minimum content). The grain lacks V_2O_3 and has a lower ZnO content. When looking at the composition of individual grains, FeO is the only oxide that is devi-

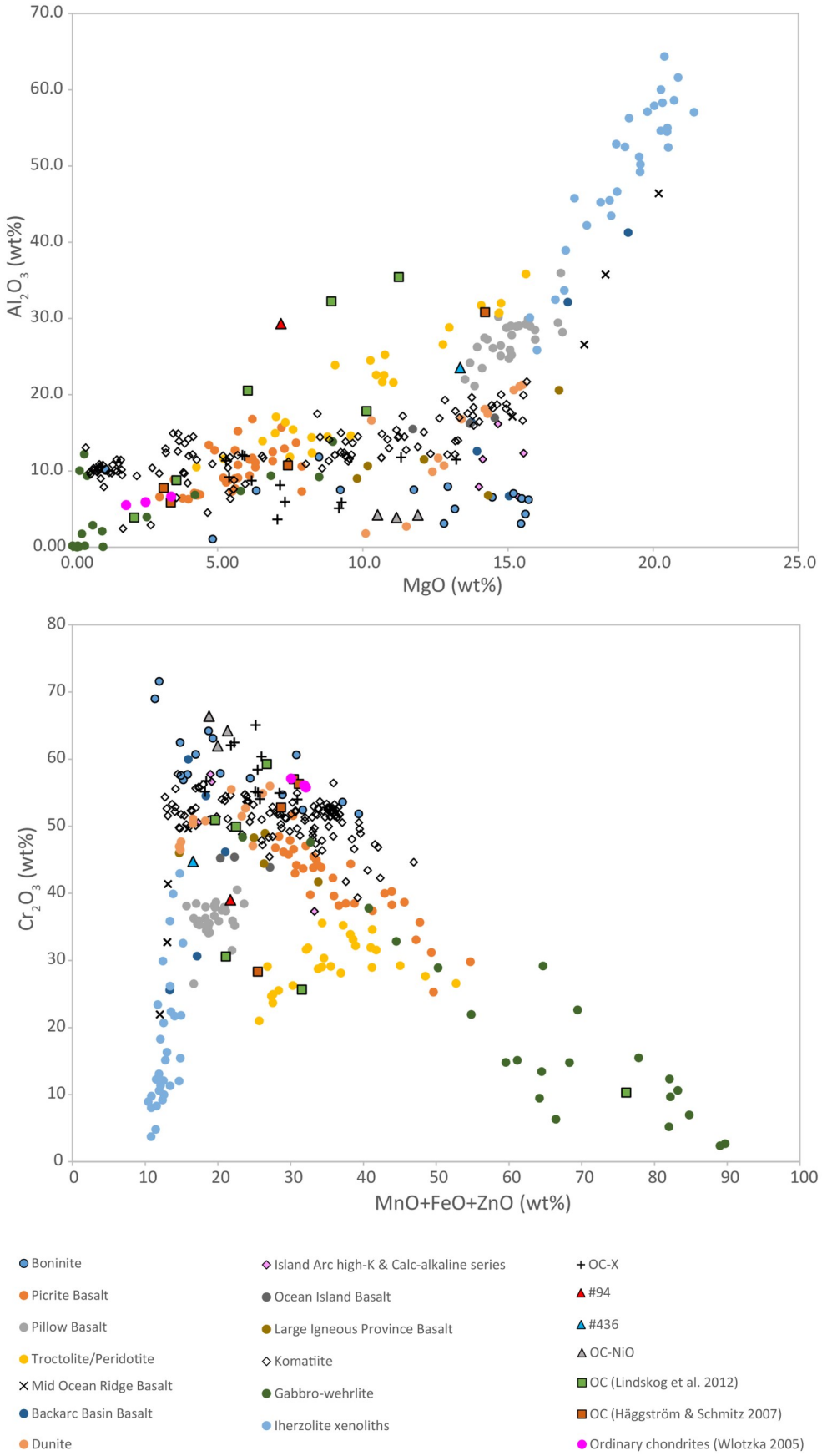

Fig. 18. Two plots with all the OC grains from this study, OC grains from Häggström & Schmitz (2007), OC grains from Lindskog et al. (2012), and terrestrial chrome spinel from a variety of igneous environments.

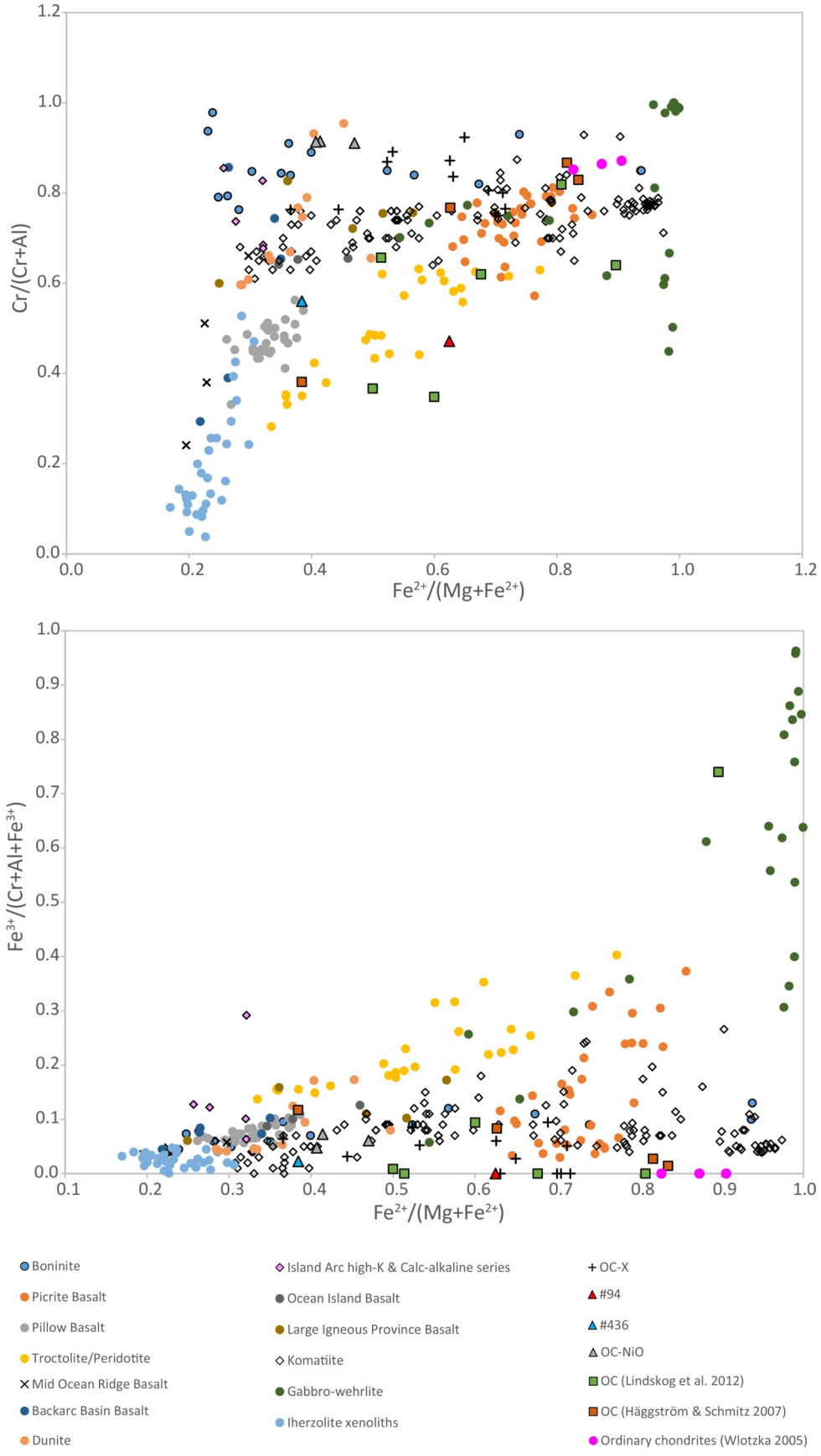

Fig. 19. Two plots showing the Cr# and Fe/3+ vs. Fe# for the 17 OC grains from this study, OC from Häggström & Schmitz (2007), OC from Lindskog et al. (2012), and terrestrial chrome spinel from a variety of igneous environments. All ratios are in mole fractions.

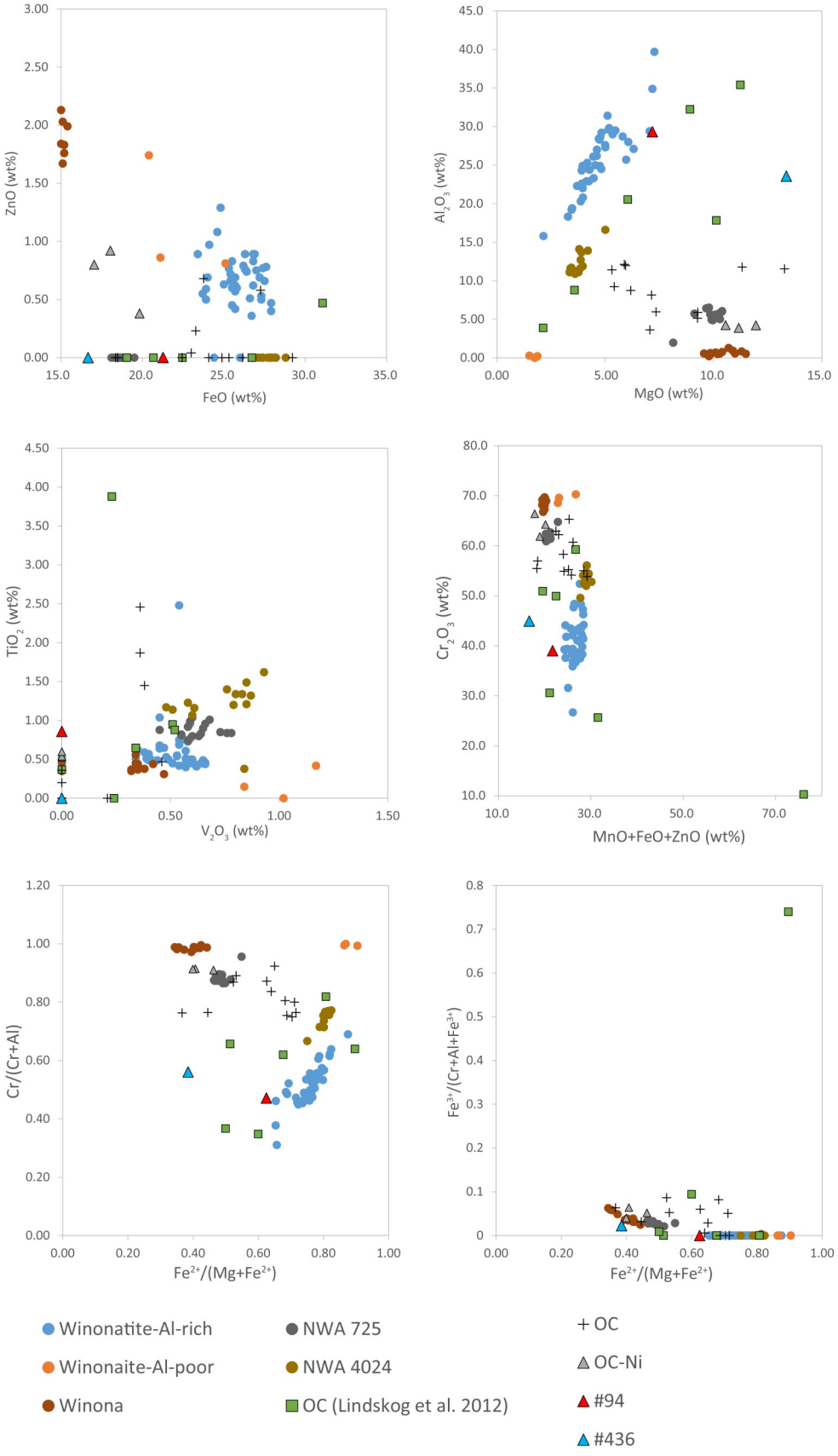

Fig. 20. Plots with the 17 OC grains from this study, the two types of grains from the fossil winonaite-like meteorite, and grains from three recent winonaite meteorites from Schmitz et al. (2014), and the OC grains from Lynna River from Lindskog et al. (2012).

ating significantly from the fossil winonaite grains. The Cr# ratio is 0.47 for grain #94. The average Cr# ratio of high aluminum winonaite grains is 0.52 and varies between 0.31-0.69 for individual grains. Fe# ratio is 0.62 for grain #94, and on average 0.76 for the fossil winonaite grains with variation between 0.65 and 0.87. The Fe/3+ ratio of the grain is zero, which is the same for the fossil winonaite grains. Grain #94 is sub-angular and measures 160 × 70 µm.

The other anomalous OC grain (#436) has a Cr# ratio of 0.56 and a Fe# ratio of 0.38 but lacks both TiO_2 and V_2O_3. Compared to the average composition of the Al-rich chromite from the fossil winonaite, the grain has a much higher MgO content (8.63 wt% more), slightly lower Al_2O_3 (2.37 wt% less), TiO_2 and V_2O_3 is absent or not detected, Cr_2O_3 is lower with ~4.0 wt%, MnO is lacking or not detected, and FeO is much lower (9.24 wt% less). ZnO is not detected. Compared with individual grains, MgO is higher with ~6.0 wt%, FeO is lower with ~7.0 wt%, and TiO_2 is absent, where the lowest amount in the fossil winonaite grains is 0.40 wt%. The Fe/3+ for this grain is 0.02. Grain #436 is a medium sized angular tetrahedral grain that measures 89 × 78 µm.

5.4 The fossil meteorite Grå 002

The fossil meteorite Grå 002 has narrow ranges in its chromite composition (see Appendix A Table 9). The average composition is displayed in Table 2. In the graphs in Fig. 14, Grå 002 comes closest to recent L chondrites in terms of Al_2O_3 vs. MgO and TiO_2 vs. V_2O_3. For the plot with ZnO vs. FeO the meteorite plots between H and L chondritic compositions, but slightly closer to recent H chondrites and in the plot Cr_2O_3 vs. MnO+FeO+ZnO the fossil meteorite grains plot together with all the other studies closer to recent H chondrites. Compared to the average composition of 26 other fossil meteorites from Kinnekulle, this deviates slightly with higher FeO and TiO_2, and much lower ZnO. The maximum diameters of the grains were measured, and lie between 77 and 197 µm, with a mean diameter of 125 µm.

6 Discussion

6.1 Sedimentologic analysis

The environment starts out in relatively calm waters with fewer large skeletal grains. The turbulence increases with time and the sea level is lowering with more large grains in the environment as a result. The hematite coated and iron stained grains increase which indicates that the waters are becoming more oxygenated and shallow and also that the deposition rate is slow (Trela 2008). The intraclasts indicate a more active environment, together with the increase in shell borings. Oncoids are microorganisms that grow cyclically around a grain core in response to environmental factors (light, sediment, temperature, and salinity flux). These are usually indicative of shallow water environments (Lindskog 2014, and references therein). In the top subinterval it is more difficult to interpret the environment as the inside of the cephalopod could represent its own microenvironment. The abundance of cephalopods is the densest in this part of the section and can be correlated with other localities in Baltoscandia (Kröger & Rasmussen 2014). The most common orthocerid genus in the Komstad Limestone is *Nilssonoceras*, belonging to the orthocerid biofacies, and is endemic to Baltica. Kröger & Rasmussen (2014) suggested cooler and deeper distal depositional environments for the orthocerid biofacies. However, based on the many cephalopods in the sediment, one conclusion could be that it is a rather shallow environment as the cephalopods were hunters of smaller animals and that these animals probably lived closer to the shore at a relatively low depth where sunlight could penetrate and upwelling of nutrients could occur. When the cephalopods died, they did so where they fed and accumulated on the sea floor. Another scenario is that the layer is a storm bed, deposited further out in the basin in deeper waters. On the other hand, that would be inconsistent with the layers below, unless there is a hiatus in between, which is not observed.

6.2 EC and OC grains

The majority of the EC grains fall within the rather limited chemical intervals of chondritic grains defined by Wlotska (2005) which would mean that, over all, alteration in the form of element exchange has been limited. In the average composition the grains have slightly more MgO than grains from other sections and previous studies from Killeröd. In the previous study by Häggström & Schmitz (2007) the MgO-depleted grains were not separated into a sub-group, but added to the average of typical EC grains, hence their lower average MgO content.

The previous study in Killeröd found somewhat more EC grains per kilogram (5.45 grains/kg) for the same interval. The amount of OC grains are however almost identical with 0.19 grains/kg. One explanation for the difference could be that the previous study had smaller samples, and that more grains were accumulated in that particular part of the rock because of

material winnowed by physical action on the sea floor. Taking a larger sample would give a more accurate estimate of the number of average grains per kilogram when covering a wider area, removing any possible lag deposit bias (this was also evident when picking grains in a one kilogram pilot sample in this study, where >10 grains/kg were extracted >63μm). As TiO_2 content between ~1.4 and 2.2 wt% is indicative of both H chondrites (where H3 has the smallest amounts) and that of L4 chondrites (Bunch et al. 1967), the 39 grains within this interval could stem from one, or both of the two types. It cannot be excluded that a small amount of chromite from chondritic meteorites other than L chondrites is present.

The overall grain shape mostly being angular, and that no grains were rounded or very rounded, indicates that many of the grains have endured little or no lateral transportation before deposition. Since the sediment shows signs of bioturbation by burrowing organisms and grain enveloping microbialites (oncoids), some grains with more rounding could have been reworked in situ. On the other hand, these metallic mineral grains might need quite extensive transportation and movement to become rounded in the relatively soft carbonate environment. Some OC grains with angular shape may be extraterrestrial, but could possibly also be grains from nearby submarine volcanism.

The fractures in 80% of the grains could also be due to transportation (even though most are angular), impacts on the asteroid parent body, compaction during diagenesis, or breakage by the method of extraction when sieving the samples. The chromite crystal has no cleavage (Nesse 2000) that would cause the irregular fractures mostly seen, but the crystal can break at its twin planes (111) which could explain the more perpendicular and parallel fractures. Alternatively, the perpendicular and parallel fractures could be a sign of shock, either by impact of a larger bolide and that the grains are from an ejecta layer, or impacts on the parent body in the asteroid belt, as in the discussion about the irregular fractures above. Russian grains have very similar amount of fracturing and crossed/ parallel fractures. This might indicate that the fractures have the same origin, and that it might very well be that the grains acquired their fractures when residing in the regolith of the parent body. The difference is less grains with reaction rims in Lynna. Perhaps the higher percentage in Killeröd could also have a connection to the same process that caused some grains to lack MgO. The tectonic history in southern Scania could play a role in the variance seen in the grains between the two localities. A hypothesis would be that more grains with fractures could be present in samples, where more gentle hydrofluoric acid treatment was used, such as in the case of samples from Lynna River (3.8 M). The harsher treatment could cause fractured grains to disintegrate more easily and go through the 63 μm sieve. However, even stronger HF than that used in this study (11 M) was used for the previous study in Killeröd (18 M), yet more grains were found per kilogram. Of course, the more treatment the grains go through the more susceptible they will be to breakage, but chemically, the HF should only remove silicates.

6.2.1 'True' EC grains

The chemical composition of these grains are in accordance with the strict definition of extraterrestrial chondritic chromite grains. The increased ZnO with decreased FeO content of the sediment-dispersed grains and fossil meteorites is a sign of diagenetic alteration as the grains do not match any of the averages of the recent ordinary chondrites. The ZnO content varies in the true EC grains between 0 and 4.21 wt%. As noted by Cronholm & Schmitz (2010), many unpolished grains display a higher ZnO content than when polished. The surface of the grains has been in contact with the sediment and the sea water and would likely be more susceptible to alteration. If the grains are diagenetically altered L-chondritic grains as indicated by their V_2O_3 and TiO_2 contents then the most mobile elements are the divalent oxides minus MgO which seems rather stable (at least in these plots) together with Cr_2O_3 that also is a bit elevated. The increase in Cr_2O_3 could be explained by a coupled substitution where $Fe^{2+} + Ti^{4+} \longrightarrow 2(Cr, Al)^{3+}$ as seen in chrome spinel of the anoxic environment of the Moon (Papike et al. 1991). This could be possible, however, the grains are already slightly enriched in TiO_2 compared with recent ordinary chondritic grains. With all these factors in mind it is still reasonable that most of the grains indeed have an L-chondritic source. The Cr# and Fe# for L-chondritic chromite is 0.86 and 0.87 respectively (Table 2). In the scatter plots with all EC grains represented (Fig. 13) more overlapping of the ordinary chondrites are shown, hence some of the grains could probably have an H or LL chondritic origin.

6.2.2 Outlier EC grains

The results for the outlier EC grains could possibly be a sampling bias, as a larger amount of rock was extracted in Killeröd. Also, more grains were lost during polishing in this study (5% in Killeröd compared to 1% in Lynna), even though the difference is rather small. In the Lynna study a low-molar HF acid was

used. This could keep more fragile and possibly altered grains intact. However, the majority of the outlier EC grains in Killeröd survived the harsher HF treatment as most of them have fractures. The fractures would allow the grains to be more susceptible to chemical alteration. The average composition of the outlier grains, together with the high elemental ratios of Cr# and Fe#, strongly indicate an extraterrestrial origin.

6.2.3 MgO-depleted EC grains

Except for a slightly lower percentage of FeO compared to the true EC grains the average composition is within errors. This type of grains has not been recorded in other sections than Killeröd. If this were to be grains from another type of meteorite, a local shower could have hit the Scanian region, and that is why these grains cannot be found elsewhere. Chromite compositional data from non-chondritic meteorites was looked into but nothing similar was found. Otherwise it is reasonable to think that the lack of magnesium is due to post-depositional alteration, since Mg^{2+} and Fe^{2+} ions can be exchanged with Zn^{2+} ions and would explain the elevated ZnO content. In the study of the ejecta deposit in the Lockne crater there was also an increase of ZnO. Also the appearance of the grains is an indication of this, with a high frequency of fractured grains and more than half with an altered appearance throughout the grains. Chromite from recent LL chondrites have a higher Fe# ratio than H- and L-chondritic chromite (Table 2), however, that elevation is due to the enrichment in FeO as well as a small deficit in MgO rather than what is seen here with absent MgO and a bit of deficiency in FeO.

The tectonically active area of the Tornquist zone that formed in the closing of the Tornquist Sea at approximately 445 Ma (Cocks & Torsvik 2005) could have caused hydrothermal alteration of some of the grains, exchanging MgO and some iron for ZnO. The effects of hydrothermal alteration largely depends on the type of host rock that the chromite resides in (Kimball 1990). In general there is an increase in the Cr# and/or Fe#. In e.g. serpentine host rocks altered chromite usually displays an enhanced Fe# but not necessarily Cr#.

6.2.4 EC low-TiO_2 grains

Three of the low-TiO_2 grains had low total oxide weight percentage (91.2-94.0 wt%) and were normalized to 100.0 wt%. The oxide percentages of these grains could thus be somewhat inaccurate. However, the three grains when normalized show similar high Cr_2O_3 and low TiO_2 as grains that have an accepted total oxide weight percentage (see Table 3 in Appendix A). The two grains that have 0.49 and 0.51 wt% TiO_2, could be remnants of an L3 chondrite that has TiO_2 in chromite between 0.25 and 0.6 wt%. L3 chondrites however, contain only small amounts of chromite compared to chondrites of petrological types 4 to 6 (Wlotska 2005) and therefore this type of grains might be sparse in the sediment. Also they are usually smaller than 63 μm (Bridges et al. 2007). One of the grains has elevated amounts of both Al_2O_3 and Cr_2O_3 with a deficit in TiO_2 and FeO, which is a common substitution in chromite on the Moon (Papike et al. 1991). The grains were also compared with chromite grains from non-chondritic meteorites (pallasites, eucrites, etc.), but no complete match was found. Some elements matched, but then one or two diverged significantly. Their high Cr# and Fe# could still be indicating an extraterrestrial origin (Roeder 1994).

6.2.5 Nickel-bearing EC and OC grains

Sediment-dispersed chromite grains containing nickel have only been found previously among both EC and OC grains from resurge deposits of the Lockne crater (Alwmark & Schmitz 2007) and from EC grains in the Russian section (Lindskog et al. 2012). The source of these grains were further discussed by Lindskog et al. (2012). A possible explanation for the rarity of these grains in other studies was that the harsh hydrofluoric acid used in previous studies could have destroyed these grains. However, that explanation is not viable anymore as 11 M hydrofluoric acid has been used also in this study. As for the origin of nickel in these grains, one explanation could be the effect of alteration, since exchange between elements like Mg and Fe is noticeable. However, as noted in the surface of grains, and by Alwmark & Schmitz (2007), a larger increase of ZnO is believed to be caused by post-depositional alteration. The grains here have only small amounts of ZnO (~0.7 wt%), where 'true' EC grains can have even more. The EC-NiO grains have all oxides within the limits of an EC composition, except for elevated MgO in two of the grains (#305 and #497) and lower FeO and slightly higher Cr_2O_3 in grain #305.

The grains with nickel may well have been chromite grains situated near or inside the fusion crust of the micrometeorite. Fusion crusts develop on most meteorites as they enter the atmosphere and the friction from the air molecules cause heating and melting of the outer meteorite layer (Ramdohr 1967; Genge & Grady 1999; Parashar et al. 2010). The melting causes enrichment of nickel in the different phases inside the crust, due to the oxidizing conditions in the atmosphere. Nickel content increases outwards in the

crust. Relict unmelted grains of refractory phases can still exist in the outer melted crust (Genge & Grady 1999). The levels of nickel in the three EC grains is higher closer to the rim for one of the grains, and with principally no NiO in the core. In the second grain the NiO content is equally high in the rim as well as the edges. And for the third grains the level of NiO is detected from rim to core but is increasing towards the rim. An explanation for the variation could be connected to the appearance of the grains. If the grains were situated in the fusion crust of a small meteorite or micrometeorite the grains could have a melted appearance as in the case for two of the grains, whereas the third grain could have been in the vicinity of the crust but not within it. At least five of the nickel bearing grains have an unpolished appearance that differ from the typical EC grain. Both the EC grains with aggregate structure (Fig. 15) and the OC grains with a zoning structure (Fig. 16) represent possible signs of heating, melting and recrystallization. The ratios for the two categories of grains support an extraterrestrial origin with high Cr# for both and with a relatively high Fe#, which is well within the span for both unequilibrated and equilibrated chondritic chromite (Roeder 1994). The EC-NiO grains also have very low Fe/3+, whereas the OC-NiO grains have a higher ratio, but this does not confirm nor support an extraterrestrial origin.

The nickel-bearing OC grains have a close similarity to EC grains, and the higher or lower content of different oxides in some cases could reflect an exchange of elements due to diagenetic factors. Mg^{2+} exchange with Fe^{2+}, and Al^{3+} can exchange with Cr^{3+} in simple substitution. Vanadium is lacking or below detection limit, and the vanadium ion can have 2+ to 5+ charge. Here vanadium is measured as a 3+ ion, which means it can be exchanged with Al and Cr and thus would explain its absence. The titanium however has a 4+ charge and is not readily exchanged with any other element, and is supposedly very stable in the spinel structure. The low concentrations (<1.4 wt%) of TiO_2 could, however, be explained by a coupled substitution, where $Fe^{2+} + Ti^{4+} \longrightarrow 2(Cr, Al)^{3+}$, which is at least, the most common substitution in the lunar chromites (Papike et al. 1998). However, when plotting these grains with all the other grains from this study they constantly plot with or near the other OC grains rather than with the EC grains. The grains are somewhat similar to the OC grains from the Loftarstone, the resurge deposits of the Lockne crater, however. The OC grains of that study have, compared with EC definition, increased MgO, lower TiO_2 and V_2O_3, slightly increased Cr_2O_3, and are slightly depleted in FeO, trends that can be found in the OC-NiO grains. The Loftarstone OC grains have similar appearance (and composition) as the aggregate EC grains from the resurge deposit (Alwmark & Schmitz 2007): a spongy look with many cavities, as the grains with nickel in this study.

When plotted with the other OC grains and terrestrial chrome spinels the grains seem to separate themselves slightly from the other grains plotted in Al_2O_3 vs. MgO, but could relate to komatiites, pillow basalts and/or mid-ocean-ridge basalts (MORBs). Those spinels did not contain any nickel, however. Plotting grains that did contain nickel with the OC-NiO grains in a TiO_2 vs. NiO plot, the closest candidate for a match were grains from basaltic andesite spinels, but looking at the other elements there is no similarity. The grains are more likely extraterrestrial; perhaps from an ordinary chondrite.

6.3 OC-X grains

Most of the OC-X grains plot well with mafic chrome spinels and deviate from chondritic compositions, and it is likely that the grains have a terrestrial origin. The grains are similar to spinels from komatiite, boninite and picrite basalt. These three rock types all originate from different melt fractions of mantle lherzolite at varying pressures and temperatures (Winter 2010). Komatiite lavas have extremely high melting point and are mostly of Archean age. They derive from 30 to 50% partial melting of the mantle, and are believed to be important in the early formation of continents (Mole et al. 2014). Since komatiites most often are metamorphosed, the chromites from komatiites are also often altered, with the chromite being gradually replaced by chromium magnetite (’ferritchromit’), which is often displayed as a rim surrounding the chromite grain (Barnes 1998; Barnes & Roeder 2001). The chromium content of the magnetite rims is significantly lower than in the chromite cores. The OC-X grains do not display any obvious chemical zonation as would be the case with magnetite rims, where at least some of the grains statistically should be zoned if having komatiitic affinity. However, during analysis visual rims were avoided when present on a grain since the total oxide percentage fell below accepted values. This did not cause much variety in the composition between rim and core, however.

Boninite is a Mg-rich basalt formed by 15 to 30% partial melting of lherzolite at low pressures and intermediate temperatures. The lavas are always set in subduction regimes in backarc to forearc settings, predominantly in submarine environments, but are unusual in the rock record (Resing et al. 2011). Boninite con-

tains much more chromite compared to most mafic rocks. Chromite from boninites have an unusually high Cr#, low Fe/3+ and very low titanium content (Barnes & Roeder 2001) much like the OC-X grains. Uncategorized basalts from ophiolites often have overlapping ratios to that of boninites, where many of the basalts in fact are boninites. It would be possible that during the tectonic evolution of the Scanian region, boninitic lava extruded during subduction events and contributed with a small amount of chrome spinel to the sediments found in Killeröd.

Picrite (picrobasalt or oceanite) is an ultramafic olivine-rich basalt produced between 15 to 30% partial melting of garnet lherzolite at high temperatures, and at a wide range of pressures (Winter 2010). The chromite data of picrite basalt is from the study of Ti-rich chromite from the Mount Ayliff intrusion, South Africa (Cawthorne et al., 1991), a sequence of rock believed to have formed through fractional crystallization of continental tholeiite. If all or some of the OC-X grains are in fact terrestrial the source had to be rather proximal to keep the grains euhedral, and similar in age to the interval studied at Killeröd. It would be of interest to be able to compare regional spinel data with the OC-X grains. Chrome spinel data of igneous rocks from Scandinavia is unfortunately sparse if not non-existent. Another approach would be oxygen isotopic analyses to confirm a terrestrial origin. The high Cr# ratio and intermediate to high Fe# ratio and the very low Fe/3+ of these grains could however be a strong evidence for an extraterrestrial origin (Roeder 1994). Some of the OC grains have slightly smaller Cr# than chrome spinel of unequilibrated ordinary chondrites, this could be a sign that they are transitional towards being equilibrated, or more metamorphosed, ordinary chondrites.

6.3.1 OC grains #94 and #436

The composition of grain #94 together with the deviation from terrestrial chrome spinels is indicating that the grain possibly originates from the winonaite impactor that caused the disruption of the L-chondrite parent body. If the grain would be terrestrial, the higher Al_2O_3 might be explained by exchange with Cr_2O_3 during diagenesis, however no ZnO is present within the grain that could be an indication of post depositional alteration. The very low (zero) Fe/3+ ratio is indicative of an extraterrestrial origin as oxidation of Fe^{2+} to Fe^{3+} relies on available oxygen, however, a terrestrial origin cannot completely be excluded by this ratio as some terrestrial chrome spinels can have a low ratio as well. Grain #436 is also a candidate for a winonaite origin, but has more oxides deviating. The Cr# has a good match with the fossil winonaite grains, but the Fe# is lower. The Fe/3+ is low which could be indicative of an extraterrestrial origin.

In the previous study at Killeröd by Häggström & Schmitz (2007) four OC grains were found in the same interval. One of these grains has a composition that is similar to the two grains discussed here. Compared to the average of the Al-rich grains from the fossil winonaite-like meteorite, the amount of MgO is 9.47 wt% higher, the Al_2O_3 amount is 4.89 wt% higher, the Cr_2O_3 amount is 12.5 wt% lower. The differences in the remainder oxides are negligible. Compared to individual grains it is mainly the two oxides MgO and Cr_2O_3 that deviate, all other oxides are within the ranges (see Appendix B Table 7). Compared with the two grains in this study the oxides are either matching with one or the other grain or fall somewhere between them. The only large difference is the much lower amount of Cr_2O_3 in the grain. Looking at the ratios for this grain, both Cr# and Fe# is 0.38. The Cr# is within the ranges of the fossil meteorite grains but the latter deviates with 0.27 from the lowest ratio. The Fe/3+ of the grain is high (0.12), on the other hand, and has more similarity with terrestrial chrome spinel. With all the similarities between these three grains, it cannot be excluded that also this grain could be a remnant of the mysterious impactor of the L-chondrite parent body.

6.4 Fossil meteorite Grå 002

The MgO value and the relatively high average TiO_2 value would be indicative of an L chondrite. The composition of the chromite grains corresponds with the compositional range of an L chondritic meteorite (Fig. 14). In the ZnO vs. FeO it plots slightly closer to an H chondrite. This could be explained by diagenesis where ZnO replaces FeO and does not reflect the original composition of the grains. The average chromite composition from the 26 fossil meteorites is very similar to the average composition of the fossil meteorites only extracted from the Arkeologen bed (Schmitz et al. 2001). At the time of that study, no meteorites had been found or analyzed in the Gråkarten bed. However looking at average grain composition from individual meteorites there is a large spread, with meteorites having similar composition as Grå 002. Comparing the size of the chromite grains from Grå 002 with chromite size data in Bridges et al. (2007) indicates that this is an L chondrite of petrologic type 5 (76-158 μm). The grains above the 158 μm limit lie in a gap between petrologic types 5 and 6, where the latter have maximum diameters of 253–638 μm that does not fit these grains.

6.5 Reducing and oxidizing environments and the effect on grain chemistry

The dark, organic-rich Komstad Limestone Formation is mainly indicative of deposition in a reducing environment. Pyrite and other metal sulfide precipitate during shallow burial through the reaction between iron minerals and hydrogen sulfide, H_2S (in highly calcareous sediments where terrigenous material is sparse, only small amounts of pyrite will form). H_2S is formed through the reduction of sulfate (Berner 1984). Sulfate is reduced in the presence of organic material where synchronous oxidation of the organic compounds take place. This redox-reaction can be conducted through the metabolism of sulfate reducing bacteria, and/or by thermochemical sulfate reduction (TSR) (Machel 2001). Since bacterial sulfate reduction (BSR) is the most common and widespread process in shallow burial diagenetic environments, with low temperature ranging from 0 to 60-80°C. BSR would be the most probable origin of the metal sulfide precipitates in these sediments, as TSR mainly function at higher temperatures in deep-burial settings. BSR can theoretically work in completely anoxic environments, but the organic material needed for the reduction of sulfate is often at least partially a product of aerobic bacterial metabolism (Machel 2001). Where organic matter is abundant on the depositional surface and in the sediment, the degradation of organic matter will consume the available pore water oxygen, and the sediment will become anoxic.

The assumption would be that the depositional environment of the Komstad Limestone is only partially reducing, or that the sea-floor became anoxic/dysoxic as organic matter settled, as there are signs of oxidation where hematite and limonite have formed around grains. In comparison the Lynna River section is light colored and has relatively little organic content, but different rock samples display both oxidizing and reducing conditions (Lindskog et al. 2012). Typically the rock is limitedly oxidized, where bioturbation and bioerosion locally has caused strong oxidation. Many hardground have also been somewhat oxidized before further sedimentation (A. Lindskog 2014, personal communication). The chromite-bearing samples in Lynna, compared with in this study (Ly1, Ly2Ö, and Ly5), contain residual material consisting of glauconite grains, hematite and limonite, biotite, iron-oxides and coal grains. Iron-rich spherules are also present in most samples. The overall view would be that the Lynna River section is more of an oxidizing environment compared to the section in Killeröd. What effect could these two environments have on the chemistry of the chromite? Chemical interaction between the rock and chromite grains in Lynna would be fairly easy as the limestone there is rather permeable and contains more terrigenous silt and clay. However, the alteration of the grains is rather limited as seen, though a higher fraction of the grains are altered here compared to Killeröd grains. The reducing environment in Killeröd is preferential for the chemical preservation of the grains as it would be at least similar to that of the conditions in space. The tectonic history of the Scanian region, however, with the likely influence of hydrothermal fluids has clearly affected some of the chromite grains.

6.6 A possible meteorite flux from the Moon?

Most lunar spinels have a composition between chromite and ulvöspinel. The latter have high amounts of TiO_2 that has not been seen in any of the chromium-rich grains in this study. Lunar chrome spinel grains usually have FeO contents above 30 wt%. Spinels are more common in lunar basaltic rocks, but can also be found in highland rocks, e.g. anorthosites. These spinels have lower concentrations of MgO, Al_2O_3 and TiO_2. The compositional ranges in the lunar chrome spinels are wide. In three selected studies (El Goresy et al. 1971a; El Goresy et al. 1971b; Papike et al. 1998), chrome spinel grains with relatively low TiO_2 amounts were chosen. TiO_2 amounts between 1.71 and 3.80 wt% in lunar rocks and soil (Papike et al. 1998), 5.29-10.8 wt% in Apollo 12 samples from Oceanus Procellarum (El Goresy et al. 1971b), and 2.66-7.43 wt% in chromite from a basaltic sample of the Apollo 14 mission (El Goresy et al. 1971a) (see Appendix C for the complete chemical compositions). Comparing chrome spinels from lunar rocks and soils with the OC grains of this study, an exact match cannot be found. The grain that comes closest to chrome spinel from lunar rocks and soil is OC grain #29 (Appendix A, Table 7).

7 Summary and Conclusions

The studied bed with sub-beds is a highly condensed interval, extremely rich in extraterrestrial chromite grains. The majority of the extracted chromite grains have an apparent L-chondritic origin. About 14 % of the EC grains in Killeröd show signs of alteration, which is less compared to the grains from Russia that has ca. 22% altered grains. The more oxidizing envi-

ronment in Lynna could be the cause of this. The Killeröd bed also contains a few grains with nickel, where some or all of the grains possibly originate from the fusion crust of meteorites. A total of 23 grains also lacked MgO completely or below the detection limit, which has not been found anywhere else in previously studied sections. These grains were also highly enriched in ZnO, which would indicate hydrothermal alteration. These grains are probably altered extraterrestrial grains.

Twelve of the OC grains, not containing nickel, could be terrestrial and originate from komatiites, boninites and/or picrite basalt, which are the three igneous rocks that are the most similar in both oxide composition and ratios. The latter two are the best candidates and derive from partial melting of the mantle in subduction environments. The Cr/(Cr+Al) ratio is high, as is the $Fe^{2+}/(Mg/Fe^{2+})$ ratio, which could instead be indicative of an extraterrestrial origin. Oxygen isotopic studies may unveil their true origin.

Among the OC grains, two of the grains stood out in terms of their chemical composition and their ratios compared to both terrestrial and chondritic spinel. One grain in particular, #94, is a good candidate for originating from the winonaite-like impactor that broke up the L-chondrite parent body. Further studies of the grain with oxygen isotopes could eliminate a terrestrial origin completely. The second grain #436 is less clear, but possibly has an extraterrestrial origin; however, further analysis would be needed to support this hypothesis.

8 Acknowledgements

I would like to thank my supervisors Birger Schmitz, Mats Eriksson, and Anders Lindskog for endless support and guidance. An extended gratitude to Birger Schmitz for introducing me to this fascinating subject, and to Anders Lindskog for the manufacturing of thin sections and discussions. I would like to thank Fredrik Terfelt for instructions and support in the laboratory and in field, and Anders Cronholm for instructions of the scanning electron microscope. Special thanks to Jonathan Jansson for support with computer software, without whom I would have teared my hair off. Thanks to friends and family for support, and to Faisal Iqbal who made sieving a lot less tedious. And a final thanks to the baby for entertaining me in the breaks.

9 References

Abzalov, M. Z., 1998: Chrome–spinels in gabbro–wehrlite intrusions of the Pechenga area, Kola Peninsula, Russia: emphasis on alteration features. *Lithos 43*, 109-134.

Agrell, S. O., Scoon, J. H., Muir, I. D., Long, J. V. P., McConnell, J. D. C. & Peckett, A., 1970: Mineralogy and Petrology of Some Lunar Samples. *Science, New Series 167 (3918)*, 583-586.

Alwmark, C., 2009: Shocked quartz grains in the polymict breccia of the Granby structure, Sweden-Verification of an impact. *Meteoritics & Planetary Science 44 (8)*, 1107-1113.

Alwmark, C. & Schmitz, B., 2007: Extraterrestrial chromite in the resurge deposits of the early Late Ordovician Lockne crater, central Sweden. *Earth and Planetary Science Letters 253*, 291-303.

Alwmark, C., Schmitz, B. & Kirsimaee, K., 2010: The mid-Ordovician Osmussaar breccia in Estonia linked to the disruption of the L-chondrite parent body in the asteroid belt. *Geological Society of America Bulletin 122 (7-8)*, 1039-1046.

Artemieva, N. A. & Shuvalov, V. V., 2008: Numerical simulation of high-velocity impact ejecta following falls of comets and asteroids onto the Moon. *Solar System Research 42 (4)*, 329–334.

Barnes, S. J., 1998: Chromite in komatiites, 1. Magmatic controls on crystallization and composition. *Journal of Petrology 39 (10)*, 1689-1720.

Barnes, S. J. & Roeder, P. L., 2001: The range of spinel compositions in terrestrial mafic and ultramafic rocks. *Journal of Petrology 42 (12)*, 2279-2302.

Bergerat, F., Angelier, J. & Andreasson, P.-G., 2007: Evolution of paleostress fields and brittle deformation of the Tornquist Zone in Scania (Sweden) during Permo-Mesozoic and Cenozoic times. *Tectonophysics 444*, 93–110.

Berner, R. A., 1984: Sedimentary pyrite formation: An update. *Geochimica et Cosmochimica Acta 48*, 605-615.

Bridges, J. C., Schmitz, B., Hutchison, R., Greenwood, R. C., Tassinari, M. & Franchi, I. A., 2007: Petrographic classification of Middle Ordovician fossil meteorites from Sweden. *Meteoritics & Planetary Science 42 (10)*, 1781-1789.

Bunch, T. E., Keil, K. & Snetsinger, K. G., 1967: Chromite composition in relation to chemistry and texture of ordinary chondrites. *Geochimica et Cosmochimica Acta 31*, 1569-1582.

Cawthorne, R. G., de Wet, M., Hatton, C. J. & Cassidy, K. F., 1991: Ti-rich chromite from the Mount Ayliff Intrusion, Transkei: Further evidence for high Ti tholeiitic magma. *American Mineralogist 76*, 561-573.

Chen, J. & Lindström, M., 1991: Cephalopod Septal Strength Indices (SSI) and depositional depth of the Swedish Orthoceratite limestone. *Geologica et Palaeontologica 25*, 5-18.

Clayton, R. N., 2003: Oxygen Isotopes in Meteorites. Treatise on Geochemistry 1, 129-142.

Clayton, R. N., Onuma, N. & Mayeda, T. K., 1976: A classification of meteorites based on oxygen isotopes. *Earth and Planetary Science Letters 30*, 10-18.

Cocks, L. R. M. & Torsvik, T. H., 2005: Baltica from the late Precambrian to mid-Palaeozoic times: The gain and loss of a terrane's identity. *Earth-Science Reviews 72*, 39–66.

Crawford, A. J. & Cameron, W. E., 1985: Petrology and geochemistry of cambrian boninites and low -Ti andesites from Heathcote, Victoria. *Contributions to Mineralogy and Petrology 91 (1)*, 93-104.

Cronholm, A. & Schmitz, B., 2010: Extraterrestrial chromite distribution across the mid-Ordovician Puxi River section, central China: Evidence for a global major spike in flux of L-chondritic matter. *Icarus 208*, 36-48.

Dick, H. J. B. & Bryan, W. B., 1979: Variation of basalt phenocryst mineralogy and rock compositions in DSDP Hole 396B. *Initial Reports of the Deep Sea Drilling Project 46*. United States.

Dronov, A. & Rozhnov, S., 2007: Climatic changes in the Baltoscandian Basin during the Ordovician: sedimentological and palaentological aspects. *Acta Palaentologica Sinica 46*, 108-113.

Dunham, R. J., 1962: Classification of carbonate rocks according to depositional texture. *Memoirs American Association of Petroleum Geologists 1*, 108-121.

El Goresy, A., Ramdohr, P. & Taylor, L. A., 1971a: The geochemistry of the opaque minerals in Apollo 14 crystalline rocks. *Earth and Planetary Science Letters 13*, 121-129.

El Goresy, A., Ramdohr, P. & Taylor, L. A., 1971b: The opaque minerals in the lunar rocks from Oceanus Procellarum. *Proceedings of the Second Lunar Science Conference 1*, 219-235.

Engrand, C. & Maurette, M., 1998: Carbonaceous micrometeorites from Antarctica. *Meteoritics & Planetary Science 33 (4)*, 565-580.

Eriksson, M. E., Lindskog, A., Calner, M., Mellgren, J. I. S., Bergström, S. M., Terfelt, F., Schmitz, B., 2012: Biotic dynamics and carbonate microfacies of the conspicuous Darriwilian (Middle Ordovician) 'Täljsten' interval, south-central Sweden. *Palaeogeography, Palaeoclimatology, Palaeoecology 367–368*, 89-103.

Erlström, M., Sivhed, U. & Wikman, H. 1999: Skånes berggrund. In: Germundsson, T. & Schlyter, P. (eds.) *Atlas över Skåne*. Sveriges nationalatlas förlag.

Genge, M. J. & Grady, M., 1999: The fusion crusts of stony meteorites: Implications for the atmospheric reprocessing of extraterrestrial materials. *Meteoritics & Planetary Science 34*, 341-356.

Gounelle, M., 2011: The Asteroid-Comet Continuum: In Search of Lost Primitivity. *Elements 7 (1)*, 29 -34.

Heck, P. R., Schmitz, B., Bauer, H. & Wieler, R., 2008: Noble gases in fossil micrometeorites and meteorites from 470 Myr old sediments from southern Sweden, and new evidence for the L-chondrite parent body breakup event. *Meteoritics & Planetary Science 43 (3)*, 517–528.

Henderson, P., 1975: Reaction trends shown by chrome-spinels of the Rhum layered intrusion. *Geochimica et Cosmochimica Acta 39*, 1035-1044.

Häggström, T. & Schmitz, B., 2007: Distribution of extraterrestrial chromite in Middle Ordovician Komstad Limestone in the Killeröd quarry, Scania, Sweden. *Bulletin of the Geological Society of Denmark 55*, 37-58.

Jaanusson, V., 1973: Aspects of carbonate sedimentation in the Ordovician of Baltoscandia. *Lethaia 6*, 11-34.

Joy, K. H. & Arai, T., 2013: Lunar meteorites: new insights into the geological history of the Moon. *Astronomy & Astrophysics 54 (4)*, 28-32.

Kamenetsky, V. S., Crawford, A. J. & Meffre, S., 2001: Factors controlling chemistry of magmatic spinel: an empirical study of associated olivine, cr-spinel and melt inclusions from primitive rocks. *Journal of Petrology 42 (4)*, 655-671.

Keil, K., Haack, H. & Scott, E. R. D., 1994: Catastrophic fragmentation of asteroids : evidence from meteorites. *Planetary Space Science 42 (12)*, 1109-1122.

Kimball, K. L., 1990: Effect fo hydrothermal alteration on the composition of chromian spinels. *Contributions to Mineralogy and Petrology 105*, 337-346.

Korochantseva, V. E., Trieloff, M., Lorenz, C. A., Buykin, A. I., Ivanova, M. A., Schwarz, W. H., Hopp, J. & Jessberger, E. K., 2007: L-chondrite asteroid breakup tied to Ordovician meteorite shower by multiple isochron ^{40}Ar-^{39}Ar dating. *Meteoritics & Planetary Science 1*, 113–130.

Kröger, B. & Rasmussen, J. A., 2014: Middle Ordovician cephalopod biofacies and palaeoenvironments of Baltoscandia. *Lethaia 47 (2)*, 275-295.

Lindskog, A., 2014: Palaeoenvironmental significance of cool-water microbialites in the Darriwilian (Middle Ordovician) of Sweden. *Lethaia 47*, 187–204.

Lindskog, A., Schmitz, B., Cronholm, A. & Dronov, A., 2012: A Russian record of a Middle Ordovician meteorite shower: Extraterrestrial chromite at Lynna River, St. Petersburg region. *Meteoritics & Planetary Science 47 (8)*, 1274-1290.

Lindström, M., Floden, T., Grahn, Y. & Kathol, B., 1994: Postimpact deposits in Tvaren, a marine Middle Ordovician crater south of Stockholm, Sweden. *Geological Magazine 131 (1)*, 91-103.

Lindström, M., 1963: Sedimentary folds and the developement of limestone in an early Ordovician sea. *Sedimentology 2*, 243-292.

Machel, H. G., 2001: Bacterial and thermochemical sulfate reduction in diagenetic settings - old and new insights. *Sedimentary Geology 140*, 143-175.

Meier, M. M. M., Schmitz, B., Bauer, H. & Wieler, R., 2010: Noble gases in individual L chondritic micrometeorites preserved in an Ordovician limestone. *Earth and Planetary Science Letters 290*, 54–63.

Mole, D. R., Fiorentini, M. L., Thebaud, N., Cassidy, K. F., McCuaig, T. C., Kirkland, C. L., Romano, S. S., Doublier, M. P., Belousova, E. A., Barnes, S. J. & Miller, J., 2014: Archean komatiite volcanism controlled by the evolution of early continents. *Proceedings of the National Academy of Sciences of the United States of America 111 (28)*, 10083-10088.

NASA. 2014. *The Asteroid Belt* [Online]. Lunar and Planetary Institute. Available: http://solarsystem.nasa.gov/multimedia/display.cfm?Category=Planets&IM_ID=850 2014].

Nesse, W. D. 2000. *Introduction to Mineralogy*, Oxford University Press.

Nesvorny, D., Vokrouhlicky, D., Bottke, W. F., Gladman, B. & Haggstrom, T., 2007: Express delivery of fossil meteorites from the inner asteroid belt to Sweden. *Icarus 188 (2)*, 400-413.

Nesvorny, D., Vokrouhlicky, D., Morbidelli, A. & Bottle, W. F., 2009: Asteroidal source of L chondrite meteorites. *Icarus 200 (2)*, 698-701.

Nielsen, A. T., 1995: Trilobite systematies, biostratigraphy and palaeoecology of the Lower Ordovician Komstad Limestone and Huk Forrnations, southern Scandinavia. *Fossils and Strata 38*, 1-374.

Nordlund, U., 1989: Lithostratigraphy and sedimentology of a Lower Ordovician limestone sequence at Hälludden Öland Sweden. *Geologiska Foreningens i Stockholm Forhandlingar 111 (1)*, 65-94.

Onyeagocha, A. C., 1974: Alteration of chromite from the Twin Sister Dunite, Washington. *American Mineralogist 59*, 608-612.

Papike, J. J., Ryder, G. & Shearer, C. K. 1998. Lunar samples. *In*: Papike, J. J. (ed.) *Planetary Materials*. Washington: The Mineralogical Society of America.

Papike, J. J., Taylor, L. & Simon, S. 1991. Lunar minerals. *In*: Heiken, G. H., Vaniman, D. T. & French, B. M. (eds.) *Lunar Sourcebook, a User's Guide to the Moon*. Cambridge University Press.

Parashar, K., Prasad, M. S. & Chauhan, S. S. S., 2010: Investigations on a large collection of cosmic dust from the Central Indian Ocean. *Earth Moon Planets 107*, 197-217.

Pieters, C. M., Besse, S., Boardman, J., Buratti, B., Cheek, L., Clark, R. N., Combe, J. P., Dhingra, D., Goswami, J. N., Green, R. O., Head, J. W., Isaacson, P., Klima, R., Kramer, G., Lundeen, S., Malaret, E., McCord, T., Mustard, J., Nettles, J., Petro, N., Runyon, C., Staid, M., Sunshine, J., Taylor, L. A., Thaisen, K., Tompkins, S. & Whitten, J., 2011: Mg-spinel lithology: A new rock type on the lunar farside. *Journal of Geophysical Research-Planets 116*, 1-14.

Puura, V. & Suuroja, K., 1992: Ordovician impact crater at Kardla, Hiiumaa Island, Estonia. *Tectonophysics 216 (1-2)*, 143-156.

Ramdohr, P., 1967: Die schmelzkruste der meteoriten. *Earth and Planetary Science Letters 2*, 197-209.

Resing, J. A., Rubin, K. H., Embley, R. W., Lupton, J. E., Baker, E. T., Dziak, R. P., Baumberger, T., Lilley, M. D., Huber, J. A., Shank, T. M., Butterfield, D. A., Clague, D. A., Keller, N. S., Merle, S. G., Buck, N. J., Michael, P. J., Soule, A., Caress, D. W., Walker, S. L., Davis, R., Cowen, J. P., Reysenbach, A.-L. & Thomas, H., 2011: Active submarine eruption of boninite in the northeastern Lau Basin. *Nature Geoscience 4 (11)*, 799-806.

Roeder, P. L., 1994: Chromite: from the fiery rain of chondrules to the Kilauea Iki Lava lake. *The Canadian Mineralogist 32*, 729-746.

Schmitz, B., 2013: Extraterrestrial spinels and the astronomical perspective on Earth's geological record and evolution of life. *Chemie der Erde/ Geochemistry 73 (2)*, 117-145.

Schmitz, B., Harper, D. A. T., Peucker-Ehrenbrink, B., Stouge, S., Alwmark, C., Cronholm, A., Bergström, S. M., Tassinari, M. & Xiaofeng, W., 2008: Asteroid breakup linked to the Great Ordovician Biodiversification Event. *Nature Geoscience 1 (1)*, 49-53.

Schmitz, B., Huss, G. R., Meier, M. M. M., Peucker-Ehrenbrink, B., Churche, R. P., Cronholm, A., Davies, M. B., Heck, P. R., Johansen, A., Keil, K., Kristiansson, P., Ravizza, G., Tassinari, M. & Terfelt, F., 2014: A fossil winonaite-like meteorite in Ordovician limestone: A piece of the impactor that broke up the L-chondrite parent body? *Earth and Planetary Science Letters 400*, 145–152.

Schmitz, B. & Häggström, T., 2006: Extraterrestrial chromite in Middle Ordovician marine limestone at Kinnekulle, southern Sweden—Traces of a major asteroid breakup event. *Meteoritics & Planetary Science 41 (3)*, 455-466.

Schmitz, B., Lindström, M., Asaro, F. & Tassinari, M., 1996: Geochemistry of meteorite-rich marine limestone strata and fossil meteorites from the lower Ordovician at Kinnekulle, Sweden. *Earth and Planetary Science Letters 145*, 31-48.

Schmitz, B., Tassinari, M. & Peucker-Ehrenbrink, B., 2001: A rain of ordinary chondritic meteorites in the early Ordovician. *Earth and Planetary Science Letters 194*, 1-15.

Stevens, R. E., 1944: Composition of some chromites of the western hemisphere. *Journal of The Mineralogical Society of America 29*, 1-34.

Thorslund, P., Wickman, F. E. & Nyström, J. O., 1984: The Ordovician chondrite from Brunflo, central Sweden, I. General description and primary minerals. *Lithos 17*, 87-100.

Torsvik, T. H., Smethurst, M. A., Van der Voo, R., Trench, A., Abrahamsen, N. & Halvorsen, E., 1992: Baltica. A synopsis of Vendian-Permian palaeomagnetic data and their palaeotectonic implications. *Earth-Science Reviews 33*, 133-152.

Trela, W., 2008: Sedimentary and microbial record of the Middle/Late Ordovician phosphogenetic episode in the northern Holy Cross Mountains, Poland. *Sedimentary Geology 203*, 131–142.

Weisberg, M. K., McCoy, T. J. & Krot, A. N. 2006. Systematics and evaluation of meteorite classification. *In*: Lauretta, D. S. & Mcsween, H. Y. (eds.) *Meteorites and the Early Solar System II*. The University of Arizona Press.

Vernazza, P., Binzel, R. P., Thomas, C. A., DeMeo, F. E., Bus, S. J., Rivkin, A. S. & Tokunaga, A. T., 2008: Compositional differences between meteorites and near-Earth asteroids. *Nature 454 (7206)*, 858-860.

Winter, J. D. 2010. *Principles of Igneous and Metamorphic Petrology*, United States of America, Pearson Education, Inc.

Wlotzka, F., 2005: Cr spinel and chromite as petrogenetic indicators in ordinary chondrites: Equilibration temperatures of petrologic types 3.7 to 6. *Meteoritics & Planetary Science 40 (11)*, 1673–1702.

Wood, B. J. & Virgo, D., 1989: Upper mantle oxidation state: Ferric iron contents of lherzolite spinels by ^{57}Fe Mössbauer spectroscopy and resultant oxygen fugacities. *Geochimica et Cosmochimica Acta 53*, 1277-1291.

Appendix A

Element signatures of chrome spinel grains 63-355 μm from this study

Table 1. 405 'true' EC grains. Oxide wt% ± 1 s.d. Oxide wt% ± 1 s.d., n.d. = not detected.
Cr# = Cr/(Cr+Al), **Fe#** = $Fe^{2+}/(Mg+Fe^{2+})$

Grain	MgO	Al_2O_3	TiO_2	V_2O_3	Cr_2O_3	MnO	FeO	ZnO	Total	Cr#	Fe#
1	3.78	5.74	3.32	0.71	58.28	0.84	26.76	0.35	99.79	0.87	0.80
2	3.32	6.00	2.76	0.67	57.40	0.96	25.54	1.50	98.17	0.87	0.81
3	2.65	6.11	2.88	0.76	58.71	0.89	27.66	1.30	100.96	0.87	0.85
4	2.82	6.47	3.08	0.74	57.59	1.16	25.95	0.57	98.39	0.86	0.84
5	2.85	6.01	3.01	0.69	58.29	0.72	27.91	n.d.	99.47	0.87	0.85
6	3.53	6.18	3.21	0.69	57.64	0.76	27.14	0.33	99.47	0.86	0.81
7	2.44	5.72	3.13	0.77	57.01	0.92	28.17	0.69	98.85	0.87	0.87
8	2.69	5.17	3.21	0.83	59.49	0.73	25.91	0.52	98.54	0.89	0.84
9	2.61	7.16	2.20	0.78	57.97	0.92	27.11	0.58	99.33	0.84	0.85
11	2.11	6.03	2.52	0.72	57.39	1.06	28.01	1.01	98.85	0.86	0.88
12	3.59	6.39	2.89	0.71	57.26	0.89	27.14	0.50	99.37	0.86	0.81
13	2.82	6.01	3.22	0.79	59.96	0.76	27.49	0.37	101.41	0.87	0.85
14	3.33	6.28	2.85	0.83	59.25	0.97	26.69	0.56	100.47	0.86	0.82
15	2.61	6.64	2.02	0.75	57.44	1.04	27.70	0.56	98.77	0.85	0.86
16	2.94	6.13	2.64	0.85	57.62	0.91	28.15	0.27	99.50	0.86	0.84
18	2.37	5.96	2.41	0.71	56.45	1.12	27.92	0.99	97.93	0.86	0.87
19	3.35	6.06	3.15	0.81	58.35	0.98	27.37	0.45	100.53	0.87	0.82
21	3.16	6.04	3.04	0.87	58.14	0.85	27.44	0.51	100.06	0.87	0.83
22	3.16	6.73	1.45	0.60	58.27	0.77	25.75	0.94	97.67	0.85	0.82
23	1.50	6.25	3.05	0.71	55.27	0.93	29.92	0.91	98.54	0.86	0.92
25	2.32	5.95	3.08	0.69	57.03	0.63	29.13	n.d.	98.83	0.87	0.88
26	3.22	5.94	3.23	0.67	58.19	0.62	27.77	0.40	100.04	0.87	0.83
27	2.54	6.03	2.89	0.72	58.98	n.d.	28.91	0.49	100.58	0.87	0.86
28	3.31	5.92	3.49	0.71	59.20	0.78	27.75	0.63	101.79	0.87	0.83
30	3.43	5.89	2.91	0.82	59.01	0.89	27.15	0.68	100.77	0.87	0.82
31	3.27	6.02	3.02	0.77	58.50	0.91	28.81	n.d.	101.29	0.87	0.83
32	1.81	5.15	3.25	0.88	60.06	0.85	27.49	0.67	100.17	0.89	0.90
33	2.75	6.00	3.29	0.88	58.46	1.04	28.09	0.56	101.06	0.87	0.85
34	2.80	5.57	2.40	0.76	58.85	0.58	29.01	0.71	100.67	0.88	0.85
35	3.30	6.28	2.97	0.69	58.87	0.76	28.46	n.d.	101.33	0.86	0.83
37	4.10	5.73	3.01	0.71	57.26	0.72	26.89	0.64	99.07	0.87	0.79
38	3.59	6.17	3.20	0.77	59.72	0.90	26.84	0.53	101.72	0.87	0.81
42	3.27	6.04	3.11	0.88	60.14	1.12	26.81	0.62	101.98	0.87	0.82
44	3.49	6.16	3.10	0.66	58.40	0.76	27.41	1.17	101.15	0.86	0.82
45	2.49	6.04	3.03	0.72	58.32	0.95	30.12	n.d.	101.66	0.87	0.87
51	3.24	5.84	3.49	0.78	58.72	1.12	27.93	0.57	101.70	0.87	0.83
52	3.28	5.93	3.19	0.85	58.55	1.03	28.22	0.81	101.86	0.87	0.83
53	3.54	5.90	2.99	0.87	58.30	0.90	26.73	0.66	99.89	0.87	0.81

54	3.45	5.71	3.27	0.84	59.14	1.10	27.98	n.d.	101.48	0.87	0.82
55	3.74	5.87	3.06	0.65	59.44	0.75	27.36	0.46	101.32	0.87	0.80
56	2.82	5.83	3.11	0.64	59.18	0.82	27.71	0.22	100.33	0.87	0.85
58	1.81	6.15	2.21	0.59	58.01	1.03	26.17	3.10	99.06	0.86	0.89
59	4.97	6.50	3.02	0.61	59.70	0.84	25.59	0.60	101.84	0.86	0.74
60	5.31	6.30	2.61	0.71	59.70	0.85	24.60	n.d.	100.09	0.86	0.72
61	2.79	6.03	2.89	0.76	57.64	0.78	29.01	0.47	100.37	0.87	0.85
62	2.46	5.85	1.83	0.75	58.88	0.73	26.85	0.65	97.98	0.87	0.86
67	3.34	5.70	3.12	0.67	57.24	0.84	26.83	0.64	98.38	0.87	0.82
68	1.56	6.03	2.92	0.73	56.55	0.89	28.69	1.14	98.50	0.86	0.91
69	2.66	5.91	2.97	0.65	57.61	0.95	28.09	0.65	99.50	0.87	0.86
72	2.37	5.58	3.17	0.68	56.73	0.72	28.39	0.50	98.15	0.87	0.87
73	2.66	6.30	2.42	0.74	57.22	1.09	27.23	0.75	98.42	0.86	0.85
74	2.58	5.63	3.17	0.62	57.93	0.82	27.83	0.26	98.86	0.87	0.86
75	2.18	6.00	2.65	0.81	57.06	0.62	28.70	0.33	98.36	0.86	0.88
76	1.84	5.72	2.33	0.68	56.72	0.87	28.74	1.31	98.20	0.87	0.90
77	2.66	6.42	3.10	0.65	58.10	0.85	25.81	0.51	98.10	0.86	0.85
78	1.92	6.34	2.83	0.73	56.39	0.91	29.05	0.36	98.54	0.86	0.89
79	3.07	5.81	2.87	0.68	58.57	0.66	24.75	0.84	97.25	0.87	0.82
80	2.54	6.03	3.06	0.72	59.56	0.89	27.49	0.56	100.86	0.87	0.86
81	1.44	5.38	2.27	0.73	57.76	0.85	27.29	2.35	98.06	0.88	0.91
82	3.04	5.85	2.73	0.66	57.72	0.85	26.34	0.90	98.10	0.87	0.83
83	1.91	5.38	3.14	0.62	56.96	0.63	29.66	0.28	98.59	0.88	0.90
84	5.62	5.88	3.23	0.64	58.50	0.76	24.05	0.29	98.96	0.87	0.71
85	3.27	5.73	3.25	0.69	58.67	0.91	27.70	0.46	100.69	0.87	0.83
86	3.14	6.06	3.06	0.78	57.37	1.02	27.68	0.41	99.53	0.86	0.83
87	2.78	6.18	2.55	0.75	58.06	1.27	26.61	0.66	98.89	0.86	0.84
88	2.53	5.81	2.47	0.6	57.69	1.03	27.88	0.55	98.57	0.87	0.86
89	2.08	6.32	3.30	0.72	57.22	1.07	26.12	1.52	98.36	0.86	0.88
90	2.30	5.84	3.13	0.73	56.43	1.11	26.04	2.43	98.03	0.87	0.86
91a	2,88	7.20	3.33	0.78	56.82	1.12	27.14	0.72	100.00	0.84	0.84
92	3.62	5.69	1.38	0.58	57.16	0.87	27.75	0.82	98.00	0.87	0.81
95	3.06	5.74	2.93	0.70	57.98	0.89	27.18	0.77	99.25	0.87	0.83
96	2.76	5.92	1.80	0.64	58.03	0.86	28.31	0.82	99.14	0.87	0.85
98	4.48	5.64	3.54	0.79	59.22	0.66	23.89	n.d.	98.22	0.88	0.75
99	3.70	5.73	3.07	0.66	57.74	0.98	26.72	0.25	98.85	0.87	0.80
101	2.76	6.21	3.00	0.60	57.84	0.94	28.27	0.36	99.95	0.86	0.85
102	3.74	6.03	3.02	0.74	57.10	0.82	26.82	0.31	98.59	0.86	0.80
103	3.00	5.87	2.70	0.96	56.98	1.04	27.27	0.27	98.09	0.87	0.84
104	3.06	5.92	3.03	0.70	57.21	0.91	27.12	0.45	98.41	0.87	0.83
106	3.01	5.82	3.13	0.67	57.02	0.80	27.90	0.43	98.78	0.87	0.84
109	2.29	6.44	2.80	0.79	58.17	0.64	29.32	0.28	100.73	0.86	0.88
111	3.69	6.34	3.23	0.80	58.07	0.88	27.02	0.43	100.45	0.86	0.80
113	3.95	5.96	3.36	0.62	56.34	0.82	26.35	0.55	97.95	0.86	0.79
114	2.43	5.76	3.18	0.72	58.51	0.82	27.83	n.d.	99.25	0.87	0.87
115	2.60	5.98	2.96	0.78	59.02	0.88	28.40	0.57	101.20	0.87	0.86
116	3.05	5.90	2.51	0.68	57.95	0.75	28.79	0.57	100.20	0.87	0.84

117	3.43	6.27	3.20	0.68	58.74	1.18	27.74	0.57	101.80	0.86	0.82
118	3.52	5.89	3.53	0.74	58.58	0.83	27.87	0.72	101.68	0.87	0.82
120	3.13	6.03	3.08	0.67	58.37	0.72	27.83	0.35	100.17	0.87	0.83
121	2.25	5.97	3.15	0.60	58.05	0.85	28.50	0.31	99.69	0.87	0.88
122	3.52	6.26	2.96	0.70	57.56	0.86	27.54	0.67	100.07	0.86	0.81
123	3.85	6.01	3.24	0.85	58.10	0.74	27.45	0.49	100.72	0.87	0.80
124	2.98	6.15	3.01	0.68	59.44	1.08	28.62	0.39	102.34	0.87	0.84
125	2.77	6.09	3.13	0.74	58.59	1.00	29.25	0.39	101.96	0.87	0.86
127	3.52	6.32	3.37	0.85	58.61	1.10	26.41	n.d.	100.18	0.86	0.81
128	2.58	6.22	2.99	0.78	57.83	0.98	27.34	n.d.	98.71	0.86	0.86
129	2.49	5.59	3.45	0.71	59.27	1.05	27.61	1.02	101.18	0.88	0.86
130	4.05	5.90	3.07	0.71	57.90	0.75	26.98	0.57	99.94	0.87	0.79
131	2.16	6.22	2.82	0.73	57.45	0.95	29.28	0.41	100.02	0.86	0.88
132	2.64	6.15	3.06	0.69	56.55	0.59	27.92	0.40	98.00	0.86	0.86
135	2.24	6.34	3.26	0.86	56.39	0.98	28.39	0.95	99.41	0.86	0.88
137	3.05	5.86	3.20	0.63	57.07	0.70	28.15	0.42	99.09	0.87	0.84
138	1.66	6.17	3.84	0.73	54.23	1.07	26.33	4.21	98.24	0.86	0.90
139	1.45	6.16	2.89	0.67	56.60	0.83	27.26	3.16	99.00	0.86	0.91
142	3.17	5.97	3.08	0.74	57.36	0.95	27.53	0.43	99.24	0.87	0.83
143	2.51	5.96	3.24	0.86	59.59	0.96	25.89	n.d.	99.00	0.87	0.85
144	2.45	5.68	3.09	0.71	56.99	0.92	28.17	0.69	98.70	0.87	0.87
145	2.71	6.06	3.08	0.75	57.79	0.86	28.54	0.39	100.17	0.86	0.86
146	2.08	5.31	2.72	0.66	57.87	1.03	28.11	1.07	98.85	0.88	0.88
148	3.01	6.15	2.81	0.83	58.01	1.05	27.92	0.80	100.58	0.86	0.84
149	2.90	6.42	3.04	0.78	57.21	1.01	27.90	0.38	99.64	0.86	0.84
150	2.98	6.21	2.99	0.72	58.40	0.84	27.12	0.39	99.65	0.86	0.84
155	2.53	6.32	2.85	0.76	57.21	0.93	27.62	0.33	98.56	0.86	0.86
158	2.93	5.65	3.15	0.74	58.27	0.82	27.01	0.70	99.27	0.87	0.84
159	2.78	5.87	2.54	0.73	57.53	0.94	27.63	0.85	98.86	0.87	0.85
160	3.71	6.63	2.61	0.83	57.64	0.82	26.84	0.55	99.62	0.85	0.80
161	3.32	5.69	3.08	0.71	58.08	1.21	27.37	0.50	99.98	0.87	0.82
162	3.35	6.26	3.12	0.67	57.28	0.69	27.32	0.33	99.04	0.86	0.82
163	3.49	6.43	3.17	0.79	57.83	1.14	27.71	0.63	101.19	0.86	0.82
168	3.12	5.83	3.04	0.67	57.63	1.00	27.38	0.12	98.80	0.87	0.83
169	2.61	6.28	3.17	0.75	57.87	0.84	28.50	0.21	100.24	0.86	0.86
172	2.46	5.94	2.70	0.73	56.63	0.94	27.67	0.64	97.70	0.86	0.86
173	2.39	5.48	1.89	0.64	59.62	1.00	27.69	0.83	99.54	0.88	0.87
174	2.64	5.54	3.06	0.77	57.94	1.11	28.00	0.37	99.43	0.88	0.86
175	2.06	6.02	1.75	0.64	56.66	0.71	28.45	0.82	97.11	0.86	0.89
176	2.30	5.79	3.36	0.66	57.51	0.93	28.63	0.85	100.02	0.87	0.88
177	2.76	5.87	2.84	0.72	57.73	0.61	28.29	0.76	99.58	0.87	0.85
178	3.73	6.28	3.00	0.82	58.77	0.83	24.82	0.91	99.15	0.86	0.79
179	2.33	5.88	3.45	0.64	58.21	0.62	26.74	0.76	98.64	0.87	0.87
180	3.10	6.14	2.92	0.86	56.84	1.02	27.76	0.41	99.05	0.86	0.83
181	4.17	5.71	3.43	0.66	58.49	0.67	25.08	0.59	98.78	0.87	0.77
182	2.91	5.94	3.11	0.73	58.72	0.69	27.68	0.51	100.30	0.87	0.84
183	3.13	6.09	3.04	0.71	58.84	0.79	27.12	0.74	100.44	0.87	0.83
184	2.53	5.91	3.29	0.70	58.17	0.86	27.64	0.34	99.45	0.87	0.86

185	2.46	6.24	3.04	0.62	58.22	1.06	23.85	1.81	97.31	0.86	0.85
186	3.30	6.04	3.06	0.80	58.45	0.85	27.46	0.48	100.44	0.87	0.82
189	3.38	5.81	3.33	0.77	58.53	0.92	27.83	n.d.	100.56	0.87	0.82
191	3.02	6.27	3.09	0.69	58.36	0.91	28.63	0.51	101.49	0.86	0.84
193	3.36	6.56	1.92	0.69	59.57	0.70	27.70	0.40	100.90	0.86	0.82
194	2.63	5.00	2.69	0.70	59.66	1.01	28.42	1.42	101.54	0.89	0.86
195	2.32	5.93	2.90	0.61	56.29	0.72	28.69	0.79	98.26	0.86	0.87
196	2.66	5.99	2.41	0.58	58.43	0.86	27.85	0.84	99.61	0.87	0.85
197	2.89	6.01	3.24	0.73	57.92	0.78	26.80	0.31	98.69	0.87	0.84
198	5.48	5.54	3.18	0.77	60.47	0.82	25.19	0.48	101.94	0.88	0.72
199	2.84	5.99	2.87	0.65	58.44	0.72	27.56	0.28	99.35	0.87	0.85
200	3.23	5.96	2.96	0.80	58.20	0.87	27.79	n.d.	99.82	0.87	0.83
201	1.90	6.43	2.55	0.75	59.13	1.09	26.38	2.35	100.58	0.86	0.89
202	4.82	5.84	3.25	0.70	59.19	0.83	26.67	0.25	101.55	0.87	0.76
203	1.94	5.95	2.68	0.60	58.15	0.84	26.75	2.74	99.65	0.87	0.89
205	3.50	5.87	3.00	0.68	58.16	0.94	27.25	0.80	100.19	0.87	0.81
206	6.34	6.27	3.21	0.72	58.11	0.89	24.28	0.56	100.38	0.86	0.68
207	5.48	5.95	2.80	0.68	58.21	0.75	27.41	n.d.	101.29	0.87	0.74
208	5.43	6.01	3.24	0.64	58.32	0.65	24.15	n.d.	98.45	0.87	0.71
210	3.23	6.16	2.65	0.72	58.74	0.77	28.33	0.47	101.08	0.86	0.83
211	2.80	6.17	3.13	0.68	57.53	1.02	28.26	0.14	99.72	0.86	0.85
212	5.14	5.87	2.50	0.72	57.75	0.73	25.58	0.50	98.78	0.87	0.74
214	2.67	5.87	2.76	0.67	59.21	0.94	28.41	0.34	100.87	0.87	0.86
215	2.57	6.67	2.99	0.69	58.33	0.95	28.42	0.51	101.14	0.85	0.86
217	2.86	5.78	3.44	0.67	58.46	0.87	28.62	0.52	101.21	0.87	0.85
218	3.53	5.96	3.06	0.80	59.12	0.97	27.74	0.31	101.47	0.87	0.82
219	2.66	6.29	3.06	0.70	58.63	1.12	27.84	0.40	100.69	0.86	0.85
220	2.27	5.99	2.19	0.56	57.82	0.88	28.64	0.70	99.05	0.87	0.88
221	2.33	6.08	3.07	0.76	58.99	0.75	27.23	0.48	99.68	0.87	0.87
222	2.14	5.77	3.14	0.74	57.12	0.83	26.90	2.64	99.28	0.87	0.88
223	3.70	6.16	2.85	0.79	58.82	0.90	26.85	0.66	100.73	0.87	0.80
224	2.86	6.01	2.70	0.78	59.10	0.86	27.19	0.55	100.06	0.87	0.84
225	2.68	5.85	2.62	0.61	58.50	0.78	28.06	0.45	99.56	0.87	0.85
226	3.74	6.08	3.04	0.85	58.12	0.80	27.35	0.43	100.42	0.87	0.80
228	2.50	5.97	2.96	0.69	58.71	0.85	26.81	1.20	99.68	0.87	0.86
229	2.17	5.80	2.76	0.65	58.25	0.76	27.01	0.57	97.98	0.87	0.88
230	3.08	5.97	3.18	0.77	58.27	0.88	28.08	0.47	100.71	0.87	0.84
231	3.40	5.81	3.07	0.69	59.06	1.05	27.62	0.65	101.34	0.87	0.82
232	1.38	6.10	2.89	0.84	58.13	0.92	28.39	2.71	101.36	0.86	0.92
233	3.05	6.05	3.24	0.64	57.93	0.92	27.94	0.11	99.88	0.87	0.84
234	3.36	6.00	3.06	0.82	59.19	1.19	27.51	0.31	101.43	0.87	0.82
235	2.22	6.32	3.12	0.71	58.22	0.87	29.24	0.68	101.38	0.86	0.88
236	2.67	5.86	3.24	0.63	59.06	1.00	28.03	0.34	100.83	0.87	0.86
237	3.02	5.89	3.10	0.63	58.62	0.88	28.34	0.40	100.89	0.87	0.84
238	2.37	6.21	3.09	0.69	59.33	0.75	28.38	0.37	101.19	0.87	0.87
239	2.40	5.80	2.82	0.84	59.86	0.89	27.59	0.24	100.43	0.87	0.87
240	3.32	5.98	3.34	0.68	59.49	0.71	27.87	n.d.	101.39	0.87	0.83

241	3.30	5.98	3.21	0.66	59.33	0.77	27.42	0.46	101.13	0.87	0.82
242	3.35	5.72	3.15	0.67	59.31	0.91	27.97	n.d.	101.07	0.87	0.82
244	3.86	5.48	2.99	0.74	58.45	n.d.	27.06	0.58	99.16	0.88	0.80
245	2.45	5.96	2.14	0.84	58.98	0.76	26.94	0.76	98.83	0.87	0.86
246	2.87	5.92	3.30	0.67	58.37	0.85	28.93	n.d.	100.91	0.87	0.85
248	2.61	6.16	3.25	0.69	60.63	0.84	26.81	0.59	101.59	0.87	0.85
250	3.16	6.11	1.62	0.65	57.32	0.70	28.72	0.87	99.15	0.86	0.84
251	2.49	5.98	1.70	0.69	59.80	1.00	29.02	1.03	101.71	0.87	0.87
252	3.45	6.17	2.99	0.67	57.87	1.12	26.74	0.60	99.60	0.86	0.81
253	3.06	5.90	3.31	0.71	59.08	0.69	27.40	0.67	100.81	0.87	0.83
254	2.65	6.38	2.37	0.79	58.19	0.96	28.13	0.45	99.91	0.86	0.86
255	3.47	5.47	3.53	0.65	58.54	0.75	26.56	0.24	99.21	0.88	0.81
256	3.54	6.53	2.41	0.76	58.76	1.00	26.74	0.84	100.57	0.86	0.81
257	3.01	5.94	3.14	0.70	58.64	1.00	28.23	0.41	101.07	0.87	0.84
259	2.14	6.24	3.10	0.73	58.71	0.89	28.41	0.77	100.99	0.86	0.88
260	2.68	6.44	2.09	0.76	57.81	0.95	27.97	0.76	99.46	0.86	0.85
262	1.75	6.43	2.61	0.67	56.92	0.92	27.67	2.60	99.57	0.86	0.90
263	3.27	6.18	3.10	0.85	58.74	1.08	28.27	n.d.	101.48	0.86	0.83
264	2.48	5.94	2.33	0.67	59.61	0.79	27.67	0.44	99.94	0.87	0.86
265	2.80	5.92	3.09	0.78	57.26	0.86	27.97	0.45	99.13	0.87	0.85
266	3.59	5.95	3.09	0.70	58.93	0.77	26.59	0.29	99.92	0.87	0.81
267	2.47	6.51	2.85	0.66	59.01	0.97	26.38	0.90	99.75	0.86	0.86
268	2.70	6.56	2.10	0.61	60.17	0.96	26.20	0.62	99.92	0.86	0.85
270	3.17	5.90	3.12	0.84	57.59	0.89	27.01	0.84	99.36	0.87	0.83
271	2.90	5.89	3.04	0.77	58.07	0.90	27.25	0.43	99.26	0.87	0.84
273	2.80	6.27	2.83	0.87	58.36	1.06	28.17	0.50	100.85	0.86	0.85
274	3.15	6.18	3.13	0.65	58.55	0.80	27.91	0.54	100.90	0.86	0.83
275	2.92	6.12	3.08	0.67	58.09	0.82	28.62	0.86	101.18	0.86	0.85
276	3.40	5.90	3.39	0.69	58.63	0.96	27.70	n.d.	100.69	0.87	0.82
277	3.21	5.86	3.28	0.68	58.40	0.95	28.32	0.29	100.98	0.87	0.83
278	3.01	5.51	3.34	0.80	58.25	0.82	28.13	0.46	100.32	0.88	0.84
279	4.38	6.10	2.28	0.79	59.32	0.63	25.10	0.36	98.97	0.87	0.76
280	2.67	5.97	3.27	0.69	57.37	1.04	26.76	0.32	98.09	0.87	0.85
281	3.24	5.79	3.08	0.76	58.00	0.96	27.50	n.d.	99.32	0.87	0.83
282	1.89	5.84	3.16	0.77	57.25	0.95	29.13	0.83	99.81	0.87	0.90
283	2.39	6.03	2.96	0.75	57.56	0.73	29.06	0.67	100.14	0.86	0.87
284	2.47	6.12	2.85	0.80	57.84	0.83	29.39	n.d.	100.30	0.86	0.87
286	3.19	5.98	2.65	0.71	57.68	0.89	28.28	0.50	99.89	0.87	0.83
288	2.43	6.05	3.30	0.77	59.40	0.78	25.08	0.85	98.65	0.87	0.85
289	2.30	6.08	2.18	0.56	58.38	0.82	27.46	0.95	98.73	0.87	0.87
290	2.77	5.91	3.22	0.71	58.73	0.87	26.57	0.45	99.22	0.87	0.84
291	2.93	5.90	3.16	0.72	58.28	0.76	27.88	n.d.	99.62	0.87	0.84
293	2.80	5.64	2.61	0.62	57.65	0.87	29.02	0.65	99.87	0.87	0.85
294	2.40	5.89	2.68	0.64	58.66	0.95	27.39	1.15	99.77	0.87	0.87
295	2.97	6.09	3.06	0.76	58.02	0.75	27.47	n.d.	99.11	0.86	0.84
296	3.36	5.99	3.25	0.65	57.97	0.84	27.07	0.53	99.67	0.87	0.82
297	2.47	6.28	2.97	0.71	58.10	0.99	26.54	0.58	98.64	0.86	0.86
300	4.67	6.44	2.64	0.83	60.31	0.77	25.52	n.d.	101.17	0.86	0.75

301	3.04	6.13	3.02	0.82	58.18	0.91	28.25	1.03	101.38	0.86	0.84
302	2.21	6.04	2.83	0.76	58.39	0.96	28.55	1.27	101.02	0.87	0.88
303	2.88	5.79	3.13	0.80	57.48	0.96	27.43	0.53	99.01	0.87	0.84
306	2.25	6.06	2.33	0.75	57.04	1.14	27.01	1.53	98.11	0.86	0.87
307	1.87	6.50	2.55	0.72	56.12	1.05	26.66	2.58	98.05	0.85	0.89
309	3.51	5.22	2.95	0.59	58.21	0.68	27.47	0.36	98.98	0.88	0.81
310	2.73	6.09	2.98	0.75	58.67	0.98	27.57	0.67	100.44	0.87	0.85
311	2.43	5.88	3.14	0.73	57.07	0.95	28.67	0.49	99.36	0.87	0.87
312	2.98	6.41	3.36	0.83	59.34	1.09	26.92	0.54	101.47	0.86	0.84
313	2.91	6.23	2.53	0.68	59.96	0.65	27.92	0.72	101.61	0.87	0.84
314	2.49	6.58	2.09	0.60	60.29	0.94	24.04	1.88	98.92	0.86	0.84
320	3.16	5.97	3.16	0.74	59.49	0.91	27.67	n.d.	101.10	0.87	0.83
322	3.13	6.71	2.88	0.74	58.65	0.81	26.73	0.69	100.34	0.85	0.83
324	3.47	6.25	3.15	0.63	58.24	n.d.	27.45	0.85	100.04	0.86	0.82
325	2.59	5.81	3.20	0.70	58.72	n.d.	29.70	n.d.	100.73	0.87	0.87
326	3.43	6.13	3.16	0.66	58.46	0.82	27.24	n.d.	99.89	0.86	0.82
327	3.20	6.17	3.18	0.68	58.04	0.85	27.48	n.d.	99.61	0.86	0.83
328	3.07	6.09	3.15	0.56	59.20	0.90	27.88	n.d.	100.84	0.87	0.84
330	2.46	6.51	3.12	0.84	58.16	1.06	27.29	0.33	99.78	0.86	0.86
331	3.28	6.13	3.26	0.82	58.57	0.77	27.73	0.60	101.15	0.87	0.83
332	1.94	6.51	2.61	0.73	58.07	0.88	26.90	2.20	99.84	0.86	0.89
333	2.41	6.57	3.38	0.76	59.72	n.d.	26.27	0.65	99.76	0.86	0.86
334	3.08	6.05	3.34	0.59	58.39	n.d.	28.18	0.51	100.15	0.87	0.84
335	2.20	5.93	3.09	0.75	59.14	n.d.	27.83	0.23	99.18	0.87	0.88
337	1.92	6.26	2.82	0.77	57.16	0.93	27.56	1.24	98.65	0.86	0.89
338b	2.19	5.75	2.89	0.63	58.86	0.95	27.88	0.86	100.00	0.87	0.88
339	3.26	5.80	3.06	0.69	57.40	0.91	27.08	0.45	98.63	0.87	0.82
340	2.01	6.07	2.77	0.91	56.70	0.65	28.61	0.49	98.21	0.86	0.89
341	2.65	5.86	3.02	0.71	58.43	0.76	26.55	0.36	98.36	0.87	0.85
342	2.67	5.68	3.18	0.74	56.70	0.91	27.27	1.01	98.16	0.87	0.85
343	3.18	5.75	2.03	0.65	59.23	0.79	27.17	n.d.	98.81	0.87	0.83
344	2.46	6.20	2.84	0.80	58.25	0.73	26.05	0.42	97.76	0.86	0.86
345	2.48	5.82	3.04	0.60	56.97	0.91	27.36	0.71	97.89	0.87	0.86
346	1.82	5.22	2.47	0.72	55.81	0.75	29.84	1.16	97.78	0.88	0.90
347c	1.67	5.69	2.98	0.67	58.20	0.83	28.93	1,02	100.00	0.87	0.91
348	2.69	5.91	2.53	0.71	56.39	0.61	28.40	0.62	97.86	0.86	0.86
349	2.23	5.65	3.29	0.65	57.48	0.93	25.10	3.25	98.58	0.87	0.86
350	1.38	5.93	2.64	0.77	57.38	1.00	28.84	0.87	98.80	0.87	0.92
351	2.68	5.89	3.20	0.69	57.16	0.85	27.92	0.76	99.14	0.87	0.85
352	2.96	6.31	3.13	0.63	56.54	1.06	28.45	n.d.	99.08	0.86	0.84
354	3.19	5.94	3.36	0.71	57.63	0.56	27.60	0.66	99.64	0.87	0.83
357	2.51	5.95	3.27	0.63	58.71	0.84	25.60	0.96	98.48	0.87	0.85
358	2.34	5.31	2.62	0.57	56.58	0.72	30.16	0.14	98.44	0.88	0.88
359	2.69	5.85	2.85	0.70	57.21	1.04	27.55	0.45	98.33	0.87	0.85
360	2.42	6.05	2.62	0.74	57.96	0.77	26.07	1.39	98.01	0.87	0.86
362	2.42	6.04	2.97	0.64	57.31	0.97	28.01	0.66	99.02	0.86	0.87
363	2.38	5.97	1.95	0.69	58.55	0.74	26.68	0.79	97.76	0.87	0.86

365	3.53	4.50	2.80	0.59	60.64	0.74	25.75	0.68	99.23	0.90	0.80
367	3.19	5.85	3.12	0.60	57.85	0.91	27.66	0.62	99.80	0.87	0.83
368	2.53	5.39	1.64	0.64	58.81	0.86	26.78	0.90	97.56	0.88	0.86
369	3.27	6.07	3.43	0.65	59.64	0.85	26.33	0.70	100.95	0.87	0.82
370	3.50	5.89	3.03	0.76	57.83	0.90	27.45	0.18	99.54	0.87	0.82
371	2.80	6.14	2.35	0.58	56.95	0.78	28.50	0.56	98.66	0.86	0.85
372	3.39	5.34	3.17	0.77	58.06	1.05	26.98	0.78	99.56	0.88	0.82
373	2.49	6.06	2.93	0.73	57.14	0.68	28.29	0.40	98.70	0.86	0.86
375	2.79	5.77	3.00	0.64	57.52	0.77	28.43	n.d.	98.92	0.87	0.85
376	3.35	5.87	3.01	0.76	57.43	0.87	26.84	0.10	98.23	0.87	0.82
377	2.31	6.00	3.03	0.81	56.00	1.00	28.68	n.d.	97.83	0.86	0.87
378	2.86	5.76	3.09	0.71	57.35	0.84	28.57	0.39	99.57	0.87	0.85
379	3.46	5.91	2.85	0.73	57.26	0.99	24.78	1.68	97.65	0.87	0.80
380	4.29	5.57	3.47	0.62	58.57	0.82	25.96	0.32	99.61	0.88	0.77
381	2.31	5.77	3.06	0.60	57.47	0.90	27.40	0.68	98.18	0.87	0.87
382	3.41	6.12	2.45	0.79	58.85	0.73	25.72	0.51	98.58	0.87	0.81
383	2.96	5.78	3.54	0.72	57.54	0.78	27.62	0.36	99.30	0.87	0.84
384	1.87	6.19	3.03	0.71	56.84	0.90	28.02	1.94	99.50	0.86	0.89
385	3.04	6.02	3.04	0.68	57.79	0.90	27.86	0.39	99.74	0.87	0.84
386	3.89	5.71	3.05	0.72	57.14	0.78	26.66	0.23	98.17	0.87	0.79
389	1.64	5.60	2.89	0.61	56.91	0.93	29.80	0.41	98.80	0.87	0.91
390	2.86	6.06	3.22	0.69	59.24	1.01	28.04	n.d.	101.13	0.87	0.85
392	2.70	5.83	3.27	0.77	59.21	0.91	28.46	0.34	101.50	0.87	0.86
393	2.30	5.92	3.08	0.72	58.43	1.28	28.96	n.d.	100.69	0.87	0.88
394	2.46	5.95	3.12	0.75	58.59	0.96	28.46	n.d.	100.30	0.87	0.87
396	2.43	6.25	3.15	0.80	58.32	0.93	27.05	0.76	99.68	0.86	0.86
397	3.26	5.92	3.40	0.66	57.84	0.92	27.99	n.d.	99.99	0.87	0.83
399	3.24	5.74	3.22	0.69	58.51	0.95	28.07	n.d.	100.42	0.87	0.83
400	1.93	5.87	3.40	0.84	60.58	0.70	25.00	0.31	98.61	0.87	0.88
401	2.98	5.96	3.78	0.66	58.48	0.79	27.27	n.d.	99.92	0.87	0.84
403	2.90	5.79	3.20	0.70	57.18	0.92	27.90	0.33	98.92	0.87	0.84
406	2.41	5.86	3.31	0.74	59.34	0.81	25.63	0.71	98.81	0.87	0.86
407	2.28	5.81	3.05	0.86	57.66	0.83	27.55	0.88	98.92	0.87	0.87
408	2.69	5.62	3.24	0.65	57.78	0.90	27.50	0.82	99.20	0.87	0.85
410	2.63	5.73	3.13	0.68	57.42	0.78	27.83	n.d.	98.19	0.87	0.86
411	2.11	6.56	3.11	0.83	59.85	0.77	23.01	1.58	97.81	0.86	0.86
412	2.39	5.67	3.05	0.69	57.54	0.65	28.49	n.d.	98.47	0.87	0.87
413	1.56	5.49	2.18	0.78	59.44	0.78	24.66	3.26	98.16	0.88	0.90
414	2.96	6.58	2.32	0.69	57.77	0.92	26.71	0.67	98.63	0.85	0.84
415	2.71	5.79	3.18	0.80	57.67	0.82	27.40	n.d.	98.37	0.87	0.85
416	3.66	5.71	3.22	0.72	58.30	0.85	26.82	0.54	99.82	0.87	0.80
417	2.59	5.93	2.89	0.68	57.07	0.82	28.12	n.d.	98.09	0.87	0.86
418	3.16	5.55	3.22	0.58	57.40	0.82	27.50	n.d.	98.23	0.87	0.83
419	1.95	6.18	3.08	0.70	58.12	0.59	26.72	0.28	97.63	0.86	0.89
420	2.82	5.78	3.24	0.64	57.75	0.85	28.32	n.d.	99.40	0.87	0.85
421	2.33	5.67	3.20	0.74	59.31	0.85	26.19	0.50	98.80	0.88	0.86
423	2.74	6.11	2.74	0.81	57.33	0.84	28.02	0.77	99.37	0.86	0.85
425	2.74	5.83	2.99	0.63	58.60	0.90	28.92	0.74	101.36	0.87	0.86

426	2.39	6.70	1.84	0.65	60.01	0.81	24.95	0.78	98.12	0.86	0.85
427	2.40	6.20	3.52	0.77	60.69	0.76	26.99	n.d.	101.34	0.87	0.86
428	2.49	5.79	3.18	0.70	59.11	0.70	27.53	n.d.	99.51	0.87	0.86
431	2.71	5.69	3.13	0.82	58.89	1.12	29.05	n.d.	101.42	0.87	0.86
433	2.42	5.99	3.18	0.72	58.38	1.00	29.34	n.d.	101.03	0.87	0.87
434	2.21	5.99	3.11	0.67	58.66	0.68	28.04	n.d.	99.37	0.87	0.88
435	2.68	5.98	3.05	0.74	58.38	0.96	28.18	0.57	100.55	0.87	0.86
437	2.39	6.41	2.32	0.74	57.47	0.95	28.71	0.61	99.60	0.86	0.87
439	2.67	6.20	1.91	0.61	59.42	1.09	25.06	1.03	98.00	0.87	0.84
440	3.24	6.08	3.22	0.71	57.87	0.94	27.25	0.38	99.70	0.86	0.83
441	2.32	5.89	1.39	0.55	57.76	0.78	28.95	0.78	98.42	0.87	0.88
442	2.98	6.07	3.21	0.77	58.82	0.87	26.64	0.48	99.85	0.87	0.83
443	2.92	5.95	3.33	0.65	58.22	0.79	27.98	0.36	100.20	0.87	0.84
444	2.52	6.12	2.61	0.66	56.96	0.84	28.95	0.81	99.46	0.86	0.87
445	3.47	5.76	3.08	0.70	58.46	0.58	27.48	n.d.	99.53	0.87	0.82
446	3.06	5.96	3.21	0.67	57.47	0.93	28.30	n.d.	99.60	0.87	0.84
447	2.84	5.89	2.93	0.61	57.77	0.97	28.68	n.d.	99.70	0.87	0.85
449	2.48	5.81	3.18	0.67	58.13	0.78	27.88	0.59	99.51	0.87	0.86
450	5.27	5.83	2.79	0.74	58.16	0.78	25.29	0.45	99.31	0.87	0.73
451	2.52	5.83	3.20	0.67	58.08	n.d.	29.37	n.d.	99.68	0.87	0.87
452	2.69	5.93	3.07	0.74	58.99	0.70	27.57	n.d.	99.69	0.87	0.85
453	3.43	5.94	3.16	0.76	58.90	1.02	27.82	n.d.	101.03	0.87	0.82
454	3.79	6.09	3.14	0.75	58.78	1.15	27.12	0.34	101.15	0.87	0.80
455	1.64	5.60	3.38	0.74	57.80	0.86	29.26	1.36	100.63	0.87	0.91
456	3.20	6.07	2.96	0.70	58.71	1.00	27.70	0.31	100.66	0.87	0.83
459	2.77	5.88	2.20	0.82	59.10	0.97	26.49	1.53	99.77	0.87	0.84
460	3.22	5.83	2.73	0.76	57.49	1.03	27.34	0.92	99.33	0.87	0.83
461	2.14	5.82	3.14	0.69	58.40	0.73	26.35	3.65	100.92	0.87	0.87
462	2.76	5.89	3.35	0.72	57.46	0.87	28.95	n.d.	100.01	0.87	0.86
463	3.42	6.02	3.00	0.77	58.19	0.81	28.04	n.d.	100.26	0.87	0.82
464	2.98	6.08	3.30	0.77	58.76	0.68	27.36	n.d.	99.92	0.87	0.84
466	2.60	5.74	3.03	0.76	57.94	1.00	28.17	n.d.	99.23	0.87	0.86
467d	2.81	6.27	2.68	0.77	59.14	1.09	26.51	0.73	100.00	0.86	0.84
468	2.97	5.99	3.14	0.70	58.13	0.86	27.83	0.41	100.04	0.87	0.84
469	3.84	6.01	2.79	0.79	57.93	0.98	26.45	0.44	99.22	0.87	0.79
470	2.46	6.17	2.59	0.72	57.99	0.88	28.34	n.d.	99.16	0.86	0.87
471	3.21	6.04	3.26	0.66	58.50	0.89	27.26	0.40	100.21	0.87	0.83
473	3.11	5.69	3.09	0.80	56.99	1.16	27.3	0.58	98.74	0.87	0.83
474	2.95	5.93	3.10	0.66	57.70	0.97	27.57	0.47	99.35	0.87	0.84
475	2.52	5.96	2.94	0.71	58.15	0.72	27.61	n.d.	98.61	0.87	0.86
476	3.98	5.73	2.43	0.76	56.40	0.79	27.83	0.33	98.25	0.87	0.80
478e	3.14	6.31	1.77	0.68	60.96	0.98	25.14	1.01	100.00	0.87	0.82
479	2.96	6.11	3.13	0.76	57.91	0.80	27.80	n.d.	99.47	0.86	0.84
480	4.15	5.98	3.33	0.72	58.62	0.89	25.75	0.77	100.20	0.87	0.78
481	2.66	6.06	2.86	0.80	57.70	0.88	28.00	0.72	99.68	0.86	0.86
482	2.80	5.58	3.34	0.73	57.48	0.95	28.64	0.31	99.84	0.87	0.85
483	2.99	5.62	3.12	0.76	57.61	0.75	27.93	0.44	99.23	0.87	0.84

485	2.55	5.99	1.70	0.61	57.03	0.83	28.40	0.89	98.00	0.86	0.86
488	3.43	5.88	3.28	0.79	57.58	0.93	27.53	0.57	99.99	0.87	0.82
489	2.48	6.24	2.19	0.79	57.92	0.91	27.42	0.77	98.71	0.86	0.86
490	3.10	5.95	3.18	0.70	57.66	0.94	27.60	0.32	99.45	0.87	0.83
491	2.69	6.13	3.08	0.72	57.30	0.93	27.98	0.45	99.28	0.86	0.85
492	3.44	6.09	3.50	0.61	57.81	1.08	26.99	n.d.	99.52	0.86	0.82
493	2.45	5.83	3.10	0.72	57.37	0.80	28.47	n.d.	98.75	0.87	0.87
494	2.65	6.24	2.93	0.75	57.82	0.87	26.33	0.73	98.33	0.86	0.85
495	2.44	5.96	2.74	0.76	56.99	0.95	27.42	1.35	98.62	0.87	0.86
499	4.46	6.02	2.74	0.67	57.27	0.82	25.15	1.13	98.27	0.86	0.76
500	3.34	6.15	2.62	0.66	56.66	0.83	27.30	0.47	98.03	0.86	0.82
501	2.89	5.90	2.27	0.64	57.60	0.79	27.56	0.59	98.24	0.87	0.84
502	2.92	6.07	3.16	0.72	57.91	0.68	27.05	0.47	98.97	0.86	0.84
504	3.17	5.76	3.26	0.65	57.24	0.78	27.25	0.48	98.59	0.87	0.83
505	3.78	6.42	3.01	0.71	57.68	0.61	27.32	0.38	99.91	0.86	0.80
506	4.45	6.09	3.18	0.71	57.97	0.78	26.10	0.54	99.82	0.86	0.77
508	2.43	5.95	3.35	0.71	57.32	0.58	28.38	n.d.	98.72	0.87	0.87
509	4.23	5.81	1.91	0.70	55.44	0.79	28.18	0.60	97.64	0.86	0.79
510	3.24	5.09	3.11	0.92	57.41	0.86	25.79	1.36	97.77	0.88	0.82
511	1.89	6.20	2.66	0.74	57.02	0.78	28.85	n.d.	98.14	0.86	0.90
512	2.63	6.64	2.15	0.70	56.61	0.74	27.94	0.70	98.10	0.85	0.86
513	2.75	5.92	3.13	0.65	57.07	0.75	27.88	n.d.	98.15	0.87	0.85
514	2.77	6.22	3.20	0.69	57.66	0.82	26.95	0.36	98.67	0.86	0.85
515	3.09	5.89	2.65	0.83	58.25	1.10	27.69	n.d.	99.48	0.87	0.83
516	3.16	6.11	3.09	0.65	57.98	0.93	25.23	1.09	98.23	0.86	0.82
517	2.37	6.09	2.96	0.68	56.73	0.73	29.29	n.d.	98.84	0.86	0.87
518	2.49	6.26	2.99	0.68	57.20	0.88	28.42	0.31	99.23	0.86	0.87
519	3.06	5.79	3.04	0.71	57.53	0.87	27.63	n.d.	98.64	0.87	0.84
521	2.84	6.02	2.99	0.59	57.01	1.09	27.04	0.92	98.50	0.86	0.84
522	3.43	5.89	3.04	0.62	57.14	0.72	27.19	n.d.	98.04	0.87	0.82
523	2.50	5.76	2.98	0.70	57.84	0.84	27.04	0.55	98.20	0.87	0.86
524f	2.77	6.62	2.58	0.72	58.96	1.07	26.80	0.49	100.00	0.86	0.84
525	3.01	5.95	2.99	0.69	56.72	0.96	27.54	n.d.	97.87	0.86	0.84
526	1.96	5.54	2.94	0.62	56.43	0.67	29.32	0.43	97.90	0.87	0.89
527	3.44	5.68	3.15	0.69	57.27	0.93	26.66	0.29	98.11	0.87	0.81

a - Normalized from 82.93 wt%. b - Normalized from 93.09 wt%. c - Normalized from 96.00 wt%. d - Normalized from 96.15 wt%. e - Normalized from 97.14 wt%. f - Normalized from 95.79 wt%. g - Normalized from 96.44 wt%.

Table 2. 43 Outlier EC grains. Oxide wt% ± 1 s.d., n.d. = not detected. **Cr#** = Cr/(Cr+Al), **Fe#** = $Fe^{2+}/(Mg+Fe^{2+})$

Grain	MgO	Al_2O_3	TiO_2	V_2O_3	Cr_2O_3	MnO	FeO	ZnO	Total	Cr#	Fe#
20	4.19	4.51	2.93	0.55	62.53	0.76	24.63	1.11	101.20	0.90	0.77
40	2.94	6.13	2.94	1.02	57.83	0.78	28.29	0.15	100.07	0.86	0.84
41	4.73	6.14	3.38	0.77	59.24	0.78	27.00	n.d.	102.04	0.87	0.76
46	5.27	5.83	2.94	0.61	59.20	n.d.	25.61	1.06	100.52	0.87	0.73
66a	8.07	6.87	3.50	0.62	58.64	n.d.	22.31	n.d.	100.00	0.85	0.61
97	4.97	5.09	3.21	0.48	58.92	0.66	25.74	n.d.	99.07	0.89	0.74
100b	2.23	5.90	1.74	0.53	59.10	0.75	29.23	0.51	100.00	0.87	0.88
107	5.34	6.11	2.86	0.71	59.28	0.88	24.19	0.43	99.80	0.87	0.72
112	2.25	6.08	1.61	0.54	59.62	1.10	26.93	1.16	99.28	0.87	0.87
133	4.57	5.81	3.24	0.73	58.21	0.66	26.23	0.59	100.04	0.87	0.76
136	1.05	5.21	2.85	0.73	56.34	0.94	28.09	3.06	98.28	0.88	0.94
187	5.59	5.99	2.88	0.86	59.25	0.73	23.96	0.46	99.71	0.87	0.71
188c	2.56	6.70	1.94	0.73	61.66	1.16	32.12	0.64	100.00	0.86	0.88
192	1.38	5.96	3.13	0.67	57.19	0.91	29.06	1.78	100.07	0.87	0.92
204	1.39	5.64	3.15	0.71	59.57	0.92	26.94	3.47	101.79	0.88	0.92
209	6.48	6.12	2.43	0.78	58.29	0.61	23.41	n.d.	98.13	0.86	0.67
216	4.57	6.13	2.84	0.76	59.60	0.87	26.51	0.51	101.79	0.87	0.77
227	5.39	4.94	3.14	0.74	60.16	0.87	25.29	0.40	100.93	0.89	0.73
247	3.49	5.70	2.00	0.70	61.12	1.04	24.31	1.55	99.91	0.88	0.80
261	4.85	9.33	2.48	0.45	55.56	0.66	26.32	0.19	99.83	0.80	0.75
269	5.10	6.33	3.83	0.73	57.57	0.78	26.61	n.d.	100.94	0.86	0.75
272	4.50	5.10	1.68	0.67	62.20	0.85	24.10	1.78	100.88	0.89	0.75
285	1.21	5.88	3.05	0.62	56.38	0.90	28.28	2.88	99.20	0.87	0.93
287	1.08	5.91	2.97	0.67	56.59	1.07	29.70	1.54	99.55	0.87	0.94
292	6.45	6.08	2.50	0.78	58.67	0.87	23.70	n.d.	99.05	0.87	0.67
298	2.87	6.02	3.23	0.69	61.13	0.74	26.08	0.54	101.30	0.87	0.84
308	4.55	5.67	3.29	0.76	59.49	0.56	26.63	0.41	101.36	0.88	0.77
315	1.55	5.76	3.01	0.53	53.54	0.84	33.58	0.43	99.24	0.86	0.92
316	4.70	6.20	3.09	0.76	59.26	0.85	25.92	0.54	101.32	0.87	0.76
317	9.49	6.40	1.88	0.76	60.09	n.d.	20.07	n.d.	98.70	0.86	0.54
319	4.81	6.20	3.12	0.69	58.96	n.d.	26.82	n.d.	100.61	0.86	0.76
329	1.19	6.22	3.08	0.56	56.28	0.78	28.97	2.38	99.46	0.86	0.93
336d	2.52	6.60	1.61	0.59	56.79	0.82	30.54	0.53	100.00	0.85	0.87
355	5.37	5.64	2.76	0.66	57.90	0.76	25.58	n.d.	98.68	0.87	0.73
364	1.20	5.71	2.47	0.64	57.58	0.85	29.15	2.03	99.63	0.87	0.93
438	2.67	5.85	3.22	0.50	57.92	0.72	27.04	0.51	98.44	0.87	0.85
472	5.25	5.79	3.02	0.72	59.11	1.27	23.49	1.35	100.01	0.87	0.72
477	4.52	6.76	2.56	0.76	57.47	0.72	25.58	0.33	98.71	0.85	0.76
484	0.53	5.51	3.00	0.68	56.68	0.93	26.17	6.21	99.71	0.87	0.97
486	4.98	5.73	3.05	0.68	57.24	0.56	25.88	0.35	98.48	0.87	0.75
503	4.52	5.89	2.14	0.71	57.23	n.d.	27.52	n.d.	97.99	0.87	0.77
507	0.74	6.47	1.95	0.66	57.39	0.81	27.55	2.85	98.41	0.86	0.95
520	1.16	6.00	4.13	0.66	54.05	0.78	26.16	5.27	98.20	0.86	0.93

a - Normalized from 85.25 wt%. b - Normalized from 95.90 wt%. c – Normalized from 93.09 wt%. d - Normalized from 95.07 wt%

Table 3. EC low-TiO_2 grains. Oxide wt% ± 1 s.d., n.d. = not detected. **Cr#** = Cr/(Cr+Al), **Fe#** = $Fe^{2+}/(Mg+Fe^{2+})$

Grain	MgO	Al_2O_3	TiO_2	V_2O_3	Cr_2O_3	MnO	FeO	ZnO	Total	Cr#	Fe#
36	2.62	6.42	0.76	0.51	61.85	0.73	25.57	0.82	99.27	0.87	0.85
321	2.30	6.79	1.30	0.71	60.04	1.04	26.48	1.25	99.90	0.86	0.87
361a	2.80	6.77	0.81	0.52	60.84	1.04	26.30	0.91	100.00	0.86	0.84
405b	2.57	6.79	0.90	0.56	60.32	0.78	27.15	0.91	100.00	0.86	0.86
409c	2.61	6.40	0.49	0.59	62.26	1.07	24.81	1.78	100.00	0.87	0.84
429	2.03	5.72	1.07	0.56	59.69	1.12	26.37	1.36	97.93	0.88	0.88
448	7.54	8.59	0.51	0.88	60.97	1.20	19.81	1.08	100.58	0.83	0.60

a – normalized from 91.22 wt%. b – normalized from 94.00 wt%. c – normalized from 93.81 wt%

Table 4. 23 MgO-depleted EC grains. Oxide wt% ± 1 s.d., n.d. = not detected. **Cr#** = Cr/(Cr+Al), **Fe#** = $Fe^{2+}/(Mg+Fe^{2+})$

Grain	MgO	Al_2O_3	TiO_2	V_2O_3	Cr_2O_3	MnO	FeO	ZnO	Total	Cr#	Fe#
17	n.d.	5.96	2.55	0.81	57.31	0.85	23.28	8.51	99.27	0.87	1.00
39	n.d.	5.79	2.72	0.72	58.24	0.93	30.16	2.96	101.53	0.87	1.00
57	n.d.	5.80	2.69	0.68	57.34	0.88	25.70	7.53	100.61	0.87	1.00
105	n.d.	5.65	2.42	0.73	58.00	1.05	20.58	9.84	98.27	0.87	1.00
126	n.d.	5.77	3.22	0.67	56.00	0.92	25.23	7.03	98.84	0.87	1.00
190	n.d.	6.03	2.60	0.74	57.29	0.97	27.70	5.20	100.52	0.86	1.00
249	n.d.	5.44	3.12	0.81	56.73	1.00	24.03	8.98	100.10	0.87	1.00
318	n.d.	6.43	2.11	0.65	58.58	0.76	28.51	3.36	100.41	0.86	1.00
323	n.d.	6.45	3.02	0.76	57.50	0.80	27.95	4.92	101.41	0.86	1.00
353	n.d.	5.31	3.04	0.55	56.22	1.05	25.81	7.26	99.24	0.86	1.00
366	n.d.	6.08	2.92	0.66	56.08	0.95	28.83	4.23	99.75	0.88	1.00
387	n.d.	5.35	2.94	0.77	56.52	1.02	25.79	7.62	100.03	0.86	1.00
388	n.d.	5.67	2.53	0.67	56.48	0.67	26.54	6.13	98.70	0.88	1.00
391	n.d.	5.48	3.07	0.73	57.41	1.03	25.69	8.31	101.73	0.87	1.00
395	n.d.	5.54	3.10	0.67	57.65	0.94	25.30	8.48	101.68	0.88	1.00
398	n.d.	5.96	1.91	0.68	58.27	0.93	21.05	9.46	98.26	0.87	1.00
402	n.d.	5.89	2.01	0.72	58.08	0.90	20.46	9.86	97.93	0.87	1.00
404	n.d.	5.47	3.08	0.73	56.77	0.83	27.45	6.44	100.77	0.87	1.00
422	n.d.	5.23	2.84	0.78	56.29	1.23	24.90	8.59	99.85	0.87	1.00
430	n.d.	5.49	3.00	0.69	57.82	0.76	25.24	8.99	101.98	0.88	1.00
432	n.d.	6.43	1.96	0.65	58.97	0.92	22.85	8.33	100.11	0.88	1.00
465	n.d.	5.84	2.60	0.68	57.52	0.67	27.21	6.00	100.52	0.86	1.00
498	n.d.	5.32	2.36	0.78	56.46	0.66	25.61	7.53	98.72	0.87	1.00

Table 5. Nickel-bearing EC grains. Oxide wt% ± 1 s.d. **Cr#** = Cr/(Cr+Al), **Fe#** = $Fe^{2+}/(Mg+Fe^{2+})$

Grain	MgO	Al_2O_3	TiO_2	V_2O_3	Cr_2O_3	MnO	FeO	NiO	ZnO	Total	Cr#	Fe#
243	2.30	6.11	1.88	0.63	58.91	0.78	29.14	0.21	0.69	100.65	0.87	0.88
305	8.84	5.29	1.71	0.60	61.39	n.d.	19.15	0.62	0.85	98.45	0.89	0.55
497	5.46	5.63	2.04	0.68	56.46	0.62	26.23	0.55	0.49	98.17	0.87	0.73

Table 6. Nickel-bearing OC grains. Oxide wt% ± 1 s.d., n.d. = not detected.
Cr# = Cr/(Cr+Al), **Fe#** = $Fe^{2+}/(Mg+Fe^{2+})$

Grain	MgO	Al_2O_3	TiO_2	V_2O_3	Cr_2O_3	MnO	FeO	NiO	ZnO	Total	Cr#	Fe#
243	2.30	6.11	1.88	0.63	58.91	0.78	29.14	0.21	0.69	100.65	0.87	0.88
305	8.84	5.29	1.71	0.60	61.39	n.d.	19.15	0.62	0.85	98.45	0.89	0.55
497	5.46	5.63	2.04	0.68	56.46	0.62	26.23	0.55	0.49	98.17	0.87	0.73

Table 7. 14 OC grains. Oxide wt% ± 1 s.d., n.d. = not detected. The two OC grains 'sensu stricto' in bold.
Cr# = Cr/(Cr+Al), **Fe#** = $Fe^{2+}/(Mg+Fe^{2+})$, **Fe/3+** = $Fe^{3+}/(Cr+Al+Fe^{3+})$

Grain	MgO	Al_2O_3	TiO_2	V_2O_3	Cr_2O_3	MnO	FeO	ZnO	Total	Cr#	Fe#	Fe/3+
24	9.26	5.15	n.d.	n.d.	62.96	n.d.	22.43	n.d.	99.80	0.89	0.53	0.05
29	5.31	11.41	1.87	0.36	55.25	0.71	23.76	0.68	99.35	0.77	0.72	0.00
43	5.88	12.14	2.46	0.36	54.15	0.92	24.88	n.d.	100.77	0.75	0.70	0.00
93	7.06	3.63	0.47	0.46	65.34	n.d.	25.32	n.d.	102.28	0.92	0.65	0.03
94	**7.18**	**29.32**	**0.86**	**n.d.**	**39.03**	**0.44**	**21.28**	**n.d.**	**98.12**	**0.47**	**0.62**	**0.00**
147	6.18	8.75	n.d.	0.21	53.86	n.d.	29.21	n.d.	98.21	0.81	0.69	0.09
213	5.42	9.23	0.20	n.d.	55.05	0.66	27.25	0.58	98.39	0.80	0.71	0.05
258	7.14	8.14	n.d.	n.d.	62.22	n.d.	23	0.04	100.53	0.84	0.63	0.00
356	11.33	11.78	n.d.	n.d.	56.98	n.d.	18.49	n.d.	98.57	0.76	0.44	0.03
374	13.28	11.53	0.36	n.d.	55.48	n.d.	18.34	n.d.	98.99	0.76	0.37	0.06
424	9.28	5.89	n.d.	n.d.	58.33	n.d.	24.07	n.d.	97.57	0.87	0.52	0.09
436	**13.37**	**23.56**	**n.d.**	**n.d.**	**44.94**	**n.d.**	**16.66**	**n.d.**	**98.53**	**0.56**	**0.38**	**0.02**
487	7.35	5.97	n.d.	n.d.	60.74	n.d.	26.16	n.d.	100.22	0.87	0.63	0.06
496	5.94	11.97	1.45	0.38	54.91	0.66	23.28	0.23	98.81	0.76	0.70	0.00

Table 8. The 29 grains lost during polishing – chemical data from preliminary analyses. Not normalized. Oxide wt%. n.d. = not detected.

Type	Grain	MgO	Al_2O_3	TiO_2	V_2O_3	Cr_2O_3	MnO	FeO	ZnO	Total
EC	10	4.01	9.33	1.43	0.56	53.01	1.02	19.38	4.59	93.33
EC	47	6.97	4.51	0.68	0.61	62.84	n.d.	17.15	2.15	94.90
EC	63	2.46	5.87	2.73	0.67	57.63	n.d.	24.57	5.09	99.01
EC	64	2.63	8.05	1.84	0.91	52.02	n.d.	31.95	n.d.	97.39
EC	65	1.86	6.54	0.75	0.39	55.00	n.d.	26.54	0.95	92.02
EC	70	1.33	7.26	2.77	0.60	52.87	n.d.	24.79	5.16	94.78
EC	71	0.75	4.25	2.93	0.47	51.04	n.d.	23.41	3.60	86.44
EC	108	2.45	5.81	1.55	0.80	58.34	n.d.	21.86	6.37	97.18
EC	110	1.37	7.25	2.94	0.75	55.70	n.d.	24.56	5.96	98.54
EC	119	3.79	6.97	3.02	0.90	56.68	n.d.	17.93	0.62	89.92
EC	134	4.37	1.95	0.65	0.32	53.56	n.d.	27.90	n.d.	88.74
OC/EC	140	0.36	2.04	0.83	0.70	44.08	n.d.	29.47	0.70	78.18
EC	141	n.d.	4.53	1.84	0.61	56.48	1.85	22.72	7.11	95.14
EC	151	0.73	5.04	1.74	0.65	56.61	n.d.	33.47	n.d.	98.25
EC	152	n.d.	2.79	2.03	0.53	53.92	n.d.	33.54	n.d.	92.80
EC	153	0.86	5.23	1.84	0.40	49.94	n.d.	35.79	0.51	94.56
OC/EC	154	1.62	6.12	1.65	0.46	50.71	n.d.	37.09	n.d.	97.64
EC	156	1.82	6.95	2.84	1.03	55.97	n.d.	28.81	1.06	98.48
EC	157	0.76	4.86	1.15	0.38	58.84	n.d.	26.96	2.50	95.45
EC	164	1.59	7.18	0.96	0.71	54.22	n.d.	31.48	n.d.	96.14
EC	165	0.46	2.91	1.72	0.63	54.68	n.d.	21.40	4.61	86.41
EC	166	1.38	4.95	3.11	1.02	62.39	n.d.	21.75	n.d.	94.60
EC	167	1.42	5.07	0.63	0.68	57.09	n.d.	27.44	1.22	93.54
EC	170	0.79	5.10	3.29	0.95	56.96	n.d.	27.95	5.53	100.57
EC	171	0.79	7.25	2.44	1.03	57.09	n.d.	27.96	1.59	98.15
OC/EC	299	0.96	4.97	2.97	n.d.	57.57	1.15	25.62	4.18	97.41
EC	304	0.87	3.63	1.24	0.57	55.69	1.11	28.78	n.d.	91.88
EC	457	2.16	7.17	2.32	0.83	57.61	0.94	27.65	1.24	99.93
EC	458	0.88	4.53	2.18	0.85	56.25	n.d.	27.69	1.67	94.05

Table 9. Chemical composition of chromite grains from the fossil meteorite Grå 002. Oxide wt% ± 1 s.d.
n.d. = not detected. **Cr#** = Cr/(Cr+Al), **Fe#** = $Fe^{2+}/(Mg+Fe^{2+})$

Grain	MgO	Al_2O_3	TiO_2	V_2O_3	Cr_2O_3	MnO	FeO	ZnO	Total	Cr#	Fe#
G1	2.67	5.55	3.35	0.72	57.59	0.88	28.53	0.38	99.68	0.87	0.86
G2	2.36	5.75	3.08	0.69	57.99	0.75	29.51	n.d.	100.12	0.87	0.88
G3	2.32	5.80	2.88	0.63	56.39	0.78	29.20	n.d.	97.99	0.87	0.88
G4	2.55	5.67	3.18	0.71	57.88	0.82	29.47	n.d.	100.28	0.87	0.87
G5	2.62	5.80	3.15	0.71	57.62	0.72	29.86	0.21	100.69	0.87	0.87
G6	2.33	5.80	2.98	0.77	58.16	0.77	30.24	n.d.	101.05	0.87	0.88
G7	2.51	5.72	3.15	0.72	58.87	0.94	30.10	n.d.	102.00	0.87	0.87
G8	2.35	5.88	3.21	0.74	58.39	0.86	30.15	n.d.	101.58	0.87	0.88
G9	2.22	5.78	3.04	0.77	57.97	0.94	30.34	n.d.	101.06	0.87	0.88

Table 10. Fractures and reaction rims in different grain types.

Fractures and reaction rims in 100 random EC grains:
81% fractures
22% crossed/parallel fractures
47% reaction rims
Fractures and reaction rims in the 43 outlier EC grains:
98% fractures
9% crossed/parallel fractures
35% reaction rim
Fractures and reaction rims in the 23 MgO-depleted EC grains:
87% fractures
17% crossed/parallel fractures
52% Spotted surfaces

Appendix B

Chromite data from other EC studies used in this study

Table 1. True EC grains from three intervals of the Lynna River section (Lindskog et al. 2012). Oxide wt% ± 1 s.d. n.d. = not detected.

Grain	MgO	Al_2O_3	TiO_2	V_2O_3	Cr_2O_3	MnO	FeO	ZnO	Total
LY1									
1	2.19	6.02	3.40	0.65	59.65	0.77	26.78	0.42	99.88
2	2.47	5.85	2.91	0.75	57.08	1.06	28.49	0.36	98.97
3	2.57	6.47	2.42	0.74	59.17	0.87	24.79	2.90	99.93
4	2.35	6.03	2.83	0.82	58.28	0.81	27.32	1.67	100.10
5	2.79	5.93	3.16	0.68	58.32	0.96	26.99	0.89	99.70
6	2.72	5.67	3.24	0.71	57.62	0.90	25.53	2.86	99.25
7	3.05	5.88	3.18	0.71	58.18	0.84	27.99	0.36	100.19
8	2.65	5.85	3.13	0.76	57.74	1.05	24.49	2.36	98.03
9	2.13	6.17	3.27	0.68	57.38	0.79	26.66	1.10	98.18
10	2.67	5.75	3.13	0.62	58.88	0.68	25.21	1.41	98.35
11	2.06	5.81	3.44	0.82	59.96	0.55	26.70	0.50	99.84
13	2.78	5.77	3.11	0.69	58.13	0.89	29.01	n.d.	100.39
15	2.46	5.78	3.42	0.69	57.85	0.92	26.94	0.93	98.98
16	2.52	6.31	2.84	0.81	57.98	1.01	28.16	0.51	100.13
17	2.62	6.01	3.44	0.64	58.96	0.72	25.82	1.06	99.27
18	2.85	5.88	3.25	0.67	57.38	0.83	28.36	n.d.	99.22
19	2.35	6.01	3.08	0.68	57.09	0.89	28.38	0.64	99.11
20	2.46	5.86	3.11	0.62	57.89	0.80	26.64	2.17	99.56
21	3.68	5.25	3.07	0.63	57.61	0.78	26.99	0.42	98.43
22	2.84	6.03	3.29	0.76	58.94	0.83	25.11	1.68	99.49
23	3.10	6.08	2.80	0.79	59.04	0.84	27.29	n.d.	99.94
24	2.70	6.07	3.09	0.76	60.10	0.82	22.66	2.99	99.19
25	2.02	5.77	2.75	0.81	61.21	0.59	26.24	n.d.	99.39
26	2.01	6.24	2.91	0.66	59.90	0.74	26.97	0.66	100.10
27	2.63	5.92	3.13	0.69	59.34	0.79	23.28	2.71	98.49
28	2.65	6.08	3.01	0.77	58.60	0.84	27.55	0.31	99.82
29	2.32	6.04	3.48	0.78	60.80	n.d.	23.33	2.67	99.42
31	2.46	5.69	3.18	0.67	59.12	0.95	27.09	0.34	99.50
32	2.76	6.00	3.31	0.73	57.86	0.85	27.18	0.72	99.40
33	2.21	6.00	3.16	0.83	59.39	0.78	25.67	1.09	99.13
34	1.92	6.47	3.08	0.82	60.11	0.74	25.27	0.79	99.22
35	2.54	5.90	3.33	0.77	59.22	0.74	27.14	n.d.	99.63
36	3.21	5.85	2.99	0.81	59.29	0.90	26.41	0.42	99.88
37	2.34	6.50	3.02	0.67	60.07	0.78	24.59	2.06	100.05
38	1.47	5.42	2.65	0.55	57.86	n.d.	31.59	0.42	99.97
40	3.09	6.19	3.50	0.68	59.43	0.88	25.91	0.28	99.96
41	2.92	6.13	3.23	0.85	60.24	0.77	24.56	n.d.	98.70
42	2.40	6.41	2.88	0.68	57.74	0.85	29.04	n.d.	100.01
43	2.54	6.03	3.24	0.62	58.44	0.64	26.83	0.57	98.92
44	2.09	5.99	3.02	0.64	58.64	0.76	28.60	n.d.	99.74

46	2.77	6.04	3.30	0.83	58.60	0.93	24.99	2.06	99.52
47	2.93	6.17	3.22	0.76	58.12	1.17	24.93	3.30	100.60
48	2.76	6.33	3.02	0.85	59.32	0.84	23.56	3.80	100.48
49	2.75	6.06	3.37	0.77	59.07	0.83	22.31	4.07	99.23
50	2.53	6.30	3.50	0.77	60.81	0.71	25.67	n.d.	100.29
51	2.18	6.46	2.93	0.85	60.55	0.79	25.38	0.48	99.63
52	2.81	6.39	2.88	0.83	59.93	0.85	21.86	4.63	100.16
53	2.30	5.87	3.56	0.68	60.08	0.77	24.64	2.02	99.92
54	2.15	5.89	3.04	0.68	60.50	0.93	26.57	0.46	100.22
55	2.66	6.18	2.60	0.86	59.31	0.86	27.13	0.53	100.13
56	3.20	5.83	2.83	0.76	58.22	0.88	26.91	0.85	99.47
57	3.14	6.10	3.31	0.75	58.65	0.78	26.83	0.47	100.02
58	3.00	5.93	2.96	0.65	57.61	0.81	28.24	n.d.	99.20
61	2.02	6.05	3.30	0.82	59.67	0.57	27.56	n.d.	10n.d.
62	2.84	6.08	3.26	0.67	59.66	0.82	24.81	1.65	99.79
63	2.53	6.25	3.21	0.89	59.69	1.23	21.07	4.71	99.57
64	2.90	6.22	2.73	0.90	59.07	0.85	26.53	0.77	99.96
65	2.42	6.11	3.08	0.67	58.92	1.12	18.28	8.40	99.01
66	2.70	5.67	3.30	0.63	57.95	0.79	28.61	0.65	100.30
69	2.23	6.50	2.92	0.69	59.59	0.80	27.73	0.36	100.82
70	2.16	6.11	3.13	0.81	59.82	0.68	25.76	1.44	99.90
74	2.66	6.47	2.94	0.84	60.48	0.91	23.41	2.89	100.60
77	2.15	5.91	3.01	0.67	58.81	0.88	28.94	n.d.	100.38
81	3.11	5.89	3.21	0.78	58.66	0.96	27.26	0.67	100.54
82	3.05	6.02	3.26	0.66	59.88	1.01	23.08	2.80	99.77
83	2.54	5.92	2.98	0.68	58.39	0.80	28.83	0.62	100.76
84	2.70	5.88	3.56	0.75	59.25	0.72	26.90	n.d.	99.75
85	2.26	5.97	2.72	0.81	59.26	0.79	27.97	0.67	100.45
86	3.36	5.88	3.57	0.71	59.96	0.69	26.80	n.d.	100.98
87	2.12	6.32	3.01	0.78	58.77	0.63	27.97	0.05	99.65
88	2.23	5.74	3.27	0.75	59.86	0.76	27.30	n.d.	99.91
89	3.27	5.87	2.71	0.74	58.23	1.01	26.52	0.37	98.72
90	3.20	5.70	3.04	0.59	58.11	0.92	26.55	1.02	99.12
91	2.27	5.81	3.36	0.61	57.65	0.95	27.80	0.52	98.97
92	2.46	5.84	3.20	0.68	58.57	n.d.	28.17	0.36	99.29
93	2.22	6.22	3.12	0.74	59.45	0.77	26.81	0.69	100.02
94	2.44	6.15	2.93	0.78	57.53	0.85	27.22	2.12	100.02
95	2.17	6.48	2.40	0.82	60.01	0.69	25.00	1.85	99.41
96	2.81	5.78	3.18	0.67	57.69	0.83	28.48	n.d.	99.45
97	1.88	5.94	3.42	0.77	60.71	n.d.	25.74	0.49	98.94
98	2.73	6.21	2.55	0.77	57.85	1.12	28.67	0.86	100.76
99	2.77	5.77	2.92	0.79	57.58	0.94	27.52	1.16	99.45
100	2.43	5.94	3.07	0.79	58.98	0.77	27.13	1.49	100.60
101	2.80	5.54	3.31	0.64	59.20	0.80	24.42	2.48	99.18
103	2.46	5.89	3.07	0.90	59.01	0.72	27.19	0.61	99.85
104	2.48	5.95	3.02	0.72	57.62	0.88	28.88	0.47	100.03
105	3.33	6.37	2.98	0.84	58.90	0.60	25.66	0.33	99.01

106	2.90	5.90	3.23	0.69	58.94	0.64	28.03	0.51	100.84
107	2.29	5.73	2.71	0.89	58.25	0.95	27.96	0.94	99.73
108	2.09	6.37	2.74	0.88	59.52	1.02	27.28	0.43	100.33
110	2.50	6.01	3.13	0.77	59.50	0.75	26.27	0.65	99.58
111	2.30	5.92	3.22	0.71	59.47	0.81	26.34	1.45	100.22
112	2.77	6.21	2.57	0.76	59.73	1.06	26.56	0.83	100.49
113	2.58	5.88	3.19	0.65	59.43	0.92	25.99	1.70	100.33
115	3.15	6.72	2.53	0.79	57.93	0.83	27.86	0.19	99.99
116	2.29	6.14	3.41	0.79	60.27	0.66	27.25	0.20	101.00
117	3.07	5.61	2.62	0.62	58.76	0.70	28.76	0.29	100.43
118	2.84	5.93	2.93	0.59	57.95	0.75	29.40	n.d.	100.40
120	2.24	5.68	3.08	0.69	58.00	0.82	28.80	0.78	100.08
122	2.04	6.05	3.58	0.82	59.84	0.64	26.80	0.40	100.17
123	2.74	6.12	3.43	0.78	59.89	0.86	21.89	4.12	99.83

Table 2. 60 Outlier EC grains from the three intervals from the Lynna River section (Lindskog et al. 2012). Oxide wt% ± 1 s.d. n.d. = not detected

Grain	MgO	Al_2O_3	TiO_2	V_2O_3	Cr_2O_3	MnO	FeO	ZnO	Total
LY1									
12	7.69	5.98	3.23	0.67	58.45	0.50	22.40	n.d.	98.93
30	5.31	6.01	3.31	0.77	60.01	1.13	21.52	1.28	99.35
39	2.15	6.31	1.75	0.72	61.25	0.86	21.79	3.77	98.60
47	1.65	6.31	3.47	0.86	61.24	0.61	24.03	0.43	98.60
48	1.43	5.94	3.24	0.65	60.34	0.56	26.58	n.d.	98.75
49	4.14	6.10	2.08	0.59	61.70	n.d.	24.98	0.41	10n.d.[b]
50	2.41	5.18	2.32	0.78	61.95	0.81	25.45	0.49	99.38
51	2.13	6.35	3.07	0.84	60.72	0.62	25.55	0.78	100.05
56	1.86	6.24	3.59	0.82	62.62	0.59	22.05	2.84	100.60
64	2.32	5.70	3.29	0.64	61.19	0.77	24.79	1.47	100.17
67	2.05	6.60	1.42	0.77	61.32	0.80	19.59	6.82	99.37
70	2.95	6.33	2.23	0.77	62.23	0.77	22.06	2.05	99.39
74	2.81	5.94	2.30	0.95	61.02	0.92	24.79	1.47	100.20
75	2.89	6.50	2.55	0.98	60.38	0.89	21.15	5.37	100.71
LY2Ö									
6	1.63	5.96	3.34	0.83	62.57	0.96	21.43	3.53	100.25
13	1.70	7.66	2.27	0.83	55.00	0.42	32.11	n.d.	10n.d.[c]
18	2.43	4.76	3.00	0.72	61.77	0.95	27.08	n.d.	100.71
23	3.85	5.64	3.08	0.80	61.70	0.76	22.52	1.33	99.68
29	1.59	6.27	2.91	0.87	62.98	0.67	25.02	0.38	100.69
30	1.41	6.70	3.22	0.80	63.54	0.63	23.54	0.40	100.24
31	1.93	5.68	1.98	1.02	64.10	1.15	20.89	2.93	99.66
32	2.10	6.64	3.19	0.74	62.66	0.92	21.19	3.03	100.48
33	1.79	6.11	3.28	0.67	62.31	0.73	25.11	0.32	100.32
34	1.88	6.38	3.34	0.71	61.28	0.71	22.36	3.41	100.07
35	1.41	5.44	2.05	1.02	64.89	0.75	23.14	0.74	99.44
38	2.46	6.04	3.40	0.82	61.33	0.74	23.52	1.16	99.47

40	2.73	6.75	2.27	0.69	61.13	1.03	24.10	1.36	100.06
41	2.74	6.44	3.77	0.80	61.35	0.90	21.56	1.43	99.00
43	1.69	6.39	3.24	0.64	61.02	0.49	26.24	0.28	99.97
46	6.29	5.14	2.56	0.65	60.06	0.53	24.93	0.41	100.57
54	1.49	7.03	2.93	0.82	62.53	n.d.	23.44	0.98	99.21
63	1.81	6.76	2.70	0.73	61.92	0.84	21.92	3.60	100.28
93	2.01	6.22	3.78	0.89	61.24	0.49	25.08	0.22	99.93
103	5.07	6.08	3.14	0.71	59.57	0.79	24.85	0.29	100.52
110	1.91	7.09	3.23	0.97	62.17	0.64	23.21	0.99	100.21
113	1.77	6.83	2.34	0.93	61.46	0.54	24.26	1.60	99.73
LY5									
2	4.18	5.09	1.76	0.45	59.77	0.77	26.51	0.28	98.80
10	2.51	6.21	2.08	0.74	61.22	0.78	23.61	3.08	100.22
18	2.27	6.06	3.01	0.56	56.13	0.70	31.40	0.27	100.41
19	1.97	6.54	3.57	0.80	62.49	0.82	23.24	n.d.	99.44
32	1.81	4.73	2.67	0.86	61.82	1.00	21.36	4.94	99.19
35	2.72	6.02	2.05	0.75	61.55	1.18	21.11	4.69	100.06
45	3.34	5.86	2.35	0.84	61.53	0.94	20.16	5.60	100.62
59	5.65	5.72	2.91	0.71	58.86	0.87	24.82	0.25	99.80
60	4.94	6.01	3.95	0.80	57.95	0.77	24.81	0.22	99.44
67	0.93	6.29	2.45	0.89	62.38	n.d.	26.68	n.d.	99.61
68	1.34	5.19	2.85	0.66	60.57	0.67	27.64	n.d.	98.93
71	1.49	5.50	2.16	0.95	61.05	0.83	27.22	0.30	99.50
72	2.30	5.73	2.62	0.95	61.16	1.04	25.92	0.66	100.39
73	1.68	7.19	2.77	0.86	62.24	0.62	24.60	n.d.	99.96
75	2.24	6.11	3.46	0.75	61.96	0.78	23.82	0.80	99.91
76	2.37	6.41	3.34	0.78	61.95	0.96	22.74	1.35	99.90
78	1.36	7.63	4.07	0.73	64.93	0.60	20.98	0.32	100.63
79	1.54	6.40	3.30	0.73	62.20	n.d.	24.55	0.16	98.88
80	4.98	5.78	2.86	0.65	58.07	0.81	25.64	n.d.	98.80
102	2.71	6.21	2.81	0.96	59.96	0.77	22.11	4.17	99.71
109	2.69	6.40	1.98	0.75	59.61	1.07	18.04	9.15	99.69
119	4.83	5.26	3.67	0.84	58.47	0.80	26.13	0.56	100.56
121	5.06	6.16	3.05	0.73	58.71	0.70	25.40	n.d.	99.80
124	5.84	6.47	2.79	0.73	60.69	0.74	21.46	0.88	99.61

Table 3. EC low-TiO_2 grain. Lynna River section (Lindskog et al. 2012). Oxide wt% ± 1 s.d.
n.d. = not detected.

Grain	MgO	Al_2O_3	TiO_2	V_2O_3	Cr_2O_3	MnO	FeO	ZnO	Total
114	2.38	6.26	1.27	0.88	62.23	1.11	17.98	7.31	99.42

Table 4. EC-nickel from the Lynna River section. (Lindskog et al. 2012). Oxide wt% ± 1 s.d.
n.d. = not detected

Grain	MgO	Al_2O_3	TiO_2	V_2O_3	Cr_2O_3	MnO	FeO	NiO	ZnO	Total
LY1										
14	6.94	4.86	1.99	0.58	57.70	0.77	24.09	0.74	0.90	98.56
54	2.41	6.19	3.32	0.73	59.34	0.75	24.89	0.59	1.08	99.31
58	6.58	5.96	2.35	0.68	58.47	0.80	23.36	0.53	n.d.	98.73
LY2Ö										
39	2.94	6.10	1.55	0.55	61.00	0.96	27.01	0.26	0.63	101.01
50	3.08	6.00	2.63	0.68	59.25	0.75	26.37	0.37	0.62	99.75
81	5.87	6.33	2.96	0.68	60.07	0.71	21.50	0.36	0.52	99.00
82	4.84	5.83	2.48	0.70	59.55	0.78	23.54	0.39	0.74	98.85
83	2.98	5.76	2.51	0.65	58.12	0.73	27.49	0.45	0.36	99.05
84	10.98	5.19	1.92	0.66	59.69	0.69	19.49	0.77	0.20	99.57
85	7.09	5.45	2.67	0.55	58.84	0.92	22.36	0.52	0.46	98.86
86	8.78	4.70	1.96	0.64	57.57	0.54	24.23	0.70	0.61	99.72
109	2.60	6.28	2.78	0.89	62.53	n.d.	23.48	0.32	0.61	99.48
LY5										
8	2.75	6.38	3.25	0.72	60.03	1.08	21.63	0.48	4.03	100.35

Table 5. OC grains from the Lynna River section. (Lindskog et al. 2012). Oxide wt% ± 1 s.d.
n.d. = not detected

Grain	MgO	Al_2O_3	TiO_2	V_2O_3	Cr_2O_3	MnO	FeO	ZnO	Total
LY1									
1	2.13	3.89	3.88	0.23	10.31	n.d.	76.1	n.d.	96.53
2	8.92	32.24	0.65	0.34	25.66	n.d.	31.06	0.47	99.32
LY2Ö									
1	6.04	20.53	n.d.	0.24	49.96	n.d.	22.46	n.d.	99.22
2	11.24	35.42	0.37	n.d.	30.61	0.41	20.68	n.d.	98.74
LY5									
1	11.95	24.12	0.65	n.d.	42.96	n.d.	20.84	n.d.	100.54
2	3.03	7.96	0.34	0.94	61.06	0.77	23.10	2.73	99.92
3	9.86	27.25	0.88	0.30	37.87	0.52	22.54	n.d.	99.23

Table 6. Fractures and reaction rims in EC grains from the Lynna River section (Lindskog et al. 2012).

Fractures and reaction rims in 100 random EC grains:
79% fractures
20% crossed and/or parallel fractures
8% reaction rims

Table 7. OC grains from the previous study at Killeröd (Häggström & Schmitz 2007). Oxide wt% ± 1 s.d.

Grain	MgO	Al_2O_3	TiO_2	V_2O_3	Cr_2O_3	MnO	FeO	ZnO	Total
9.71 to 9.73 m	7.42	10.72	0.17	0.17	52.8	0.54	28.04	0.11	99.97
9.73 to 9.79 m	14.21	30.82	0.57	0.50	28.34	0.35	25.1	0.04	99.93
	3.39	5.85	1.06	0.56	57.03	1.01	28.61	0.81	98.32
	3.14	7.77	1.34	0.51	56.32	0.92	29.23	0.97	100.20

Table 8. High-aluminium chromite grains from the fossil winonaite-like meteorite (Schmitz et al. 2014). Oxide wt% ± 1 s.d. n.d. = not detected. **Cr#** = Cr/(Cr+Al), **Fe#** = $Fe^{2+}/(Mg+Fe^{2+})$

Grain	MgO	Al_2O_3	TiO_2	V_2O_3	Cr_2O_3	MnO	FeO	ZnO	Total	Cr#	Fe#
Cr1	4.17	25.30	1.04	0.45	44.10	n.d.	23.90	0.59	99.53	0.54	0.76
Cr2	2.15	15.80	2.48	0.54	52.40	n.d.	26.80	0.83	101.00	0.69	0.87
Cr3	4.76	28.60	0.59	0.38	38.60	n.d.	26.30	0.89	100.10	0.48	0.76
Cr4	5.11	31.40	0.49	0.65	39.30	n.d.	23.40	0.89	101.30	0.46	0.72
Cr5	3.70	22.30	0.77	0.59	43.60	0.49	26.60	0.51	98.47	0.57	0.80
Cr6	5.15	29.60	0.50	0.59	36.70	0.37	25.50	0.83	99.17	0.45	0.74
Cr7	4.82	24.50	0.64	0.45	42.10	n.d.	25.30	0.77	98.52	0.54	0.75
Cr8	3.47	19.40	0.50	0.60	46.30	n.d.	27.90	0.47	98.59	0.62	0.82
Cr9	4.73	28.30	0.53	0.48	38.80	n.d.	26.90	0.89	100.60	0.48	0.76
Cr10	5.81	28.70	0.45	0.64	38.40	n.d.	26.00	n.d.	100.00	0.47	0.72
Cr11	3.97	20.80	0.69	0.54	47.70	n.d.	25.70	0.57	100.00	0.61	0.78
Cr12	3.96	22.00	0.61	0.57	44.20	0.64	27.30	0.50	99.73	0.57	0.79
Cr13	3.91	24.30	0.51	0.34	41.40	n.d.	27.60	0.78	98.79	0.53	0.80
Cr14	5.97	25.70	0.45	0.60	41.80	n.d.	24.00	0.69	99.25	0.52	0.69
Cr15	5.18	29.80	0.45	0.51	37.80	n.d.	25.80	0.60	100.20	0.46	0.74
Cr16	3.95	24.90	0.43	0.62	43.20	0.54	25.70	0.69	99.99	0.54	0.78
Cr17	4.70	28.40	0.55	0.53	38.30	n.d.	27.40	0.77	100.80	0.47	0.77
Cr18	5.00	27.60	0.51	0.39	39.10	n.d.	25.50	0.60	98.72	0.49	0.74
Cr19	6.07	28.00	0.68	0.45	39.40	0.51	23.90	0.50	99.60	0.49	0.69
Cr20	4.45	26.10	0.44	0.66	39.80	0.43	27.00	0.75	99.61	0.51	0.77
Cr21	4.77	28.60	0.46	0.66	39.40	0.38	24.60	1.08	99.94	0.48	0.74
Cr22	4.83	29.20	0.41	0.62	37.50	n.d.	26.80	0.89	100.20	0.46	0.76
Cr23	3.45	19.20	0.76	0.56	47.30	n.d.	27.90	0.40	99.54	0.62	0.82
Cr24	3.92	22.60	0.54	0.53	43.50	n.d.	27.20	0.69	98.88	0.56	0.80
Cr25	4.75	24.90	0.73	0.58	41.80	n.d.	27.50	0.66	100.90	0.53	0.76
Cr26	7.27	39.70	0.45	n.d.	26.70	n.d.	24.80	1.29	100.20	0.31	0.66
Cr27	4.47	23.30	0.54	0.40	43.50	n.d.	25.00	0.63	97.81	0.56	0.76
Cr28	3.87	20.30	0.75	0.54	48.40	0.47	25.50	0.45	100.20	0.62	0.79
Cr29	3.28	18.30	0.96	0.59	48.30	n.d.	27.30	0.53	99.21	0.64	0.82
Cr30	4.27	24.40	0.65	0.47	40.90	0.49	26.20	0.79	98.17	0.53	0.77
Cr31	4.62	27.00	0.50	0.41	38.00	n.d.	26.40	0.74	97.69	0.49	0.76
Cr32	7.05	29.40	0.49	0.40	37.60	0.27	23.70	0.55	99.46	0.46	0.65
Cr33	5.01	27.30	0.42	0.54	39.10	n.d.	25.40	0.72	98.49	0.49	0.74
Cr34	4.25	22.90	0.62	0.35	42.90	0.53	26.70	0.36	98.64	0.56	0.78

Cr35	4.13	22.90	0.50	0.49	42.30	0.59	26.80	0.62	98.36	0.55	0.78
Cr36	6.31	27.10	0.51	0.57	39.20	n.d.	24.40	n.d.	98.16	0.49	0.68
Cr37	7.18	34.90	0.52	n.d.	31.60	n.d.	24.10	0.97	99.28	0.38	0.65
Cr38	4.61	26.20	0.45	0.57	38.70	0.60	25.70	0.62	97.45	0.50	0.76
Cr39	5.34	29.00	0.49	0.44	36.80	n.d.	25.70	0.42	98.13	0.46	0.73
Cr40	4.54	25.00	0.57	0.40	41.10	n.d.	26.30	0.76	98.60	0.52	0.76
Cr41	5.47	29.50	0.40	0.57	35.90	n.d.	25.40	0.66	97.97	0.45	0.72

Table 9. Low-aluminium chromite grains from the fossil winonaite-like meteorite (Schmitz et al. 2014).
n.d. = not detected. **Cr#** = Cr/(Cr+Al), **Fe#** = $Fe^{2+}/(Mg+Fe^{2+})$

Grain	MgO	Al_2O_3	TiO_2	V_2O_3	Cr_2O_3	MnO	FeO	ZnO	Total	Cr#	Fe#
Cr42	1.50	0.29	0.42	1.17	70.30	0.83	25.10	0.81	100.40	0.99	0.90
Cr43	1.87	0.22	0.15	0.84	68.60	0.89	21.10	0.86	94.51	1.00	0.86
Cr44	1.74	n.d.	n.d.	1.02	69.60	0.96	20.40	1.74	95.38	1.00	0.87

Table 10. Elemental composition (wt%) of chrome spinels from winonaite Winona (Schmitz et al. 2014).
n.d. = not detected. **Cr#** = Cr/(Cr+Al), **Fe#** = $Fe^{2+}/(Mg+Fe^{2+})$, **Fe/3+** = $Fe^{3+}/(Cr+Al+Fe^{3+})$

Grain	MgO	Al_2O_3	TiO_2	V_2O_3	Cr_2O_3	MnO	FeO	ZnO	Total	Cr#	Fe#	Fe/3+
Cr1	11.50	0.52	0.31	0.47	68.20	3.24	15.10	1.67	100.90	0.99	0.34	0.06
Cr2	11.00	0.56	0.38	0.38	67.30	3.08	14.80	2.09	99.53	0.99	0.36	0.06
Cr3	10.90	0.93	0.37	0.32	67.90	2.66	14.90	2.14	100.20	0.98	0.37	0.05
Cr4	11.30	0.83	0.44	0.42	66.80	2.39	14.90	2.39	99.49	0.98	0.35	0.06
Cr5	10.10	0.68	0.37	0.35	69.70	2.95	15.20	1.83	101.20	0.99	0.42	0.03
Cr6	10.40	0.77	0.48	n.d.	69.20	2.37	15.10	2.03	100.30	0.98	0.41	0.04
Cr7	10.30	0.56	0.45	0.34	69.20	3.04	14.90	1.84	100.50	0.99	0.41	0.03
Cr8	10.70	1.29	0.56	0.34	68.20	2.41	14.90	2.15	100.50	0.97	0.39	0.04
Cr9	9.79	0.22	0.35	0.32	69.60	3.22	15.00	1.84	100.40	1.00	0.42	0.03
Cr10	9.57	0.58	0.44	0.35	69.30	3.10	15.20	1.76	100.30	0.99	0.44	0.02
Cr11	10.20	0.51	0.37	n.d.	69.50	2.87	14.90	2.16	100.50	0.99	0.40	0.04
Cr12	9.89	0.53	0.47	n.d.	69.00	2.81	15.00	2.13	99.87	0.99	0.42	0.03
Cr13	9.85	0.61	0.35	n.d.	69.00	2.93	15.40	1.99	100.10	0.99	0.42	0.04

Table 11. Elemental composition (wt%) of chrome spinels from winonaite NWA 725 (Schmitz et al. 2014).
n.d. = not detected. **Cr#** = Cr/(Cr+Al), **Fe#** = $Fe^{2+}/(Mg+Fe^{2+})$, **Fe/3+** = $Fe^{3+}/(Cr+Al+Fe^{3+})$

Grain	MgO	Al_2O_3	TiO_2	V_2O_3	Cr_2O_3	MnO	FeO	ZnO	Total	Cr#	Fe#	Fe/3+
Cr1	10.20	5.55	1.01	0.68	61.60	1.90	18.80	n.d.	99.73	0.88	0.48	0.03
Cr2	10.30	5.02	0.96	0.66	61.80	1.90	18.50	n.d.	99.15	0.89	0.47	0.03
Cr3	9.67	6.41	0.80	0.60	61.40	2.35	18.90	n.d.	100.10	0.87	0.50	0.03
Cr4	9.79	6.51	0.74	0.58	62.00	2.54	18.60	n.d.	100.80	0.86	0.49	0.02
Cr5	10.20	5.62	0.92	0.58	62.10	2.23	18.60	n.d.	100.30	0.88	0.47	0.03
Cr6	10.30	5.78	0.82	0.55	62.20	1.73	18.90	n.d.	100.20	0.88	0.48	0.03
Cr7	10.40	6.01	0.99	0.59	62.00	1.88	18.70	n.d.	100.50	0.87	0.47	0.03
Cr8	9.97	4.88	0.85	0.73	62.70	2.52	18.70	n.d.	100.30	0.90	0.48	0.03
Cr9	9.85	5.65	0.84	0.76	62.10	2.37	18.50	n.d.	100.00	0.88	0.49	0.02
Cr10	10.10	5.61	0.81	0.55	62.00	2.20	18.50	n.d.	99.73	0.88	0.48	0.03
Cr11	9.91	4.95	1.04	0.60	62.30	1.98	18.70	n.d.	99.55	0.89	0.49	0.03
Cr12	10.30	5.82	0.83	0.64	60.90	2.15	18.20	n.d.	98.79	0.88	0.46	0.03
Cr13	10.40	6.07	0.88	0.45	62.40	2.17	18.10	n.d.	100.40	0.87	0.47	0.03
Cr14	9.12	5.74	0.80	0.63	61.50	2.58	18.70	n.d.	99.06	0.88	0.52	0.02
Cr15	8.14	1.98	0.84	0.78	64.80	3.36	19.50	n.d.	99.40	0.96	0.55	0.03
Cr16	10.10	5.60	0.90	0.65	61.40	1.91	18.40	n.d.	99.05	0.88	0.48	0.03

Table 12. Elemental composition (wt%) of chrome spinels from winonaite NWA 4024 (Schmitz et al. 2014).
n.d. = not detected. **Cr#** = Cr/(Cr+Al), **Fe#** = $Fe^{2+}/(Mg+Fe^{2+})$, **Fe/3+** = $Fe^{3+}/(Cr+Al+Fe^{3+})$

Grain	MgO	Al_2O_3	TiO_2	V_2O_3	Cr_2O_3	MnO	FeO	ZnO	Total	Cr#	Fe#	Fe/3+
Cr1	3.80	14.10	1.23	0.58	52.60	1.18	27.30	n.d.	100.80	0.71	0.80	0.00
Cr2	3.44	11.70	1.21	0.85	54.20	1.24	27.40	n.d.	100.00	0.76	0.82	0.00
Cr3	3.40	11.60	1.49	0.85	54.10	1.23	27.10	n.d.	99.70	0.76	0.82	0.00
Cr4	3.96	11.90	1.62	0.93	54.50	1.33	28.10	n.d.	102.30	0.75	0.80	0.00
Cr5	3.90	13.70	1.07	0.60	52.30	1.29	27.40	n.d.	100.30	0.72	0.80	0.00
Cr6	5.01	16.60	1.17	0.48	49.60	0.93	26.80	n.d.	100.50	0.67	0.75	0.00
Cr7	3.71	11.20	1.40	0.76	54.00	1.29	27.90	n.d.	100.30	0.76	0.81	0.00
Cr8	3.61	10.90	1.34	0.83	54.40	1.33	28.20	n.d.	100.60	0.77	0.81	0.00
Cr9	3.84	11.60	1.32	0.87	54.10	1.22	27.80	n.d.	100.70	0.76	0.80	0.00
Cr10	3.68	11.20	1.34	0.80	52.80	1.34	28.80	n.d.	99.90	0.76	0.81	0.00
Cr11	3.35	11.10	0.38	0.84	56.10	1.21	27.90	n.d.	100.90	0.77	0.82	0.00
Cr12	4.20	13.90	1.16	0.61	52.00	1.21	27.80	n.d.	100.80	0.71	0.79	0.00
Cr13	3.87	12.70	1.14	0.51	52.90	1.32	27.80	n.d.	100.30	0.74	0.80	0.00
Cr14	3.77	11.10	1.20	0.79	54.50	1.34	27.70	n.d.	100.40	0.77	0.80	0.00

Appendix C

Lunar spinel data used in this study

Table 1. Lunar chromite from the Apollo 12 mission (El Goresy et al. 1971b). Oxide wt%.

sample	MgO	Al_2O_3	TiO_2	V_2O_3	Cr_2O_3	MnO	FeO	Total
12002	5.89	11.70	5.29	0.98	46.50	0.29	30.10	100.75
12063	3.94	11.00	10.80	0.92	34.90	0.20	51.60	99.56
12063	3.92	11.00	6.27	0.74	43.80	0.27	33.30	99.30
12018	3.43	11.70	4.27	0.95	46.00	0.24	32.30	98.89

Table 2. Lunar chromite from the Apollo 14 mission (El Goresy et al. 1971a). Oxide wt%.

Sample 14053,2	MgO	Al2O3	TiO2	V2O3	Cr2O3	MnO	FeO	Total
Grain 1	5.98	21.74	2.79	0.56	38.17	0.18	29.24	98.66
Grain 2	6.18	21.72	2.66	0.56	38.23	0.19	28.81	98.35
Grain 3	4.02	16.11	4.95	0.70	39.56	0.25	33.29	98.88
Grain 4	4.78	13.20	7.43	0.73	38.81	0.29	33.43	98.67

Table 3. Spinel analyses from lunar rocks and soil, (Papike et al. 1998). Oxide wt%. n.d. = not detected.

Sample	MgO	Al_2O_3	TiO_2	V_2O_3	Cr_2O_3	MnO	FeO	SiO_2	CaO	ZrO_2	Total
4	7.80	12.20	3.80	n.d.	49.10	n.d.	26.80	n.d.	n.d.	n.d.	99.70
28	4.62	20.10	3.31	0.63	39.10	0.24	31.70	n.d.	n.d.	0.04	99.74
29	0.98	21.74	2.79	0.56	38.17	0.18	29.24	n.d.	n.d.	n.d.	98.66
36	7.23	10.64	1.71	1.33	54.87	0.27	24.38	0.19	0.05	n.d.	100.67
37	6.15	10.84	2.46	n.d.	53.30	0.41	26.38	n.d.	n.d.	n.d.	100.36

Table 4. (Agrell et al. 1970)

Sample	MgO	Al2O3	TiO2	V2O3	Cr2O3	MnO	FeO	SiO2	CaO	Total
7 (85/4/14.2)	5.72	6.23	25.12	0.00	21.40	0.34	40.71	0.40	0.01	99.93

Appendix D

Terrestrial spinel data used in this study

Table 1. Representative compositions of spinel inclusions trapped in the most primitive olivines found in the studied samples (Kamenetsky et al. 2001). **Cr#** = Cr/(Cr+Al), **Fe#** = Fe^{2+}/(Mg+Fe^{2+}), **Fe/3+** = Fe^{3+}/(Cr+Al+Fe^{3+}).

Sample	MgO	Al_2O_3	TiO_2	Cr_2O_3	MnO	Fe_2O_3	FeO	FeOT	Total	Cr#	Fe#	Fe/3+
1	17.63	26.55	0.27	41.39	0.12	4.31	9.15	13.02	99.43	0.51	0.23	0.05
2	18.36	35.76	0.19	32.72	0.17	3.77	9.48	12.87	100.44	0.38	0.23	0.04
3	20.19	46.42	0.08	21.95	0.11	3.72	8.57	11.91	101.03	0.24	0.20	0.04
4	15.15	17.11	0.48	49.67	0.16	4.93	11.30	15.73	98.79	0.66	0.30	0.06
5	19.14	41.26	0.30	25.58	0.00	4.29	9.51	13.37	100.08	0.29	0.22	0.04
6	13.93	12.59	0.17	54.53	0.11	6.10	12.76	18.24	100.19	0.74	0.34	0.07
7	17.06	32.15	0.69	30.66	0.16	6.67	10.98	16.98	98.37	0.39	0.26	0.08
8	13.74	16.38	0.40	46.20	0.24	8.58	13.07	20.78	98.61	0.65	0.35	0.10
9	15.04	6.71	0.30	59.99	0.21	6.75	9.65	15.72	98.64	0.86	0.26	0.08
10	15.36	6.56	0.24	57.76	0.20	10.25	9.56	18.77	99.93	0.86	0.26	0.13
11	14.13	11.53	0.47	37.33	0.14	23.31	12.17	33.13	99.08	0.68	0.32	0.29
12	14.66	16.15	0.55	50.53	0.18	5.33	12.34	17.13	99.72	0.68	0.32	0.06
13	15.54	12.31	0.43	51.44	0.08	10.26	10.52	19.74	100.58	0.74	0.28	0.12
14	14.00	7.93	0.46	56.64	0.13	8.03	11.80	19.02	98.99	0.83	0.32	0.10
15	15.45	1.05	0.01	71.59	0.06	3.53	8.69	11.86	100.38	0.98	0.24	0.04
16	15.60	3.10	0.02	69.00	0.13	3.53	8.03	11.20	99.41	0.94	0.23	0.04
17	13.17	7.53	0.02	60.73	0.05	4.72	12.66	16.90	98.88	0.84	0.35	0.06
18	15.47	10.07	0.17	57.73	0.19	5.96	10.28	15.64	99.87	0.79	0.26	0.08
19	15.19	11.83	0.22	56.91	0.20	4.68	10.84	15.05	99.87	0.76	0.28	0.06
20	12.93	7.42	0.26	57.90	0.18	7.78	13.16	20.15	99.63	0.84	0.37	0.10
21	15.71	10.22	0.18	57.58	0.25	6.28	9.02	14.67	99.25	0.79	0.25	0.07
22	14.46	7.52	0.16	62.49	0.00	4.33	10.91	14.80	99.88	0.85	0.30	0.05
23	14.54	16.95	1.84	45.25	0.21	7.05	13.78	20.12	99.62	0.64	0.35	0.09
24	13.69	16.19	1.55	45.42	0.15	8.17	14.78	22.12	99.95	0.65	0.38	0.10
25	11.72	15.49	1.48	43.89	0.26	10.20	17.72	26.89	100.76	0.66	0.46	0.13
26	12.11	11.52	4.43	44.43	0.22	8.34	18.61	26.11	99.64	0.72	0.47	0.11
27	10.17	10.67	1.92	48.95	0.15	8.02	19.12	26.33	98.99	0.75	0.52	0.10
28	9.80	9.01	4.95	41.72	0.25	12.30	22.49	33.55	100.53	0.76	0.57	0.17
29	14.32	6.79	4.02	48.30	0.13	11.77	14.23	24.81	99.56	0.83	0.36	0.16
30	16.76	20.59	0.69	46.04	0.09	5.46	9.70	14.61	99.32	0.60	0.25	0.06

1-4 MORB; 5-9 Backarc basin basalt; 10-14 Island arc high-k & calc-alkaline series; 15-22 Island arc boninitic & tholeitic series; 23-25 Ocean Island basalts; 26-30 Large Igneous Province basalt.

Table 2. Representative electron microprobe analyses of chromite microphenocrysts in Heathcote boninites (Crawford & Cameron 1985). **Cr#** = Cr/(Cr+Al), **Fe#** = $Fe^{2+}/(Mg+Fe^{2+})$, **Fe/3+** = $Fe^{3+}/(Cr+Al+Fe^{3+})$. n.d. = not detected.

Sample	MgO	Al_2O_3	TiO_2	Cr_2O_3	MnO	Fe_2O_3	FeO	FeOT	NiO	Total
26282	4.83	3.08	n.d.	60.65	0.73	6.43	24.29	30.07	n.d.	100.21
26268	12.80	4.34	0.10	64.22	0.39	5.95	12.97	18.32	0.10	100.87
26281	11.76	5.01	n.d.	63.13	0.79	5.14	13.92	18.54	n.d.	99.76
26281	1.15	6.38	n.d.	53.62	0.77	6.93	30.13	36.36	n.d.	98.98
26279	8.49	7.05	0.31	54.72	0.54	9.47	19.82	28.33	0.16	100.56
26280	6.33	7.94	0.33	52.44	0.40	9.58	22.66	31.27	0.17	99.85
26271	1.15	6.23	0.29	51.86	0.55	9.48	30.28	38.80	0.15	99.99
26269	9.23	6.54	0.22	57.15	0.37	6.91	17.85	24.06	0.17	98.44

Cr#	Fe#	Fe/3+
0.93	0.74	0.09
0.91	0.36	0.07
0.89	0.40	0.07
0.85	0.94	0.10
0.84	0.57	0.12
0.82	0.67	0.11
0.85	0.94	0.13
0.85	0.52	0.09

Table 3. Electron Microprobe Analyses of Chromite and Ferritchromite from the TwinSisters Dunite, Washington (Onyeagocha 1974). **Cr#** = Cr/(Cr+Al), **Fe#** = $Fe^{2+}/(Mg+Fe^{2+})$, **Fe/3+** = $Fe^{3+}/(Cr+Al+Fe^{3+})$

Sample	MgO	Al_2O_3	TiO_2	V_2O_3	V_2O_5	Cr_2O_3	MnO	Fe_2O_3	FeO	FeOT	ZnO
2-4	15.50	21.30	0.03	0.11	0.13	47.00	0.23	3.80	11.00	14.42	0.05
2-4A#1	15.20	20.60	0.05	0.12	0.15	47.70	0.24	3.70	11.30	14.63	0.07
2-4A#2	15.40	21.10	0.05	0.12	0.15	46.50	0.41	4.00	10.80	14.40	0.03
5-4B	12.60	11.70	0.10	0.16	0.19	51.50	0.50	9.70	13.90	22.62	0.14
5-4C	12.80	10.70	0.13	0.19	0.23	52.70	0.58	10.40	13.70	23.05	0.14
5-4D	10.30	16.60	0.08	0.21	0.25	47.10	0.52	6.80	17.90	24.01	0.27
5-5	14.30	17.50	0.08	0.16	0.19	51.10	0.44	4.10	12.40	16.09	0.05
5-5D	13.40	16.80	0.08	0.18	0.22	50.80	0.47	4.60	13.60	17.74	0.08
5-7	14.20	18.10	0.05	0.12	0.15	50.40	0.40	3.90	12.60	16.11	0.05
2-4A#1	10.10	1.80	0.12	0.16	0.19	56.00	0.47	13.10	14.70	26.48	0.20
2-4A#2	11.50	2.70	0.90	0.16	0.19	54.90	0.63	13.00	13.70	25.39	0.14
5-5	12.40	9.90	0.13	0.19	0.23	55.50	0.55	7.90	14.10	21.20	0.10

NiO	CoO	Total	Cr#	Fe#	Fe/3+
0.10	0.04	99.16	0.60	0.29	0.04
0.10	0.03	99.11	0.61	0.30	0.04
0.09	0.04	98.54	0.60	0.28	0.05
0.11	0.08	100.49	0.75	0.38	0.12
0.15	0.11	101.60	0.77	0.38	0.12
0.09	0.11	99.98	0.66	0.50	0.08
0.08	0.07	100.28	0.66	0.33	0.05
0.09	0.08	100.18	0.67	0.36	0.05
0.09	0.05	99.99	0.65	0.33	0.04
0.49	0.04	97.18	0.95	0.45	0.17
0.34	0.08	98.05	0.93	0.40	0.17
0.13	0.10	101.00	0.79	0.39	0.09

Table 4. Ti-rich chromite from the Mount Ayliff Intrusion, Transkei, picrite basalt (Cawthorne et al. 1991). **Cr#** = Cr/(Cr+Al), **Fe#** = $Fe^{2+}/(Mg+Fe^{2+})$, **Fe/3+** = $Fe^{3+}/(Cr+Al+Fe^{3+})$.

Sample	MgO	Al_2O_3	TiO_2	Cr_2O_3	MnO	Fe_2O_3	FeO	FeOT	Total	Cr#	Fe#	Fe/3+
21/2	5.20	9.10	4.70	47.10	0.30	3.20	28.90	31.78	98.50	0.78	0.76	0.05
21/2	5.60	7.70	7.00	44.40	0.40	3.50	30.10	33.25	98.70	0.79	0.75	0.06
21/3	7.90	10.60	5.20	46.80	0.30	2.00	25.80	27.60	98.60	0.75	0.64	0.03
21/3	5.40	8.80	6.00	45.50	0.40	3.30	29.80	32.77	99.20	0.78	0.76	0.05
21/4	6.20	11.70	3.00	48.50	0.30	2.20	26.10	28.08	98.00	0.74	0.70	0.03
21/4	6.90	11.30	4.50	46.20	0.30	2.70	26.30	28.73	98.20	0.73	0.68	0.04
21/5	5.30	8.50	3.30	51.60	0.30	2.60	27.70	30.04	99.30	0.80	0.75	0.04
21/5	5.60	9.00	5.10	43.90	0.40	5.90	28.50	33.80	98.40	0.77	0.74	0.09
21/6	6.30	10.50	3.20	47.90	0.30	3.90	26.10	29.61	98.20	0.75	0.70	0.06
21/6	6.10	9.40	6.30	43.80	0.40	3.90	29.20	32.71	99.10	0.76	0.73	0.06
21/7	6.10	11.50	3.40	46.60	0.30	3.90	26.60	30.11	98.40	0.73	0.71	0.05
21/7	6.90	12.50	3.40	45.80	0.30	4.00	25.80	29.40	98.70	0.71	0.68	0.06
21/8	4.40	6.90	4.80	44.40	0.40	8.40	30.30	37.85	99.60	0.81	0.79	0.13
21/8	7.90	7.30	8.80	38.20	0.30	8.70	28.50	36.32	99.70	0.78	0.67	0.14
16/3	4.20	7.10	2.50	40.30	0.40	16.90	28.30	43.49	99.70	0.79	0.79	0.24
16/3	5.50	7.30	4.70	33.10	0.40	20.60	28.30	46.82	99.90	0.75	0.74	0.31
16/4	4.00	6.30	4.00	38.30	0.40	15.70	29.40	43.51	98.10	0.80	0.80	0.24
16/4	3.80	6.40	6.40	31.20	0.40	18.50	32.30	48.93	98.90	0.77	0.83	0.30
16/5	4.30	7.00	2.40	40.00	0.40	16.60	27.60	42.52	98.30	0.79	0.78	0.24
16/5	4.30	6.80	3.60	35.70	0.50	20.20	29.10	47.26	100.20	0.78	0.79	0.30
16/7	5.70	9.10	4.30	37.40	0.40	14.40	27.90	40.85	99.20	0.73	0.73	0.21
16/7	4.90	12.70	3.30	25.30	0.40	23.50	28.10	49.23	98.20	0.57	0.76	0.33
NGL/9	6.30	11.10	4.10	38.50	0.40	11.10	27.20	37.18	98.70	0.70	0.71	0.16
NGL/11	7.30	12.90	2.30	44.20	0.40	7.10	24.00	30.38	98.20	0.70	0.65	0.10
NGL/11	7.20	15.70	1.40	43.00	0.40	6.90	24.00	30.20	98.60	0.65	0.65	0.09
NGL/54	7.70	13.70	1.80	43.70	0.40	8.80	23.40	31.31	99.50	0.68	0.63	0.12
NGL/54	5.70	10.80	3.80	38.50	0.50	12.20	27.30	38.27	98.80	0.71	0.73	0.17
WG/1	4.70	13.40	2.60	45.00	0.40	4.70	28.90	33.13	99.70	0.69	0.77	0.07
WG/1	6.20	16.80	2.80	39.80	0.40	6.00	26.90	32.29	98.90	0.61	0.71	0.08
GC692	5.60	12.70	0.60	42.30	0.40	10.80	25.70	35.41	98.10	0.69	0.71	0.15
GC692	5.70	15.20	0.90	39.60	0.40	10.30	26.30	35.56	98.40	0.64	0.72	0.15
GC697	3.50	8.90	2.70	38.70	0.50	15.50	31.20	45.13	101.00	0.74	0.83	0.23
GC697	3.00	6.60	4.40	29.80	0.40	23.70	33.00	54.31	100.90	0.75	0.86	0.37

Table 5. Chrome spinel analyses from DSDP Hole 396B pillow basalts (Dick & Bryan 1979). **Cr#** = Cr/(Cr+Al), **Fe#** = Fe^{2+}/(Mg+Fe^{2+}), **Fe/3+** = Fe^{3+}/(Cr+Al+Fe^{3+}).

Sample	MgO	Al_2O_3	TiO_2	Cr_2O_3	MnO	FeO	Fe_2O_3	FeOT	Total	Cr#	Fe#	Fe/3+
22-1	15.62	29.22	0.48	34.50	0.11	12.59	6.34	18.29	98.90	0.44	0.31	0.99
	15.76	29.00	0.45	35.31	0.11	12.23	5.70	17.35	98.60	0.45	0.30	0.99
	15.13	27.80	0.45	36.29	0.12	13.04	5.70	18.16	98.50	0.47	0.33	0.99
	14.95	28.77	0.35	35.08	0.11	13.35	5.79	18.56	98.40	0.45	0.33	0.99
8-2	16.72	29.43	0.38	36.30	0.14	11.26	5.86	16.53	100.10	0.45	0.27	0.99
	15.73	29.87	0.43	34.09	0.15	12.61	6.62	18.56	99.50	0.43	0.31	0.99
10-1	14.48	26.11	0.69	35.22	0.19	14.20	8.81	22.12	99.70	0.47	0.36	0.99
	13.85	21.13	0.88	40.54	0.19	14.66	8.67	22.45	99.90	0.56	0.37	0.99
12-1	16.88	28.20	0.32	38.11	0.17	10.61	5.46	15.52	99.75	0.48	0.26	0.99
	15.94	27.23	0.34	38.47	0.18	11.86	5.53	16.83	99.55	0.49	0.29	0.99
16-1	14.28	27.24	0.20	37.99	0.13	14.00	4.65	18.18	98.50	0.48	0.36	0.99
	13.94	26.23	0.55	35.94	0.13	14.97	7.69	21.88	99.50	0.48	0.38	0.99
16-2	15.69	29.90	0.46	34.17	0.17	12.76	6.60	18.69	99.80	0.43	0.31	0.99
	16.82	35.96	0.27	26.52	0.16	11.00	6.13	16.51	96.90	0.33	0.27	0.99
	13.52	22.00	0.96	38.45	0.22	15.14	9.15	23.37	99.40	0.54	0.39	0.99
	15.93	28.49	0.57	35.53	0.20	12.39	6.92	18.61	100.00	0.46	0.30	0.99

Table 6. Composition of Rhum unit 7/unit 8 chrome-spinels, troctolite/peridotite (Henderson 1975). **Cr#** = Cr/(Cr+Al), **Fe#** = Fe^{2+}/(Mg+Fe^{2+}), **Fe/3+** = Fe^{3+}/(Cr+Al+Fe^{3+}). n.d. = not detected

Sample	MgO	Al_2O_3	TiO_2	Cr_2O_3	MnO	FeO	Fe_2O_3	FeOT	Total	Cr#	Fe#	Fe/3+
1	7.01	17.09	n.d.	32.21	n.d.	22.83	17.90	38.92	97.04	0.56	0.65	0.23
2	10.67	21.69	1.77	30.37	0.69	20.03	15.41	33.88	100.63	0.48	0.51	0.19
3	11.05	21.59	1.66	29.04	0.81	18.77	16.38	33.50	99.3	0.47	0.49	0.20
4	12.98	28.81	1.00	26.26	0.69	17.00	14.03	29.61	100.77	0.38	0.42	0.16
5	14.70	30.74	1.09	24.67	0.55	14.63	13.53	26.79	99.91	0.35	0.36	0.15
6	14.68	30.68	0.98	24.94	0.61	14.58	13.76	26.95	100.23	0.35	0.36	0.16
7	14.76	32.00	1.01	23.68	0.57	14.78	13.57	26.98	100.37	0.33	0.36	0.15
8	15.62	35.83	0.85	21.02	0.49	13.98	12.45	25.17	100.24	0.28	0.33	0.14
9	9.05	23.87	0.82	28.12	0.74	21.85	15.92	36.16	100.37	0.44	0.58	0.19
10	7.33	16.35	n.d.	33.92	n.d.	22.40	17.59	38.21	97.59	0.58	0.63	0.22
11	8.24	14.38	n.d.	33.15	n.d.	20.27	20.35	38.56	96.39	0.61	0.58	0.26
12	6.55	13.90	n.d.	34.63	n.d.	23.40	19.81	41.21	98.29	0.63	0.67	0.25
13	10.76	25.22	n.d.	28.77	n.d.	19.39	16.01	33.78	100.15	0.43	0.50	0.19
14	14.08	31.73	n.d.	25.54	n.d.	15.67	14.08	28.33	101.1	0.35	0.38	0.16
15	10.26	24.49	n.d.	29.12	n.d.	20.33	16.89	35.51	101.09	0.44	0.53	0.20
16	12.76	26.58	n.d.	29.10	n.d.	15.42	12.67	26.81	96.53	0.42	0.40	0.15
17	10.46	22.58	n.d.	31.65	n.d.	18.87	14.75	32.13	98.31	0.48	0.50	0.18
18	7.60	15.42	n.d.	35.26	n.d.	21.73	17.23	37.22	97.24	0.61	0.62	0.22
19	10.73	22.57	n.d.	31.88	n.d.	18.70	15.23	32.39	99.11	0.49	0.49	0.18
20	9.59	14.62	n.d.	35.60	n.d.	18.14	18.01	34.33	95.96	0.62	0.51	0.23
21	6.98	14.94	n.d.	31.93	n.d.	22.46	20.63	41.01	96.94	0.59	0.64	0.27
22	4.27	10.50	n.d.	26.59	n.d.	20.52	35.84	52.74	97.72	0.63	0.77	0.40
23	5.22	11.58	n.d.	27.66	n.d.	24.13	27.12	48.51	95.71	0.62	0.72	0.36
24	8.25	12.36	n.d.	31.56	n.d.	19.87	24.33	41.74	96.37	0.63	0.57	0.32
25	7.49	11.84	n.d.	29.23	n.d.	20.89	26.86	45.04	96.31	0.62	0.61	0.35

Table 7. Microprobe data of spinels from lherzolite xenoliths (Wood & Virgo 1989). Oxide wt%.
Cr# = Cr/(Cr+Al), **Fe#** = $Fe^{2+}/(Mg+Fe^{2+})$, **Fe/3+** = $Fe^{3+}/(Cr+Al+Fe^{3+})$.

Sample	MgO	Al_2O_3	TiO_2	Cr_2O_3	MnO	FeO	NiO	SiO_2	Total	Cr#	Fe#	Fe/3+
KLB 8301	19.80	57.12	0.10	10.61	0.11	11.82	0.39	0.05	100.00	0.11	0.23	0.02
KLB 8304	20.86	61.61	0.13	4.82	0.10	11.34	0.37	0.03	99.26	0.05	0.20	0.02
KLB 8305	21.41	57.04	0.08	9.80	0.10	10.75	0.44	0.04	99.66	0.10	0.17	0.03
KLB 8311	16.00	25.85	0.05	42.98	0.16	14.60	0.14	0.08	99.86	0.53	0.29	0.04
KLB 8313	18.76	46.64	0.08	20.69	0.11	12.41	0.31	0.11	99.11	0.23	0.23	0.03
KLB 8315	20.72	58.61	0.11	8.97	0.09	10.34	0.38	0.04	99.26	0.09	0.20	0.01
KLB 8316	16.94	33.68	0.54	32.60	0.22	14.97	0.28	0.11	99.34	0.39	0.27	0.04
KLB 8320	20.04	57.89	0.12	9.21	0.08	12.30	0.37	0.07	100.08	0.10	0.22	0.02
MBR 8305	20.48	54.49	0.09	12.29	0.07	11.43	0.32	0.06	99.23	0.13	0.19	0.03
MBR 8306	20.46	54.60	0.51	10.02	0.10	12.47	0.32	0.15	98.63	0.11	0.20	0.04
MBR 8307	19.55	49.22	0.07	18.27	0.11	11.98	0.29	0.05	99.54	0.20	0.21	0.03
MBR 8309	20.52	52.43	0.14	13.10	0.10	11.79	0.30	0.08	98.46	0.14	0.18	0.04
MBR 8313	19.56	50.20	0.23	16.33	0.09	12.89	0.26	0.06	99.62	0.18	0.22	0.03
SC 8804B	18.50	45.50	0.22	23.44	0.12	11.60	0.20	0.05	99.63	0.26	0.25	0.01
SC 8803B	17.71	42.20	0.24	26.20	0.10	13.33	0.18	0.04	100.00	0.29	0.27	0.02
SC 1-27	15.75	30.10	0.01	39.93	0.17	13.68	0.16	0.06	99.86	0.47	0.31	0.02
SC 8805	16.63	32.47	0.17	35.87	0.11	13.29	0.13	0.02	98.69	0.43	0.28	0.02
SC 8803B	19.17	56.28	0.17	11.32	0.11	13.32	0.35	0.05	100.77	0.12	0.25	0.02
SC 8802	18.73	52.86	0.28	15.15	0.08	12.70	0.28	0.08	100.16	0.16	0.26	0.01
SC 8804	17.29	45.76	0.44	21.82	0.12	14.81	0.25	0.06	100.55	0.24	0.30	0.02
IM 8701	20.26	54.62	0.07	12.11	0.10	12.40	0.37	0.10	100.03	0.13	0.21	0.03
IM 8702	20.49	54.99	0.05	11.39	0.04	12.07	0.40	0.10	99.53	0.12	0.20	0.03
IM 8703	19.03	52.50	0.06	12.02	0.12	14.55	0.40	0.10	98.78	0.13	0.24	0.05
IM 8705	19.52	51.20	0.07	15.44	0.11	14.72	0.37	0.13	101.56	0.17	0.23	0.05
MO 4334-11	20.32	58.30	0.32	8.33	0.10	11.46	0.38	0.12	99.33	0.09	0.21	0.02
MO 4334-14	20.39	64.36	0.22	3.76	0.11	10.71	0.49	0.11	100.15	0.04	0.23	0.00
MHP 79-1	20.27	60.01	0.29	8.07	0.13	10.70	0.39	0.11	99.97	0.08	0.22	0.01
VI 313-5	18.19	45.25	0.64	21.72	0.23	13.82	0.37	0.18	100.40	0.24	0.26	0.03
VI 313-37	18.55	43.47	0.43	22.37	0.13	13.42	0.22	0.13	98.72	0.26	0.24	0.04
VI 314-6	16.99	38.92	0.32	29.91	0.24	12.20	0.30	0.15	99.03	0.34	0.28	0.01

Table 8. Chrome–spinels in gabbro–wehrlite intrusions of the Pechenga area, Kola Peninsula, Russia (Abzalov 1998). Oxide wt%. n.d. = not detected.

Sample	MgO	Al_2O_3	TiO_2	V_2O_5	Cr_2O_3	MnO	FeO	Fe_2O_3	FeOT	NiO	ZnO
1788-560(4)	6.84	9.38	0.92	0.22	47.63	0.27	19.86	13.84	32.30	0.08	0.15
2986-1029	8.97	13.82	0.35	0.18	48.38	0.29	17.35	6.32	23.03	0.08	0.06
A90-2/2	0.51	9.38	8.79	0.23	21.97	1.46	30.41	23.96	51.95	0.09	1.40
A90-7/2(5)	8.50	9.21	3.31	0.29	37.79	1.34	18.18	22.88	38.75	0.10	0.64
A90-3/1,1	0.25	10.05	10.33	0.20	15.14	0.82	31.42	30.37	58.72	0.10	1.61
A90-3/1,2	0.41	12.20	10.88	0.23	14.82	0.82	32.49	27.40	57.12	0.06	1.62
557b(2/5)	4.22	6.84	4.65	0.11	28.93	1.55	23.06	28.38	48.57	0.21	0.14
561b(1/1)	5.79	7.37	4.39	0.09	32.85	0.30	21.23	25.38	44.05	0.30	0.16
369(4/1)	1.03	2.10	16.01	n.d.	13.46	1.21	33.07	33.60	63.28	n.d.	n.d.
369(4/2)	1.06	0.04	14.40	n.d.	14.78	1.03	31.81	39.47	67.29	0.06	n.d.
369M	0.70	2.88	21.06	0.25	6.36	2.86	36.22	29.65	62.88	0.10	0.73
369M(d)	0.33	1.75	5.14	0.28	5.22	0.87	28.64	58.09	80.86	0.11	0.27
561b(3/3)	2.56	3.95	15.26	n.d.	9.48	6.05	27.27	32.82	56.78	0.37	1.37
1583(4)	0.17	0.00	0.14	0.21	2.71	0.03	28.30	68.23	89.64	0.08	0.03
1877(2/1)	0.19	0.09	0.38	0.48	15.49	0.17	27.20	55.75	77.32	0.11	0.35
1877(3/5)	0.19	0.19	0.93	0.71	29.19	0.35	26.32	41.37	63.51	0.03	0.83
1906	0.01	0.18	0.64	0.18	22.63	0.77	25.75	46.52	67.57	0.08	1.09
1581(1)	0.24	0.06	0.31	0.31	10.64	0.14	27.87	61.26	82.94	0.11	0.13
1583(1)	0.16	0.00	0.17	0.20	2.40	0.01	28.02	67.78	88.95	0.11	0.04
1875(2/6)	0.43	0.19	0.44	0.44	12.34	0.06	27.80	60.03	81.77	0.08	0.25
1887(1)	0.05	0.06	0.32	0.76	9.70	0.10	27.64	60.51	82.04	0.15	0.05
1887(2)	0.11	0.09	0.33	0.65	6.98	0.06	27.74	63.14	84.50	0.08	0.22

CaO	SiO_2	Total	Cr#	Fe#	Fe/3+
n.d.	0.24	99.42	0.77	0.65	0.14
n.d.	0.21	96.00	0.70	0.54	0.06
n.d.	0.11	98.31	0.61	0.98	0.31
0.04	0.18	102.46	0.73	0.59	0.26
0.02	0.06	100.37	0.50	0.99	0.40
0.01	0.03	100.98	0.45	0.98	0.35
0.04	0.20	98.32	0.74	0.79	0.36
0.02	0.05	97.93	0.75	0.72	0.30
n.d.	n.d.	100.48	0.81	0.96	0.56
n.d.	n.d.	102.65	1.00	0.96	0.64
0.03	0.11	100.95	0.60	0.97	0.62
0.01	0.14	100.85	0.67	0.98	0.86
n.d.	n.d.	99.13	0.62	0.88	0.61
0.05	0.21	100.16	1.00	0.99	0.96
0.04	0.17	100.42	0.99	0.99	0.76
n.d.	0.10	100.21	0.99	0.99	0.54
0.05	0.15	98.05	0.99	1.00	0.64
n.d.	0.07	101.14	0.99	0.99	0.84
0.06	0.04	98.99	1.00	0.99	0.96
0.02	0.32	102.40	0.98	0.98	0.81
n.d.	0.19	99.53	0.99	1.00	0.85
0.02	0.19	99.61	0.98	0.99	0.89

Tidigare skrifter i serien ”Examensarbeten i Geologi vid Lunds universitet”:

372. Svantesson, Fredrik, 2013: Alunskiffern i Östergötland – utbredning, mäktigheter, stratigrafi och egenskaper. (15 hp)
373. Iqbal, Faisal Javed, 2013: Paleoecology and sedimentology of the Upper Cretaceous (Campanian), marine strata at Åsen, Kristianstad Basin, Southern Sweden, Scania. (45 hp)
374. Kristinsdóttir, Bára Dröfn, 2013: U-Pb, O and Lu-Hf isotope ratios of detrital zircon from Ghana, West-African Craton – Formation of juvenile, Palaeoproterozoic crust. (45 hp)
375. Grenholm, Mikael, 2014: The Birimian event in the Baoulé Mossi domain (West African Craton) — regional and global context. (45 hp)
376. Hafnadóttir, Marín Ósk, 2014: Understanding igneous processes through zircon trace element systematics: prospects and pitfalls. (45 hp)
377. Jönsson, Cecilia A. M., 2014: Geophysical ground surveys of the Matchless Amphibolite Belt in Namibia. (45 hp)
378. Åkesson, Sofia, 2014: Skjutbanors påverkan på mark och miljö. (15 hp)
379. Härling, Jesper, 2014: Food partitioning and dietary habits of mosasaurs (Reptilia, Mosasauridae) from the Campanian (Upper Cretaceous) of the Kristianstad Basin, southern Sweden. (45 hp)
380. Kristensson, Johan, 2014: Ordovicium i Fågelsångskärnan-2, Skåne – stratigrafi och faciesvariationer. (15 hp)
381. Höglund, Ida, 2014: Hiatus - Sveriges första sällskapsspel i sedimentologi. (15 hp)
382. Malmer, Edit, 2014: Vulkanism - en fara för vår hälsa? (15 hp)
383. Stamsnijder, Joaen, 2014: Bestämning av kvartshalt i sandprov - metodutveckling med OSL-, SEM– och EDS-analys. (15 hp)
384. Helmfrid, Annelie, 2014: Konceptuell modell över spridningsvägar för glasbruksföroreningar i Rejmyre samhälle. (15 hp)
385. Adolfsson, Max, 2014: Visualizing the volcanic history of the Kaapvaal Craton using ArcGIS. (15 hp)
386. Hajny, Casandra, 2014: Ett mystiskt ryggradsdjursfossil från Åsen och dess koppling till den skånska, krittida ryggradsdjursfaunan. (15 hp)
387. Ekström, Elin, 2014: – Geologins betydelse för geotekniker i Skåne. (15 hp)
388. Thuresson, Emma, 2014: Systematisk sammanställning av större geoenergianläggningar i Sverige. (15 hp)
389. Redmo, Malin, 2014: Paleontologiska och impaktrelaterade studier av ett anomalt lerlager i Schweiz. (15 hp)
390. Artursson, Christopher, 2014: Comparison of radionuclide-based solar reconstructions and sunspot observations the last 2000 years. (15 hp)
391. Svahn, Fredrika, 2014: Traces of impact in crystalline rock – A summary of processes and products of shock metamorphism in crystalline rock with focus on planar deformation features in feldspars. (15 hp)
392. Järvin, Sara, 2014: Studie av faktorer som påverkar skredutbredningen vid Norsälven, Värmland. (15 hp)
393. Åberg, Gisela, 2014: Stratigrafin i Hanöbukten under senaste glaciationen: en studie av borrkärnor från IODP’s expedition nr 347. (15 hp)
394. Westlund, Kristian, 2014: Geomorphological evidence for an ongoing transgression on northwestern Svalbard. (15 hp)
395. Rooth, Richard, 2014: Uppföljning av utlastningsgrad vid Dannemora gruva; april 2012 - april 2014. (15 hp)
396. Persson, Daniel, 2014: Miljögeologisk undersökning av deponin vid Getabjär, Sölvesborg. (15 hp)
397. Jennerheim, Jessica, 2014: Undersökning av långsiktiga effekter på mark och grundvatten vid infiltration av lakvatten – fältundersökning och utvärdering av förhållanden vid Kejsarkullens avfallsanläggning, Hultsfred. (15 hp)
398. Särman, Kim, 2014: Utvärdering av befintliga vattenskyddsområden i Sverige. (15 hp)
399. Tuvesson, Henrik, 2014: Från hav till land – en beskrivning av geologin i Skrylle. (15 hp)
400. Nilsson Brunlid, Anette, 2014: Paleoekologisk och kemisk-fysikalisk undersökning av ett avvikande sedimentlager i Barsebäcks mosse, sydvästra Skåne, bil dat för ca 13 000 år sedan. (15 hp)
401. Falkenhaug, Jorunn, 2014: Vattnets kretslopp i området vid Lilla Klåveröd: ett

kunskapsprojekt med vatten i fokus. (15 hp)

402. Heingård, Miriam, 2014: Long bone and vertebral microanatomy and osteohistology of 'Platecarpus' ptychodon (Reptilia, Mosasauridae) – implications for marine adaptations. (15 hp)
403. Kall, Christoffer, 2014: Microscopic echinoderm remains from the Darriwilian (Middle Ordovician) of Västergötland, Sweden – faunal composition and applicability as environmental proxies. (15 hp)
404. Preis Bergdahl, Daniel, 2014: Geoenergi för växthusjordbruk – Möjlig anläggning av värme och kyla i Västskåne. (15 hp)
405. Jakobsson, Mikael, 2014: Geophysical characterization and petrographic analysis of cap and reservoir rocks within the Lund Sandstone in Kyrkheddinge. (15 hp)
406. Björnfors, Oliver, 2014: A comparison of size fractions in faunal assemblages of deep-water benthic foraminifera—A case study from the coast of SW-Africa.. (15 hp)
407. Rådman, Johan, 2014: U-Pb baddeleyite geochronology and geochemistry of the White Mfolozi Dyke Swarm: unravelling the complexities of 2.70-2.66 Ga dyke swarms on the eastern Kaapvaal Craton, South Africa. (45 hp)
408. Andersson, Monica, 2014: Drumliner vid moderna glaciärer — hur vanliga är de? (15 hp)
409. Olsenius, Björn, 2014: Vinderosion, sanddrift och markanvändning på Kristianstadsslätten. (15 hp)
410. Bokhari Friberg, Yasmin, 2014: Oxygen isotopes in corals and their use as proxies for El Niño. (15 hp)
411. Fullerton, Wayne, 2014: REE mineralisation and metasomatic alteration in the Olserum metasediments. (45 hp)
412. Mekhaldi, Florian, 2014: The cosmic-ray events around AD 775 and AD 993 - Assessing their causes and possible effects on climate. (45 hp)
413. Timms Eliasson, Isabelle, 2014: Is it possible to reconstruct local presence of pine on bogs during the Holocene based on pollen data? A study based on surface and stratigraphical samples from three bogs in southern Sweden. (45 hp)
414. Hjulström, Joakim., 2014: Bortforsling av kaxblandat vatten från borrningar via dagvattenledningar: Riskanalys, karaktärisering av kaxvatten och reningsmetoder. (45 hp)
415. Fredrich, Birgit, 2014: Metadolerites as quantitative P-T markers for Sveconorwegian metamorphism, SW Sweden. (45 hp)
416. Alebouyeh Semami, Farnaz, 2014: U-Pb geochronology of the Tsineng dyke swarm and paleomagnetism of the Hartley Basalt, South Africa – evidence for two separate magmatic events at 1.93-1.92 and 1.88-1.84 Ga in the Kalahari craton. (45 hp)
417. Reiche, Sophie, 2014: Ascertaining the lithological boundaries of the Yoldia Sea of the Baltic Sea – a geochemical approach. (45 hp)
418. Mroczek, Robert. 2014: Microscopic shock-metamorphic features in crystalline bedrock: A comparison between shocked and unshocked granite from the Siljan impact structure. (15 hp)
419. Balija, Fisnik. 2014: Radon ett samhällsproblem - En litteraturstudie om geologiskt sammanhang, hälsoeffekter och möjliga lösningar. (15 hp)
420. Andersson, Sandra. 2014: Undersökning av kalciumkarbonatförekomsten i infiltrationsområdet i Sydvattens vattenverk, Vombverket. (15 hp)
421. Martin, Ellinor, 2014: Chrome spinel grains from the Komstad Limestone Formation, Killeröd, southern Sweden: A high-resolution study of an increased meteorite flux in the Middle Ordovician. (45 hp)

LUNDS UNIVERSITET

Geologiska institutionen
Lunds universitet
Sölvegatan 12, 223 62 Lund